DSA Report
August 2024, number 3

Investigation into the Radioecological Status of the sunken Nuclear Submarine Komsomolets in the Norwegian Sea

Results from the 2019 Norwegian research cruise

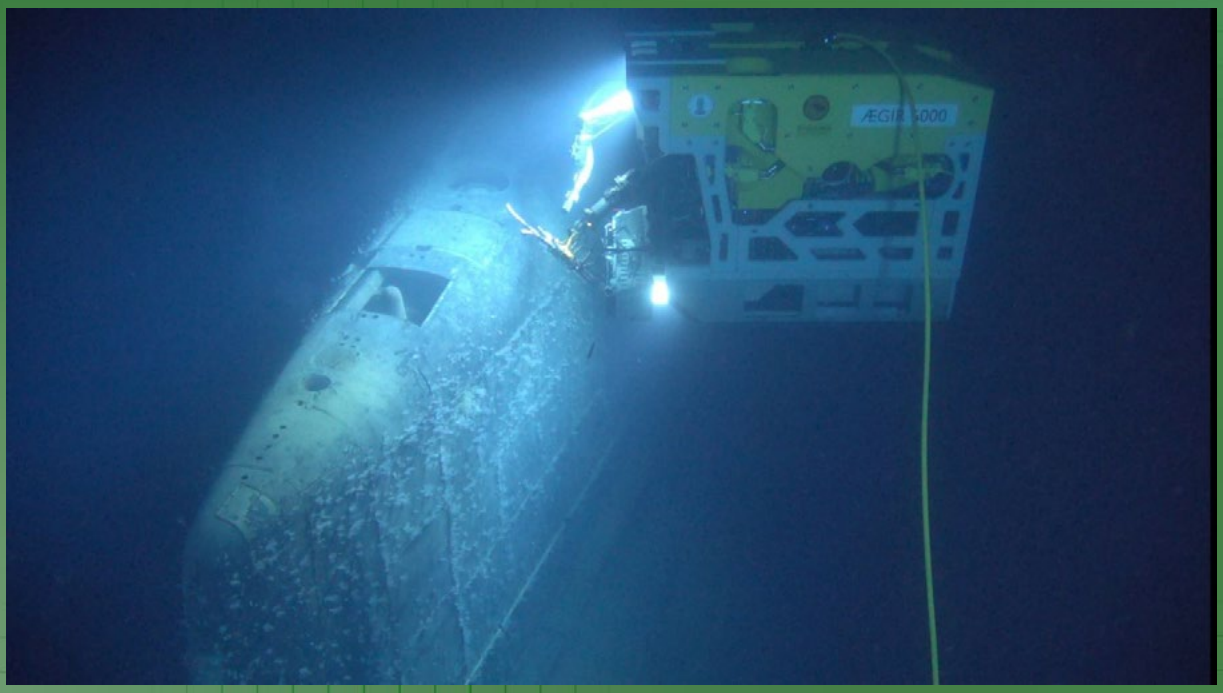

Norges miljø- og biovitenskapelige universitet

DSA

Norwegian Radiation and Nuclear Safety Authority

Referanse
Gwynn, J.P., Heldal, H.E., Teien, H.C., Volynkin, A., Jerome, S.M. Lind, O.C., 2024. Investigation into the radioecological status of the sunken nuclear submarine Komsomolets in the Norwegian Sea. Results from the 2019 Norwegian research cruise. DSA report 2024:3, Direktoratet for strålevern og atomsikkerhet, Østerås, Norge.

Emneord
Komsomolets, Norskehavet, atomubåt, radioaktiv forurensning, miljøstatus.

Resymé
Rapporten presenterer resultat fra det norske forskningstoktet i 2019 til den sunkne atomubåten Komsomolets i Norskehavet.

Reference
Gwynn, J.P., Heldal, H.E., Teien, H.C., Volynkin, A., Jerome, S.M. Lind, O.C., 2024. Investigation into the radioecological status of the sunken nuclear submarine Komsomolets in the Norwegian Sea. Results from the 2019 Norwegian research cruise. DSA report 2024:3, Norwegian Radiation and Nuclear Safety Authority, Østerås, Norway.

Key words
Komsomolets, Norwegian Sea, nuclear submarine, radioactive contamination, environmental status

Abstract
This report presents the results obtained by the Norwegian research cruise in 2019 to the site of the sunken nuclear submarine Komsomolets in the Norwegian Sea.

Prosjektleder: Justin Gwynn.
Godkjent:

Sara Skodbo, avdelingsdirektør, avdeling kunnskapsutvikling og internasjonal atomsikkerhet

Publisert 2024-08-20

Sider 108

DSA,
Postboks 329 Skøyen
0213 Oslo
Norge

Telefon 67 16 25 00
Faks 67 14 74 07
Email dsa@dsa.no
dsa.no

ISSN 2535-7339

DSA-rapport Nummer 3 **Publisert** aug 2024

Investigation into the radioecological status of the sunken nuclear submarine Komsomolets in the Norwegian sea

Results from the 2019 Norwegian research cruise

Executive summary

During the 2019 Norwegian research cruise to the nuclear submarine Komsomolets, which sank in 1989, Komsomolets was observed lying upright on the seafloor at a depth of around 1680 m approximately 250 km SSW from Bear Island. The forward section of the submarine has suffered considerable damage to both the outer hull and inner pressure hull particularly around the torpedo compartment. The coverings, plates and plugs installed around the torpedo compartment by Russia in the 1990s were observed to be still in place. The stern section showed no obvious physical damage to the external hull, except for several missing deck tiles on the starboard side adjacent to the main stern ballast tank and compartment seven. The exterior surfaces of the submarine were typically covered with a sparse layer of marine biota growth. As well as the known openings between the marine environment and the torpedo compartment, it is likely that such pathways exist between compartments two and three and possibly to all the remaining compartments either through damaged transverse bulkheads or system tube lines that ran the length of the submarine.

Releases of radionuclides from the reactor were detected via a ventilation pipe, as previously reported by Russia in the 1990s and again in 2007, but these releases were not continuous. When elevated levels of radionuclides were detected in or near the ventilation pipe, a simultaneous visual release could be observed emerging from the ventilation pipe. The cause of this is not known. Visual releases and elevated levels of radionuclides were also detected from a metal grill next to the ventilation pipe, which has not been reported previously by Russia. No obvious visual releases were observed emerging from any other opening around the submarine. There was no indication of any release of weapon grade plutonium from the two nuclear warheads that have been reported to be in the torpedo compartment.

The range of Cs-137 activity concentrations in seawater samples collected from or near the ventilation pipe and metal grill when visual releases were observed were within the range of reported values from previous Russian investigations in the 1990s and lastly in 2007. The maximum observed activity concentrations of Sr-90 and Cs-137 in these samples were 400 000 and 800 000 times higher, respectively, than typical background values for these radionuclides in seawater from the Norwegian Sea. However, based on the results for Cs-137 and Sr-90 in samples taken at different distances from the ventilation pipe, the releases of these radionuclides from the reactor in Komsomolets appear to be rapidly diluted.

The maximum observed combined activity concentration of Pu-239 and Pu-240 in seawater samples collected from or near the ventilation pipe and metal grill when visual releases were observed was 64 times higher than the average activity concentration for Pu-239,240 in bottom water sampled around Komsomolets since 1993. The maximum observed activity concentration of U-236 in seawater samples collected from or near the ventilation pipe and metal grill when visual releases were observed was 243 times higher than available data for the North Sea. The elevated levels of Cs-137, Sr-90, Pu-239, Pu-240 and U-236 as well as atom ratios of Pu-240/Pu-239 that have been detected in releases from the reactor in Komsomolets would suggest that the nuclear fuel assemblies have been damaged and that nuclear fuel is in direct contact with seawater and deteriorating.

The releases that have occurred since Komsomolets sank in 1989 appear to have had little impact on the surrounding sediments based on the available results for Cs-137, Pu-239, Pu-240, U-236 and atom ratios of Pu-240/Pu-239. There is some evidence that marine biota growing on the hull of Komsomolets have accumulated Cs-137 that has been released from the reactor, but the observed activity concentrations were low and not at a level where any significant effects would be expected.

Elevated concentrations of several trace elements in releases from or near the ventilation pipe and metal grill, in sediment around Komsomolets and in marine biota growing on the hull likely indicates other ongoing corrosion processes within the submarine. Any impacts due to the elevated levels of some trace elements (e.g., Ni, Cu and Zn) in the releases and in sediments around the submarine are likely to be limited to the immediate area around the submarine.

Releases from the reactor in Komsomolets can be expected to continue in the future. Further investigations should be carried out to determine the mechanisms behind the observed releases, the corrosion processes that are occurring within the reactor and the implications of these for further releases and the fate of the remaining nuclear material in the reactor. Komsomolets provides a unique opportunity to understand the risks and consequences of releases from other sunken or dumped reactors in the Arctic as well as risks from any further accidents involving nuclear powered vessels and any other type of nuclear technologies used at sea. It is therefore important that continued monitoring of the situation and status of the submarine is carried out.

Innholdsfortegnelse

1 Introduction

In 1992 a Norwegian-Russian expert group was established to investigate radioactive contamination in the northern areas under the joint Norwegian-Russian Commission for Cooperation in the Environmental Sector. The Norwegian-Russian expert group was formed in the light of new information concerning dumping of radioactive waste in the Barents and Kara Seas by the Former Soviet Union. The preparation of the Norwegian research cruise in 2019 was discussed under the Norwegian-Russian expert group and a Russian observer participated in the research cruise. However, at the time that this report was written, project cooperation between Norwegian and Russian authorities on nuclear safety was on hold after the full-scale invasion in Ukraine in February 2022.

The objectives defined for the expert group were:

- To obtain information on the handling, storage, discharge and dumping of radioactive material in the northern areas.
- To investigate, through field work, the actual levels of radioactive contamination in the open Kara Sea and at the dumping sites.
- To locate dumped nuclear waste and identify if any leakage of radioactive substances has taken place.
- To undertake impact and risk assessments for man and the environment.
- To inform the public of the results of these investigations

The Norwegian-Russian expert group enabled progress on issues related to nuclear safety and radiological environmental assessments, such as:

- Nuclear safety improvements at Andreeva Bay, as well as removal of spent nuclear fuel from this site.
- Risk and consequence assessments for actual and potential sources of radioactive contamination in Northwest Russia.
- The removal and safe disposal of 180 high activity radioactive sources from light beacons in Northwest Russia and 71 similar sources from the Russian coastline in the Baltic Sea.
- The impact of radioactive contamination in the area surrounding the Russian nuclear facility at Mayak and consequence assessments for potential accidents at the facility.
- Research cruises to dumping sites of radioactive waste in the Kara Sea and Novaya Zemlya fjords in 1992, 1993 and 1994.
- Investigation of potential radioactive contamination in the environment following the raising of Kursk in 2001.
- Research cruise to the Kara Sea and Stepovogo Fjord in 2012 to investigate the status of dumped radioactive waste including the nuclear submarine K-27.
- Research cruise to the site of the sunken nuclear submarine K-159 in the Barents Sea in 2014.

1.1 The nuclear submarine Komsomolets (K-278)

1.1.1 Construction and operational history of the nuclear submarine Komsomolets (K-278)

Project 685 was a Soviet nuclear powered attack submarine (Figure 1.1) designed and built in the 1970s and was accepted into service with the Soviet Northern Fleet in 1983. The submarine was assigned the tactical number K-278 in 1988 and was given the NATO designation "Mike". K-278 was the only kind of its type built by the Soviet Union, with an outer and inner pressure hull of titanium alloy and an outer layer of rubber deck tiles that increased the stealth of the submarine. The use of titanium alloy for the hulls

allowed the submarine to reach far greater depths than any other submarine in service at that time. In 1985 during test trials, it was reported that K-278 reached a depth of 1027 m. At such a depth, the submarine would have been below the operational depth of any other submarine and any other anti-submarine weapons and would have been difficult to detect acoustically. For this accomplishment, K-278 was given the name Komsomolets in 1989, one of the few Soviet submarines to be given such an honour. Komsomolets was approximately 118 m in length with an underwater displacement of 8500 tons and top speed underwater of 31 knots. Komsomolets was constructed with seven compartments (Figure 1.2), with the single 190 MW OK-650b-3 pressurised water reactor in compartment number 4. In addition, there was a backup power plant, consisting of an emergency diesel generator with a capacity of 500 kW in compartment number 3, with the main bank of batteries located in compartment number 1. At the stern of the submarine, two backup 300 kW electric motors were housed that could propel the submarine of speeds up to 5 knots. The submarine was equipped with an escape chamber in the sail (tower) of the submarine (Figure 1.1) and six 533 mm torpedo tubes at the bow that could fire torpedoes at any submerged depth. It is likely that Komsomolets would have carried a variety of different torpedo propulsion units such as SAET-60M torpedoes, C-10 "Granat" cruise missiles and VA-111 "Shkval" supercavitating torpedoes. Komsomolets carried 2 nuclear warheads along with warheads containing conventional explosives that could have been fitted to these different torpedoes. In total, Komsomolets carried 22 torpedoes, 6 of which would have been loaded in the torpedo tubes at the time of sinking.

.

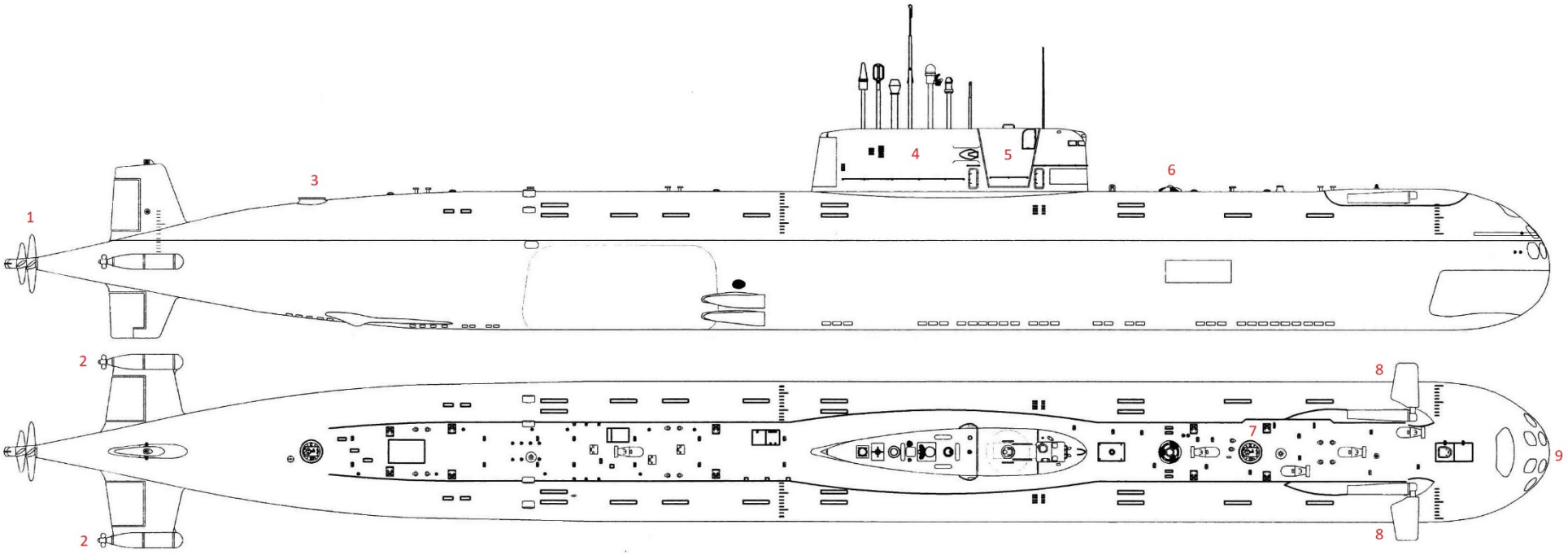

Figure 1.1. Plan drawing of the nuclear submarine Komsomolets (K-278) with some key features identified. 1. Main propeller, 2. Auxillary propellers, 3. Rear entrance hatch (to compartment seven), 4. Sail, 5. Escape chamber, 6. Emergency buoy, 7. Forward entrance hatch (to torpedo compartment), 8. Dive planes, 9. Doors to torpedo tubes (Image: Drawingdatabase.com).

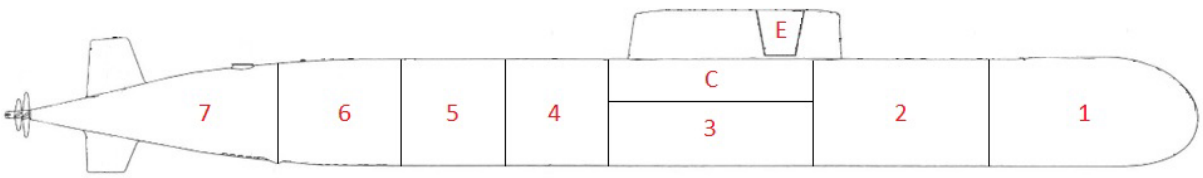

Figure 1.2. Simplistic schematic of the nuclear submarine Komsomolets (K-278), showing the general layout of the seven compartments. 1. Torpedo compartment, 2. Living quarters, 3. Diesel generator, 4. Reactor, 5. Auxiliary mechanisms, 6. Turbines, 7. Stern and control, C. Control centre, E. Escape chamber (Image: DSA).

In total, Komsomolets completed 3 combat missions; firstly, from November 30th, 1986, to February 28th, 1987, secondly from August to October 1987 and lastly when it set out on February 28th, 1989, for its third and last combat mission. There were two crews who were assigned to Komsomolets, the main one under the command of Captain 1st Rank Yu. A. Zelensky and the reserve crew under the command of Captain 1st Rank E. A. Vanin. When Komsomolets set sail on its third combat tour on February 28th, 1989, the submarine was manned by the reserve crew, which according to Romanov (2006) may have contributed to the eventual sinking of the submarine.

1.1.2 The sinking of the nuclear submarine Komsomolets (K-278)

Komsomolets set sail on its last and fatal combat mission on February 28th, 1989, with a crew of 69 onboard. On the morning of April 7th, 1989, Komsomolets was cruising at a depth of around 400 m in the Norwegian Sea. At around 11 am, there was a report of a fire in compartment seven with smoke leaking into compartment six. Shortly afterwards, the order was given to surface and the main ballast tanks were blown. The piping that connected the main stern ballast tanks to the high-pressure air system passed through compartment seven and it has been suggested that the piping to the port ballast tank failed when the order to blow the stern ballast tanks was given, resulting in high pressure air being forced into compartment seven and turning the fire into a blast furnace (Romanov, 2006). The submarine managed to surface just after 11:15 am and soon afterwards the reactor was put into emergency shutdown and the hatch to the escape chamber was opened. On the surface, eyewitnesses reported seeing deck tiles over the stern starboard ballast tank peeling off into the water and bubbling of air in the water (probably due to hot gases from the fire being pumped into the ballast tank). The port stern ballast tank was not blown and was still filled with seawater. Even though the door to compartment seven was sealed, smoke and fumes spread to the other compartments through system and ventilation lines that passed through the bulkheads. At around 2:00 pm and as the fire in compartment seven died out, it is thought that the pressure in this compartment dropped allowing seawater to start entering the submarine, possibly through a damaged Kingston valve in the cooling system to the stern propulsion tube (Romanov, 2006). Although most of the crew were already topside, the order for evacuation of the submarine was given at 4:42 pm. The last entry in the ship's log was at 4:45 pm. A few minutes later, Komsomolets started to sink stern first with a trim around 80 degrees (Romanov, 2006).

Six crew members including the commander were still onboard as the submarine sank. Five of them managed to make their way to the escape chamber and close the lower hatch after the trim of the sinking submarine levelled out. However, they could not release the escape chamber and the submarine continued to sink towards the seafloor with the escape chamber locked to the hull. At some point, the

escape chamber was rocked violently by a shock from below. It is not known if this shock was from the submarine hitting the seafloor or some other explosion, but this led to the sudden release of the escape chamber. On the way to surface three of the five crew in the escape chamber were overcome by fumes, but two of them managed to put on breathing apparatus. When the escape chamber reached the surface, the upper hatch was blown off killing one of the two conscious crew members. The remaining crew member managed to climb out before the escape chamber sank back to the seafloor. At this point there were 60 crew members alive in the water with only one life raft between them which had been inflated upside down. Water temperature at that time of year was probably no more than 5˚C (Ottersen, 2010) and most of the crew had no survival suits or life jackets. A Soviet support vessel arrived on the scene over an hour after Komsomolets sank. By this time a further 30 of the crew had died and tragically 3 others died after being rescued. In total, 42 of the crew lost their lives in the accident, with only 27 surviving, including the sole survivor from the escape chamber. The submarine now lies at a depth of 1680 m, south southwest of Bear Island (73º43'27" N, 13º15'59" E).

Figure 1.3. The nuclear submarine Komsomolets in service (Photo: Norwegian Air Force 333 Squadron).

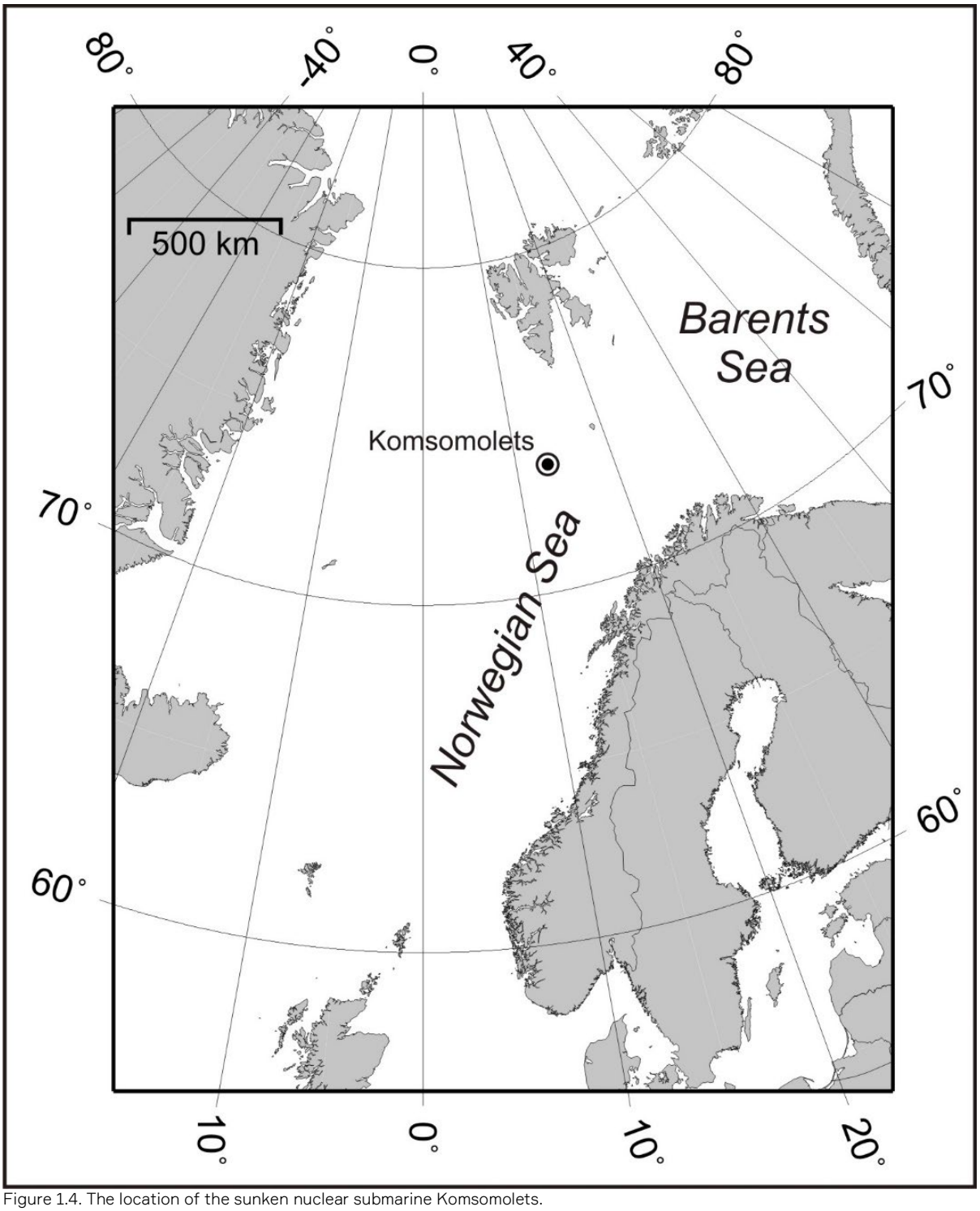

Figure 1.4. The location of the sunken nuclear submarine Komsomolets.

1.1.3 The radioactive inventory of Komsomolets

The total activity of the inventory of the reactor at the time of sinking has been estimated at 29 PBq with a further 16 TBq of plutonium (Pu-239 and Pu-240) contained within the two nuclear warheads in the torpedo compartment (Gladkov et al., 1994; Høibråten et al., 1997). Taking radioactive decay into account, the estimated inventory of 29 PBq would have decreased to 3 PBq by 2019, with almost the entire (95%) remaining activity due to Sr-90 and Cs-137 (Table 1.1). The predicted activity ratio of Cs-137 to Sr-90 in the reactor has been estimated as approximately 1:1 (Høibråten et al. 1997).

Table 1.1. Estimated inventories of selected radionuclides in the reactor of Komsomolets[a].

Radionuclide	Half-life (y)	Activity (TBq)	
		At time of sinking (1989)	2019
Co-60	5.3	53	1.0
Sr-90	28.8	2800	1371
Cs-134	2.1	1800	0.008
Cs-137	30.0	3100	1550
Pu-239	24110	4.4	4.4
Pu-240	6561	1.7	1.7

a - Taken from Gladkov et al. (1994) and Høibråten et al. (1997)

1.2 Previous investigations of the sunken nuclear submarine Komsomolets

1.2.1 Overview of Soviet and Russian investigations

Soviet and then Russian investigations were carried out between 1989 and 2007 with the aid of manned MIR submersibles to investigate the status of the sunken nuclear submarine and the surrounding marine environment. The use of manned submersibles in these investigations allowed for the visual inspection of the submarine and for the collection of samples and in situ measurements next to the hull. Initial investigations showed that the front part of the submarine had suffered considerable damage, with holes and cracks in both the outer hull and inner pressure hull (Yablokov et al., 1993). Damage to the outer and inner pressure hull was observed above the torpedo compartment (Figure 1.5) and it was reported that the nuclear material in the warheads were in contact with seawater (Yablokov et al., 1993). It has been estimated that it took Komsomolets around 7 minutes to reach the seafloor (Hollister, 1993a). The observed damage to the outer and inner hulls has been attributed to a possible explosion inside the submarine due to flooding of the main batteries or the detonation of one of the conventional warheads in the torpedo compartment. Alternatively, it has been suggested that the observed damage occurred as the result of hydraulic shockwaves from the rupturing of the remaining high pressure air tanks in the forward section (Romanov, 2006). It is not known whether it was the impact of the submarine hitting the seafloor that instigated any of the proposed means of destruction to the forward compartments or whether the impact itself was a further factor to the observed damage. In 1994, work was carried out to reduce the flow of seawater through the damaged torpedo compartment (Kasatonov, 1996). The torpedo compartment was partially filled and covered on both the port and starboard sides by taurpaulins secured by chains to the outer hull. Titanium plates were positioned over openings in the upper outer deck over the torpedo compartment and the six torpedo tubes were sealed with titanium plugs (Figure 1.6). In 1992, it was reported that the maxium activity concentration of Cs-137 in seawater in the near environment of the submarine was 180 Bq/m^3, with an average of around 30 Bq/m^3 (Hollister, 1993b). Releases of Co-60, Cs-134 and Cs-137 have been detected in a ventilation pipe that forms an open connection between the compartment (No. 5) immediately aft of the reactor compartment and the open sea during Russian

investigations by in situ measurements and through the use of sorbents (Hollister, 1993a, 1994a; Nejdanov, 1993; Gladkov et al., 1994; Kazennov, 2010). It is likely that this ventilation pipe was opened to help vent smoke when Komsomolets was on the surface and consequently would not have been closed when the submarine suddenly sank. That releases from the reactor have been detected implies that the primary cooling system and/or the reactor vessel itself have been compromised and that the reactor compartment is not sealed. According to Russian sources, it is assummed that all 'release barriers' have been breached (Hollister, 1992). In 1993, activity concentrations of Cs-137 in the ventilation pipe were reported as being between 6 and 13 kBq/m^3 (Hollister, 1993a). In 1994, activity concentrations of Cs-137 detected in the ventilation pipe were of the order of 1 MBq/m^3 decreasing to 4 kBq/m^3 in the zone around the outlet (Gladkov et al., 1994). Based on rates of water flow in the ventilation pipe, annual releases of Cs-137 from the sunken submarine were estimated at that time to be around 500 GBq/a (Gladkov et al., 1994). In 2007, annual releases of Cs-137 from the ventilation pipe were reported to have decreased by more than 30 fold (Kazennov, 2010), whilst more recently, Vysotsky et al. (2014) estimated releases of Cs-137 and Sr-90 from Komsomolets at 0.1 GBq/a.

Figure 1.5. Photo showing one of the MIR submersibles investigating damage to the torpedo compartment of Komsomolets during the 1993 Russian investigation. The photo's perspective is taken looking away from the bow of the submarine and shows the starboard side of the torpedo compartment before this area was covered with taurpaulins. (Photo: DSA).

Figure 1.6. Photo showing one of the titanium plugs that was placed over the torpedo tubes by the Russians in 1994. The plug is fastened to the side of one of the MIR submersibles used during the 1994 Russian investigation. (Photo: DSA).

In terms of the near environment around Komsomolets, activity concentrations of Cs-134 between 3 and 8 Bq/kg dry weight (d.w.) were reported for the upper layers of sediment from samples collected by Russia in 1993 (Hollister, 1994a). Otherwise, activity concentrations of Sr-90, Cs-137, Pu-238, Pu-239,240 and Am-241 in seawater and sediment samples collected by Soviet and Russian investigations between 1989 and 1995 from the area around Komsomolets did not indicate any obvious signs of releases from the submarine (Hollister, 1994a; Stepanov et al., 1999; Astakhov et al., 2000). However, above background activity concentrations of Sr-90 and Cs-137 were reported in some samples of benthic fauna collected close to Komsomolets in 1994, although not for any other year (Kuznetsov et al., 1996, 1999). Additionally, Co-60 was reported to have been detected in 3 samples of echinoderms (3.5 to 27 Bq/kg) collected close to the Komsomolets in 1993 (Kuznetsov et al., 1999). Plutonium activity concentrations and atom ratios in seawater sampled in the torpedo compartment and in sediments sampled close to Komsomolets in 1994 and 1995 were reported to be comparable to background measurements (Stepanov et al., 1999; Astakhov et al., 2000).

1.2.2 Overview of Norwegian monitoring

Norway has carried out monitoring of the marine environment in the area around Komsomolets annually since 1990. Figure 1.7 shows the outline of the submarine on the seafloor as observed in 1991 using the echo sounder from the Norwegian R.V. “Johan Hjort”. In surface sediments collected in the years 1991 to 1994 by Russia, but analysed by Norway, Cs-134 was detected (0.3 to 2.2 Bq/kg d.w.), while elevated activity concentrations of Cs-137 in bottom seawater were reported between 1991 (30 Bq/m^3) and 1993 (8 Bq/m^3) (Bøhmer & Berthelsen, 1992; Blindheim et al., 1994; Kolstad, 1995). However, since then neither Cs-134 nor any increased activity concentrations of radionuclides above values typical for the Norwegian

Sea have been observed in any environmental sample collected by Norway when sampling from surface vessels (e.g., Gwynn et al., 2018). Since 2013, Norwegian monitoring has been carried out using an acoustic transponder on the sampling gear that allows samples to be collected at precise locations, approximately 20 m from the hull of Komsomolets. Without the use of an acoustic transponder it is not possible to know the exact position of the sampling gear when the samples (seawater or sediment) are collected, or how the position of the samples collected relates to the actual location of the submarine. Even with the use of an acoustic transponder, there is still a need to maintain a safe operating distance from Komsomolets in order to avoid the possibility of fouling the sampling gear on the submarine.

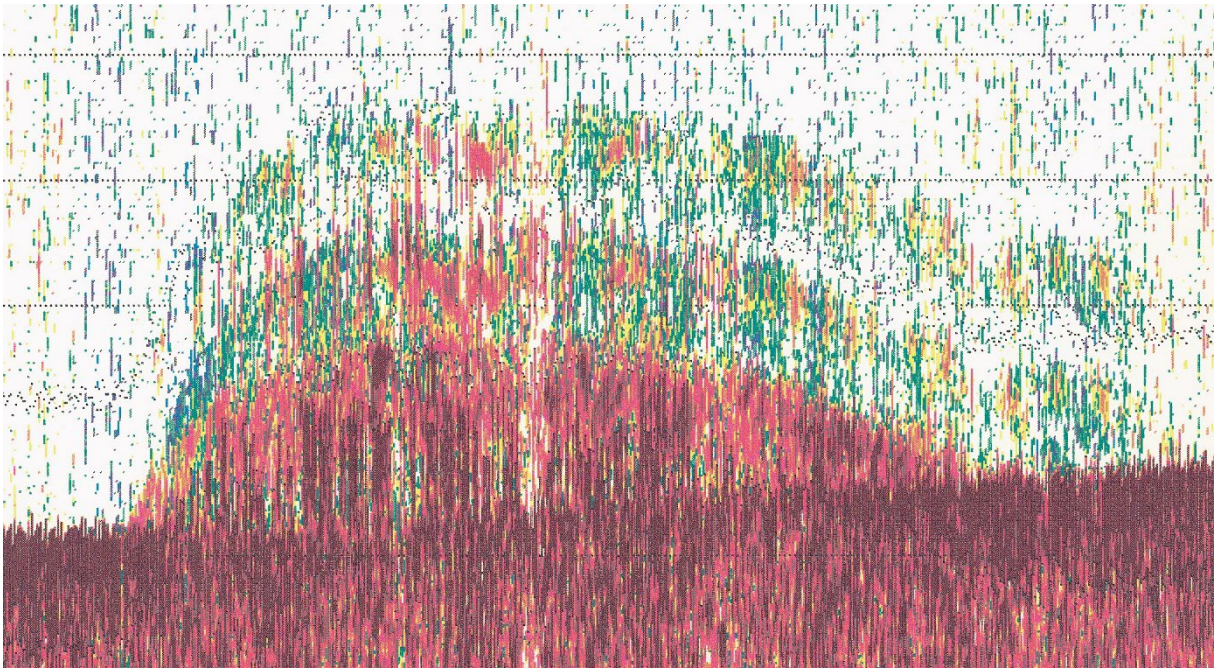

Figure 1.7. Echogram of the sunken nuclear submarine Komsomolets taken from the R.V. "Johan Hjort" in 1991 (Image: IMR).

1.2.3 Other monitoring of Komsomolets

British and German research cruises collected samples of sediment and seawater in the area around Komsomolets in 1989 and 1995, respectively. Activity concentrations of Sr-90, Cs-137, Pu-238, Pu-239,240 and Am-241 in such samples did not indicate any releases from the submarine (Camplin & Read, 1992; Grøttheim, 1999; Nies et al., 1999a, 1999b; Nies et al. unpublished).

1.3 The oceanographic setting of the sunken nuclear submarine Komsomolets

1.3.1 Bathymetry

As mentioned previously, Komsomolets sank to a depth of 1680 m south southwest of Bear Island. The bathymetric setting of Komsomolets has been described as reasonably flat in the immediate area around the submarine (Hollister, 1992). On a larger spatial scale (Figure 1.8), the submarine has been described as lying on a ledge over a submarine canyon that descends to depths deeper than 3000 m (Hollister, 1992).

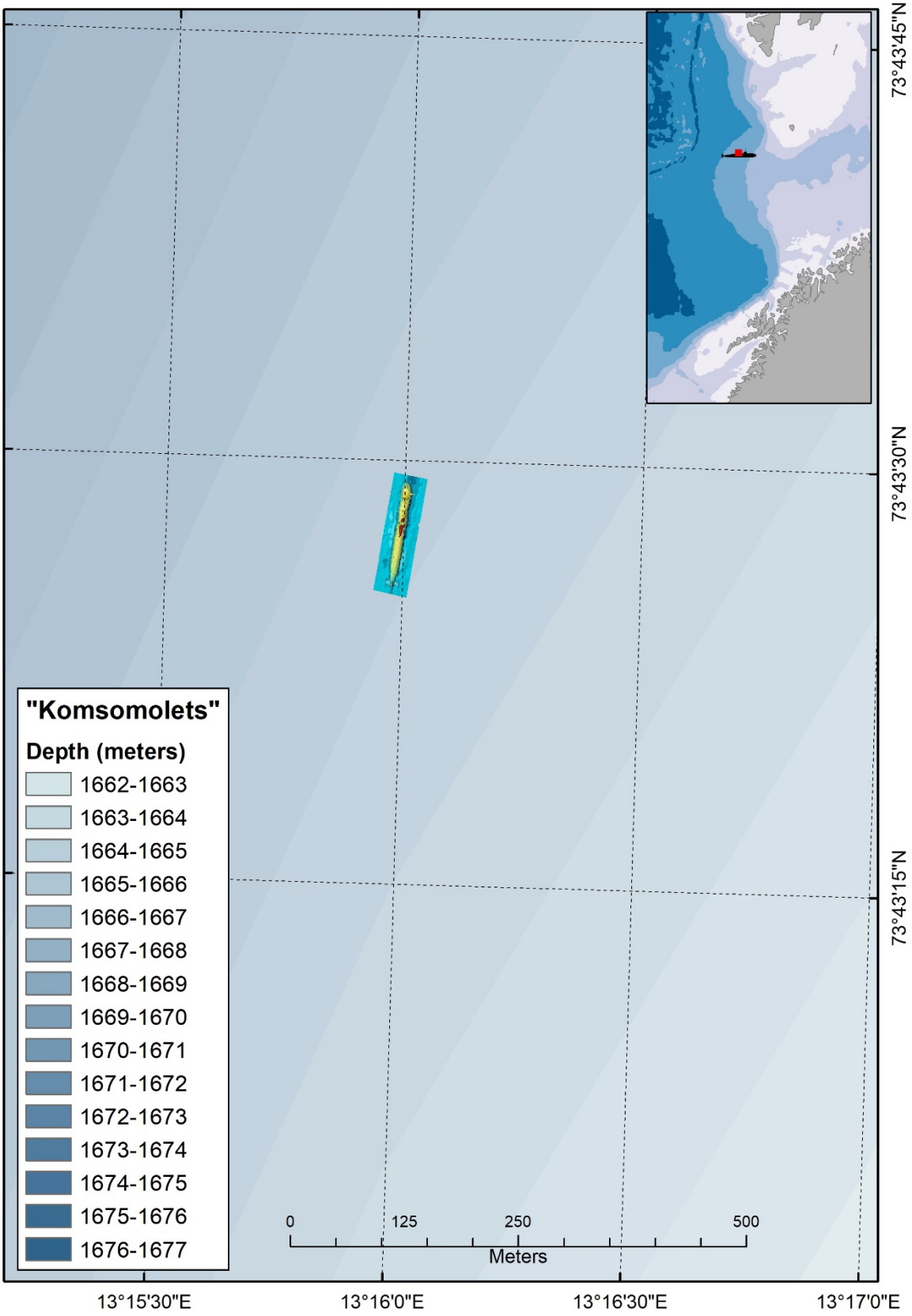

Figure 1.8. Bathymetry of seafloor in the region around the sunken nuclear submarine Komsomolets

1.3.2 Hydrography and currents

The Instititute for Marine Research routinely carries out a hydrographic transect that runs westward from Bear Island several times each year and is located about 90 km north of the position where Komsomolets lies on the seafloor (Kjell Arne Mork pers. comm.). Figure 1.6 shows the temperature, salinity, and density distributions from this section from May/June 2019. Atlantic Water (salinity >35‰) occupies the upper 500 m with temperatures above 3°C. Below the Atlantic Water in the intermediate and deep layers, the salinity does not vary much, but the temperature shows a decrease for the deeper layers. Of particular note, the water layer deeper than circa 1500 m depth is nearly homogenous (Figure 1.9).

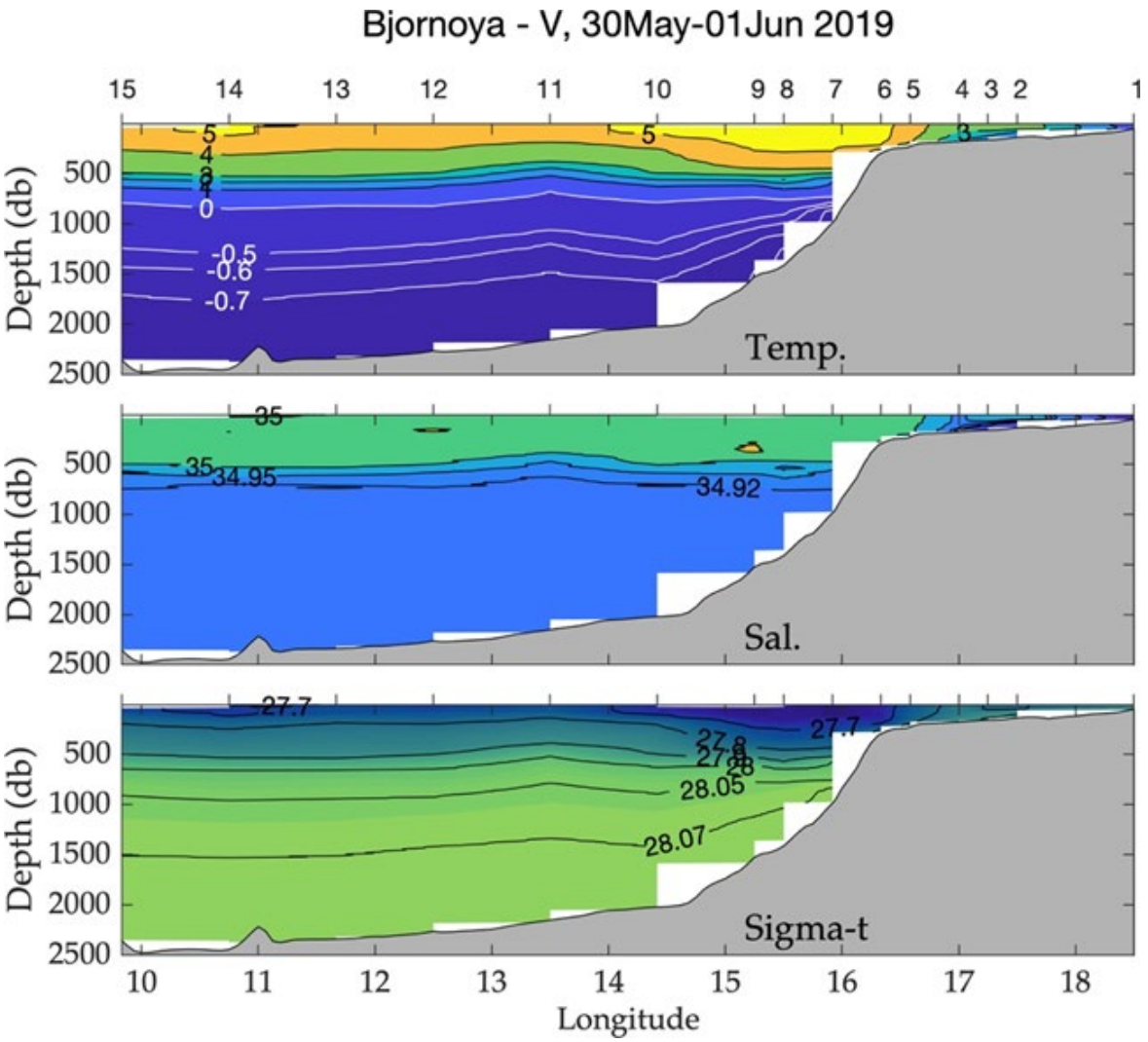

Figure 1.9. Temperature (°C), salinity (‰), density (sigma-theta; kg/m^3) distributions in the Bear Island-West section during 30 May – 1 June 2019.

In terms of surface water currents (Figure 1.10), the Norwegian Atlantic Current (NwAC) transports relative warm and saline water northwards in the upper layer. The NwAC splits into two branches at the entrance of the Barents Sea opening, where one branch flows eastwards into the Barents Sea while another branch flows northward, passing the location where Komsomolets lies, to become the West Spitsbergen Current which eventually transports water into the Central Arctic Ocean along the shelf edge North of Svalbard.

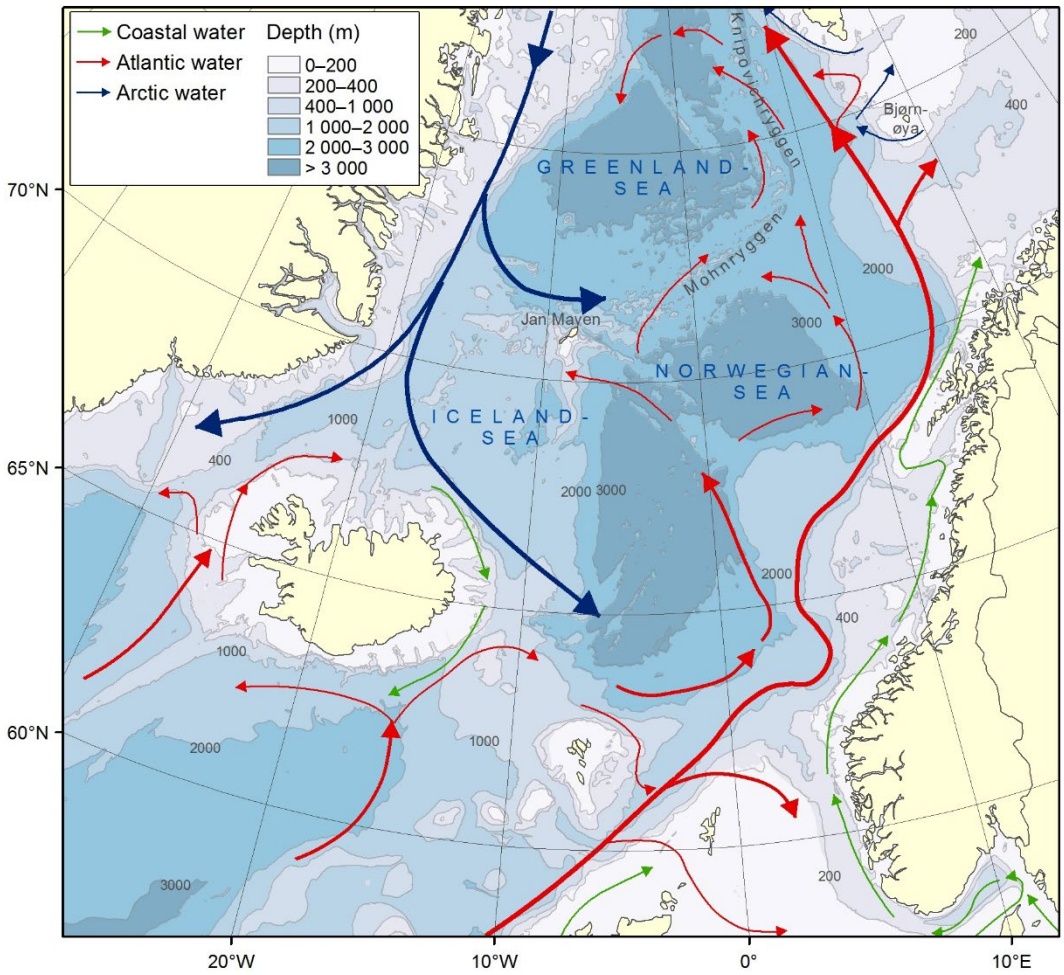

Figure 1.10. Schematic view of the main surface currents in the region around the location of the sunken nuclear submarine Komsomolets (Image: IMR).

There exist only a few direct measurements of the deep currents in the region where Komsomolets lies on the seafloor. In 1993, a mooring with 4 current meters were deployed nearby (73º 43.19´N, 13º15.60´E) between May and August 1993. The current meters were placed at depths of 167, 667, 1567 and 1642 m over a bottom depth of 1697 m, but the upper instruments were lost due to fishing activity. Measurements from the other instruments showed a strong barotropic component (i.e. the current was constant with depth) with alternating pulses along the slope (Blindheim et al., 1994). The dominant tidal component was the semidiurnal period and its amplitude decreased with depth, from about 10-15 cm/s at 667 m to less than 5 cm/s at 1642 m depth. The maximum measured velocity was found at the deepest instrument with a speed of 34.2 cm/s that flowed towards the southwest.

Between May and November 2001, another mooring with current meters was deployed south of Komsomolets' position. This mooring was deployed at depth of 1500 m with current meters at 790 m and 1290 m depths. The velocity and direction time series of currents registered by the deepest current meter where the semidiurnal and diurnal tidal currents are filtered out is shown in Figure 1.11.

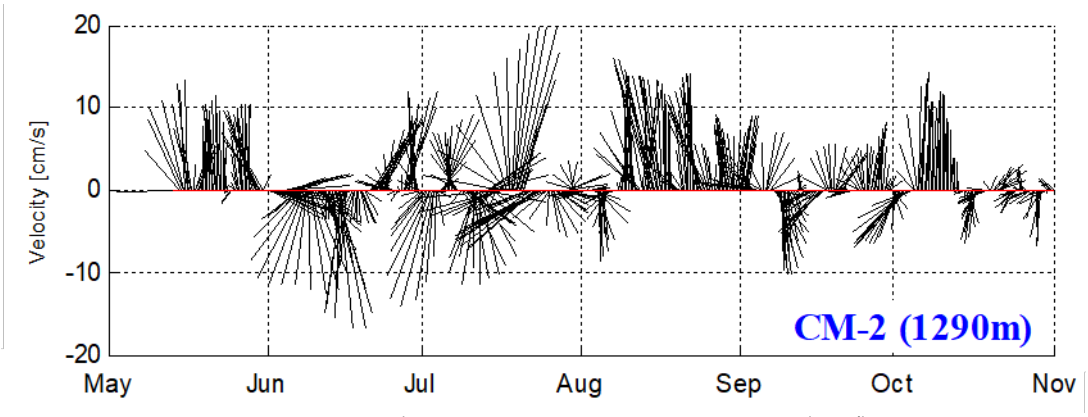

Figure 1.11. Stick plots of low pass filtered (Butterworth filter with cut-off frequency=1/26 h^{-1}) current vectors. 6 h values are plotted. Positive value indicates northward current (Mork & Søiland pers. comm.).

In the observed time series (Mork & Søiland pers. comm.), the current direction was seen to switch between northward and southward, but with an overall dominant northward direction. The maximum speed of the filtered data was 20 cm/s. In August, there was a persistent northward flow with speed of about 10 cm/s that lasted for about one month. The results from the upper current meter were similar supporting the previous observation in 1993 that currents are constant with depth. The dominant tidal component was at the semidiurnal period, and the tidal current at this location has a tendency of clockwise ellipse rotation with major and minor axis speeds of 4.5 cm/s and 2.2 cm/s.

Russian investigations reported velocities of 20 to 30 cm/s at 10 to 20 m above the seafloor during a 15 day record in 1989, with a mean flow toward the north and northeast and maximum velocities of 3.5 cm/s 20 cm above the bottom over a period of 5 days in 1993 (Hollister, 1994b).

1.3.3 Sedimentation

It has been reported that the bottom 400 m of the water column in the area around Komsomolets are associated with a nepheloid layer of high turbidity formed by the resuspension of bottom sediments (Lukashin et al., 1996, 1998; Lukashin, 2008;). Other observations suggest that this nepheloid layer begins about 200 m from the seafloor with a turbidity maximum around 40 m from the bottom (Hollister, 1994b). Water samples collected from this layer in 1993 contained between 1 and 10 mg/l of suspended sediment (Hollister, 1994b). Chemical analysis of sediment collected in sediment traps in the area, showed that concentrations of biogenic elements (e.g., C and P) were higher above the nepheloid layer, whereas the nepheloid layer itself is enriched in terregenous material that includes lithogenic elements (Si and Al) and hydroxides of Fe and Mn (Lukashin, 2008). The supply of sediment to water depths above and below the nepheloid layer has been shown to vary, with a marked increase in fluxes above the nepheloid layer in the autumn due to an increased supply of calcium carbonate material (Lukashin et al., 1996). Below the nepheloid layer, the flux of terrigenous material varied over the course of the 12 months when samples were collected from 16 to 145 mg/m^2, with the maximum value ascribed to a possible suspension stream formed upslope from the location of Komsomolets (Lukashin et al., 1996). Grain size distribution analyses of the top 1 cm of four sediment cores collected within ~20 m of the hull and at a reference site 100 m upstream from the submarine in 2013, showed that fine silt (average 57%) and clay (average 20%) were the dominant fractions (Flo, 2014).

In terms of sedimentation rates, Pb-210 dating of 2 sediment cores sampled by Norwegian monitoring in 2012 determined that sedimentation rates from these cores were of the order of 0.08 to 0.10 cm/a (Gwynn et al., 2018). This would imply that the year that Komsomolets sank (i.e. 1989) would correspond to

a sediment depth of 2 to 3 cm (Gwynn et al., 2018). Based on the distribution of Pb-210 in the uppermost layers of these cores, there was no indication of mixing in the surface sediments of these cores. The sedimentation rates reported by Gwynn et al. (2018) are in good agreemented with other reported sedimentation rates for other sediment cores sampled near or in the area around Komsomolets with a range from 0.074 to 0.12 cm/a (Hollister, 1994b; Grøttheim, 1999). However, a somewhat higher sedimentation rate of 0.26 cm/a derived from a core sampled in the area around Komsomolets in 1999 has also been reported (Heldal et al., 2002).

1.4 Other sources of radioactive contamination to the Norwegian Sea

The following main sources of radioactive contamination continue to contribute to levels of anthropogenic radionuclides in the Norwegian Sea:

- → Global fallout from atmospheric nuclear weapon testing in the 1950s and 1960s
- → Long range oceanic transport of radionuclides discharged from European reprocessing plants at Sellafield (UK) and Cap la Hague (France)
- → Long range oceanic transport of Chernobyl fallout
- → The re-entry of the SNAP-9A satellite in 1964

1.5 The 2019 Norwegian research cruise to the site of the sunken nuclear submarine Komsomolets in the Norwegian Sea.

The aim of the 2019 Norwegian research cruise was to investigate the radioecological and visual status of the sunken nuclear submarine Komsomolets in the Norwegian Sea, and provide up-to date information about any potential releases and the levels of radioactive pollution in the marine environment around the submarine that may have arisen from such releases from the reactor and the 2 nuclear warheads in the torpedo compartment. This was to be achieved through the use of a remotely operated vehicle (ROV) that would enable the collection of samples of seawater, sediment and biota far closer to the submarine than possible when using sampling gear lowered from surface ships.

2 Sampling methodologies

All sampling work was conducted onboard the R.V. “G.O. Sars” of the Institute of Marine Research between the 7th and 9th of July 2019. The ROV Ægir 6000 (Fig. 2.1) was used to conduct sonar and video surveys as well as to collect seawater, sediment and biota samples over the course of 4 dives. Independently of the ROV, large volume surface and bottom water samples were also collected.

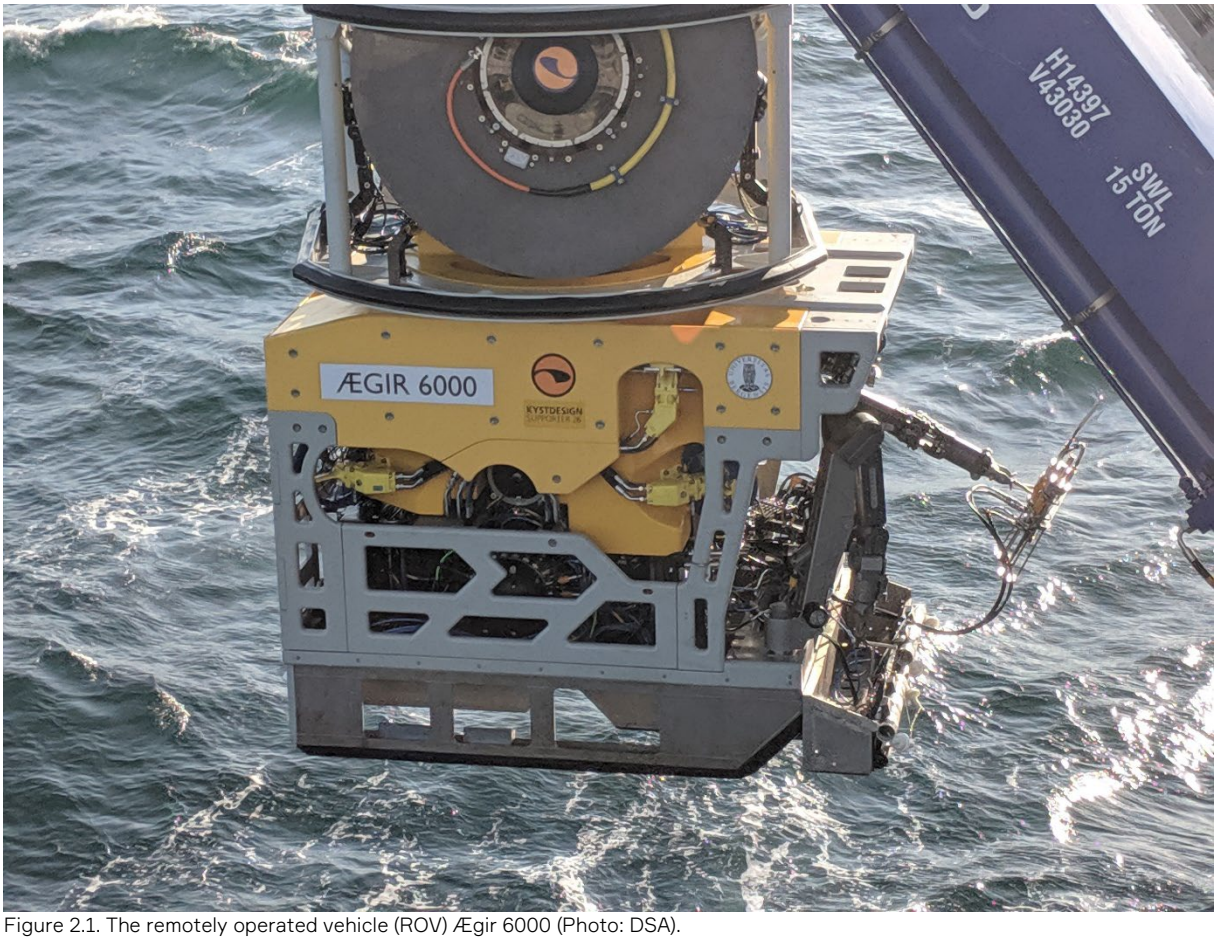

Figure 2.1. The remotely operated vehicle (ROV) Ægir 6000 (Photo: DSA).

2.1 Sonar and video surveys

After locating Komsomolets on the seafloor at the beginning of the 1st dive with the ROV an initial video survey of the submarine was carried out. Further video surveys were carried out over the course of all 4 dives with the ROV. Following the initial video survey, a high-resolution side scan sonar survey of the submarine was carried out using a Multibeam Kongsberg EM2040 unit mounted underneath the ROV.

2.2 Seawater sampling and processing onboard

Seawater samples were collected from the surface using the seawater intake supply onboard the research vessel. Large volume bottom water samples were collected using a water sampling array equipped with twelve 10 l Niskin bottles and conductivity, temperature and depth (CTD) instrumentation. For the collection of these samples, the water sampling array was lowered and then positioned accordingly using the ROV. Large volume bottom water samples were taken approximately 3 m over the ventilation pipe and

beside the torpedo compartment (port side) at two different locations (Fig 2.2). Smaller volume water samples were collected directly by the ROV, using three 1 l syringe samplers and two 2 l Niskin bottles. These samples were collected directly from or close to the ventilation pipe, at various heights above the ventilation pipe and at a distance of approximately 1 m from either side of the reactor compartment (Fig. 2.3). Samples collected directly from the ventilation pipe were taken from a depth of around 20 to 30 cm inside the ventilation pipe.

For the surface seawater samples, 75 l and 50 l were filtered through 1 µm filters for Cs-137 and Sr-90, respectively. Samples for Cs-137 and Sr-90 were collected in 25 l plastic cans, with the Sr-90 sample acidified to pH 2 with concentrated HCl. For Pu-239 and Pu-240, 40 l samples were filtered either through 0.45 µm membrane filters (Millipore) or Pall hollow fibre cartridges of 10 kDa nominal cut-off. The hollow fibres were carefully washed between each sample with 0.1 M NaOH, 0.1 M HNO_3 and MilliQ water prior to pre-conditioning with sample water prior to sample collection. The filtered samples were acidified to pH 2 using ultrapure HCl followed by the addition of a Pu-242 yield tracer. Further small volume samples (50 ml) were collected for trace element analysis, which were then filtered through either 0.45 µm membrane filters (Millipore) or Pall hollow fibre cartridges of 10 kDa nominal cut-off.

The large volume bottom sample collected over the ventilation pipe consisted of water collected from two separate casts of the water sampler. Water collected from these two casts was pooled before sub-samples were taken for different analyses. From this sample, volumes of 75 l and 50 l were taken for Cs-137 and Sr-90, respectively, and filtered through 1 µm filters. Samples for Cs-137 and Sr-90 were collected in 25l plastic cans, with the Sr-90 sample acidified to pH 2 with concentrated HCl. Further 40 l samples were taken to determine Pu-239 and Pu-240 in <0.45 µm and <10 kDa fractions as described above, as was the case for additional 50 ml samples for trace elements.

The large volume bottom samples that were collected beside the torpedo compartment at two different locations was carried out using just one cast of the water sampler, with half of the Niskin bottles on the water sampler used at one location and the other half at the second location. From each of these samples 40 l was taken to determine Pu-239 and Pu-240 and filtered through 0.45 µm membrane filters (Millipore), as was the case for 50 ml samples for trace elements.

For the small volume samples taken directly by the ROV using syringe samplers and Niskin bottles, these samples were transferred to plastic bottles and then were analysed for gamma emitters directly onboard using a NaI detector before further treatment. One sample (collected above a metal grill next to the ventilation pipe) was filtered through a 0.45 µm filter and reanalysed onboard, but otherwise the samples were stored at 5°C.

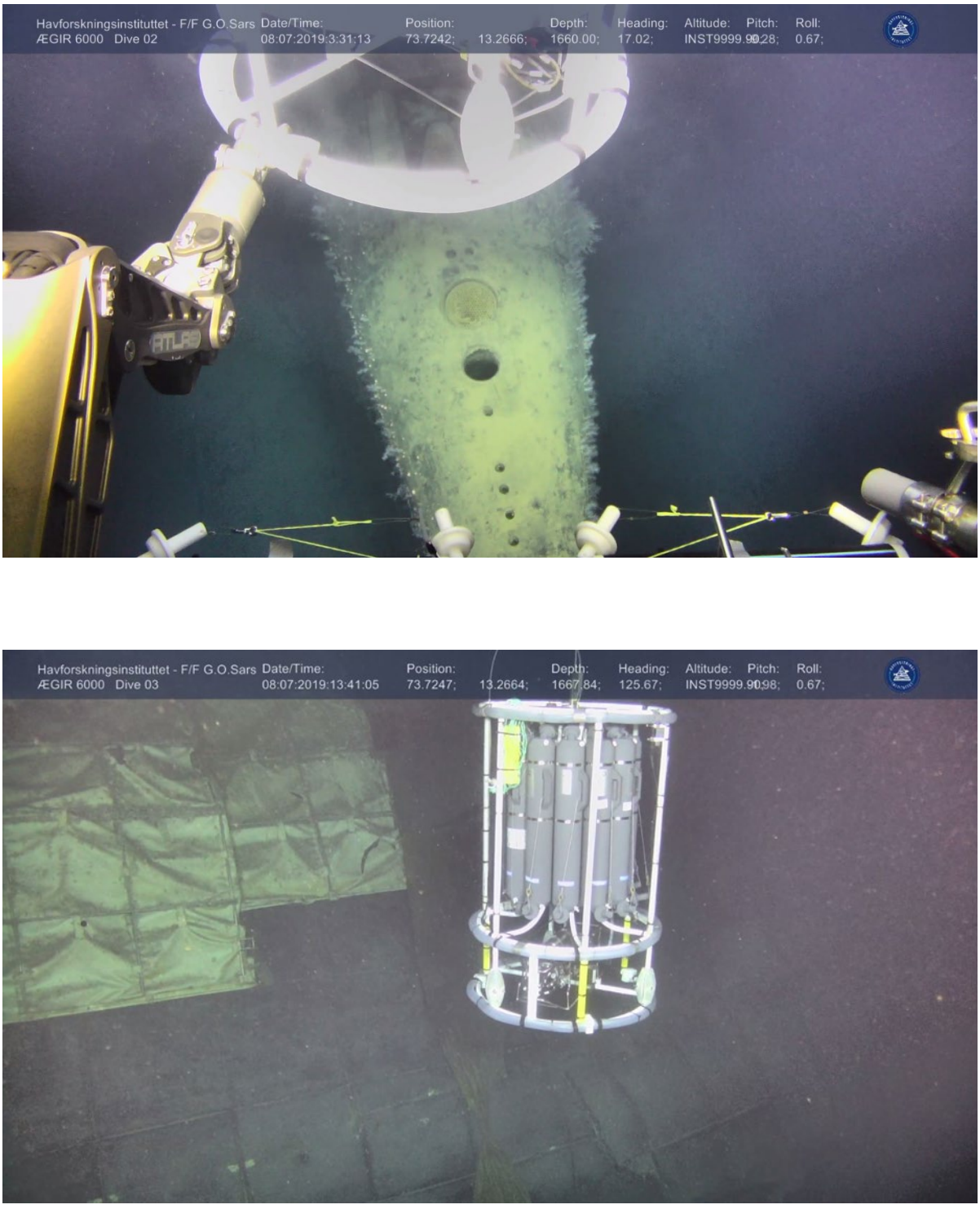

Figure 2.2. Large volume samples collected around 3 m directly over the ventilation pipe (upper photo) and next to the opening in torpedo compartment on the port side of the submarine (lower photo) (Photos: IMR).

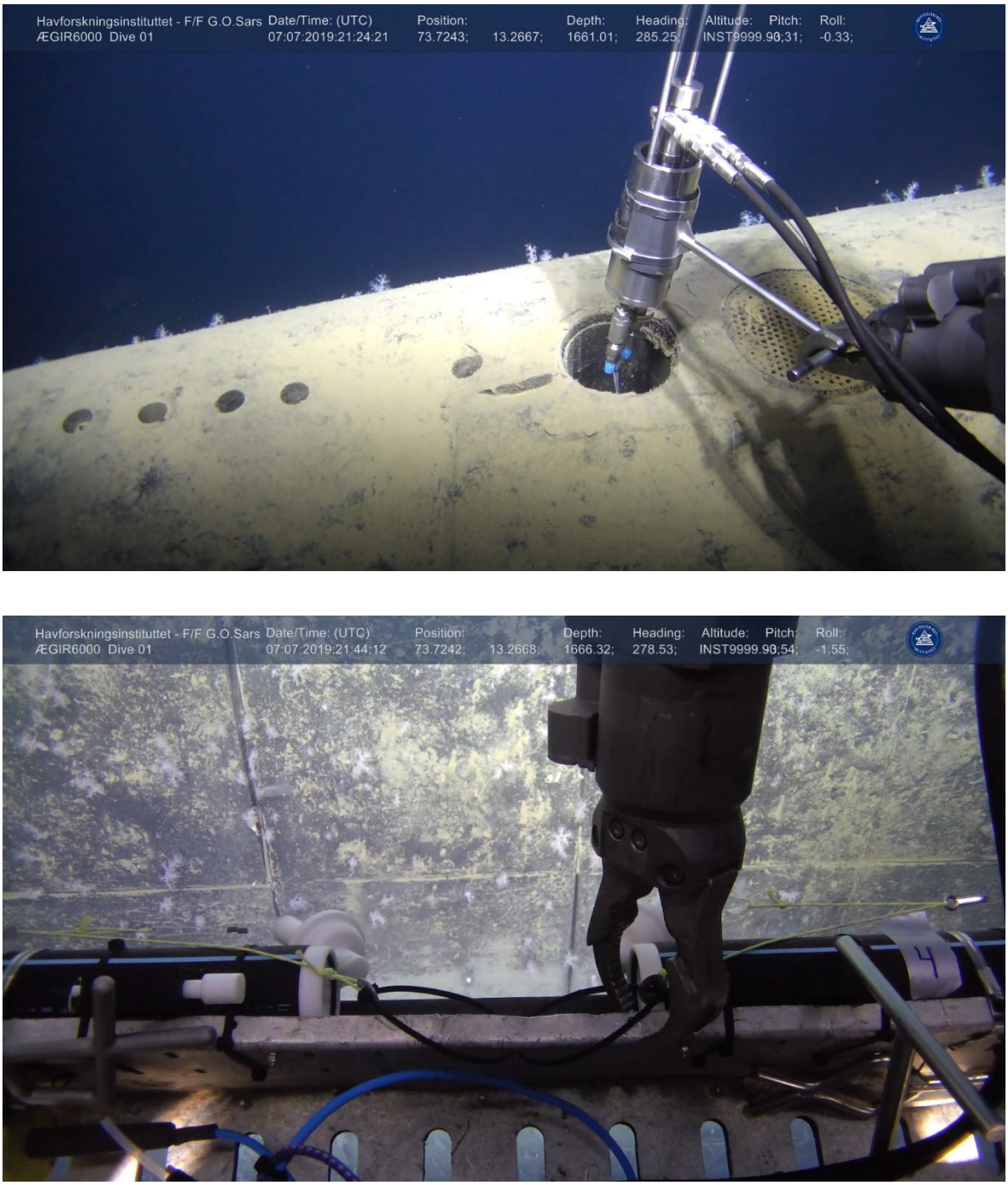

Figure 2.3. Syringe sample collected directly from the ventilation pipe (upper photo) and Niskin bottle sample collected next to reactor compartment (lower photo) (Photos: IMR).

2.3 Sediment sampling and processing onboard

Sediment samples were taken at various locations around the submarine (Fig. 2.4) using either push cores or blade cores (Fig. 2.5 a and b). Push and blade cores with sediment samples were returned to the surface using an auxiliary basket (Fig. 2.6) to allow the ROV to continue operations without surfacing. Onboard, all push core tubes were sealed and then frozen. Surface sediment samples (0 to 2 cm) were taken from blade cores collected from the port and starboard sides of the reactor compartment for screening purposes directly onboard using a NaI detector.

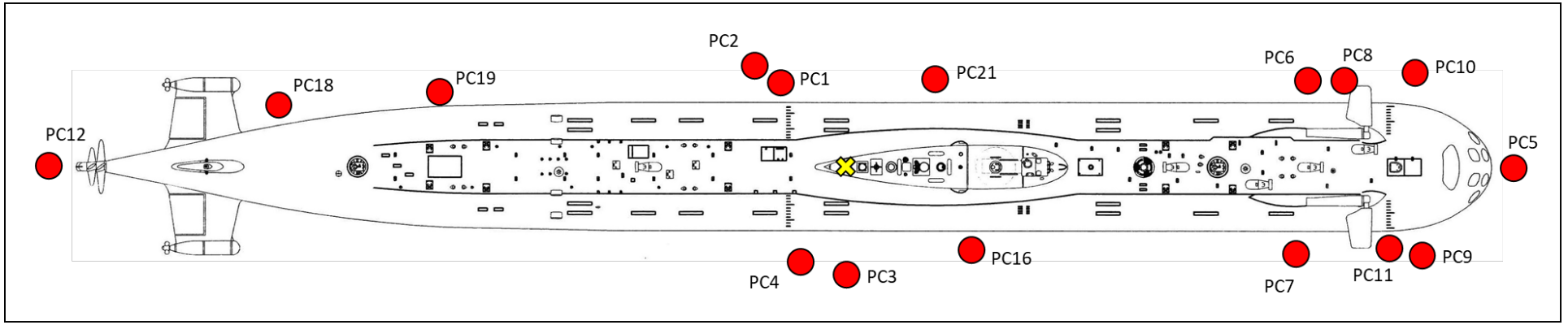

Figure 2.4. Location of successful push cores taken around the hull of Komsomolets in 2019. Samples were lost from 6 push cores and the position of these failed push cores are not shown. The prevailing current direction flows along the submarine from the stern to the bow. Location of the ventilation pipe and metal grill is indicated by the yellow cross.

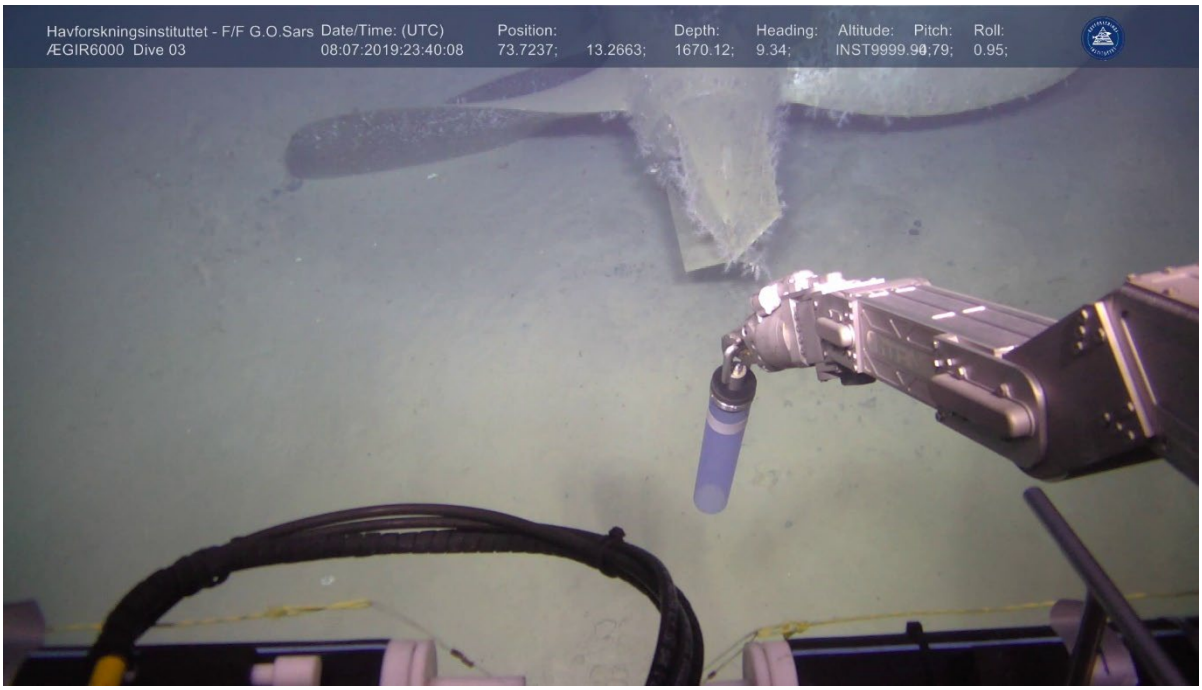

Figure 2.5. Push core being taken next to main propeller (Photos: IMR).

Figure 2.6. Auxiliary basket used in conjunction with the ROV to return sediment samples to the surface (Photo: IMR).

2.4 Biota sampling

Biota samples were collected from hull surface below the ventilation pipe and from both the port and starboard sides. One biota sample was collected directly from the seafloor and next to the hull of the submarine. Samples were collected using either the manipulator arm or a vacuum sampler (Fig. 2.7). Onboard, biota collected were roughly sorted into similar types and then frozen.

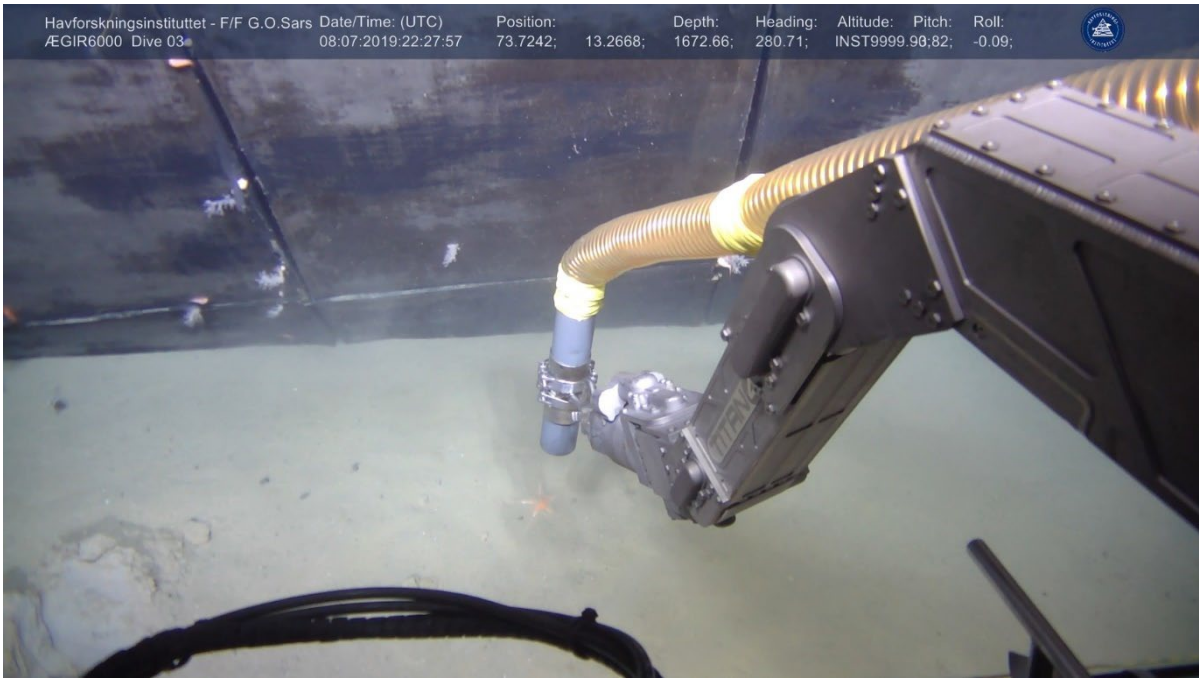

Figure 2.7. Biota sample on hull surface collected using ROV's manipulator arm (upper photo) and biota sample on seafloor collected using ROV's vacuum sampler (lower photo) (Photos: IMR).

3 Analytical methodologies

3.1 Analysis onshore

3.1.1 Determination of gamma emitters

In the laboratory, biota samples were further sorted by taxonomy for identification purposes and to ensure that pooled samples contained only the same species. All sediment and biota samples were freeze dried and homogenised before being packed into standard plastic counting geometries and counted on high-resolution gamma spectrometers (HPGe). Spectra were typically collected for periods of between 1 and 4 days.

For the analysis of Cs-137 in large volume water samples, all samples were acidified with HNO_3 to pH 2 with the addition of Cs-134 as a yield tracer. Cesium was precipitated using ammonium phosphomolybdate (AMP; $(NH_4)_3PMo_{12}O_{40}$). The AMP precipitate was transferred to 200 ml sample geometries and dissolved in 6M NaOH, before counting on a HPGe detector.

For the gamma spectrometry analysis of small volume water samples, all samples were filtered using 0.45 µm filters before they were transferred to 200 ml plastic containers and directly counted on a HPGe detector. To improve the detection limits for Cs-137, selected small volume water samples were precipitated with AMP as described above with the exception that the precipitate was packed into small counting geometries before counting on a HPGe detector. All 0.45 µm filters from the small volume water samples were also counted on a HPGe detector. Filters were not dried prior to gamma spectroscopy analysis or any further determination of Pu-239, Pu-240 and U-236, with the exception of one filter that was air dried following gamma spectroscopy analysis prior to screening with autoradiography (see section 3.1.5).

3.1.2 Determination of Sr-90

Strontium-90 in large volume water samples was determined using a method based on Harvey et al. (1989). Briefly, samples were acidified with 1ml/l of 12M HCl and then filtered to remove particulate material. Filtrates were weighed and then a known amount of Sr-85 yield tracer added. Mixed calcium and strontium oxalate precipitates were formed at pH 4 and these were separated from the bulk sample by decanting and centrifugation. The precipitate was dissolved and repeated nitrate precipitations were performed until the excess calcium was removed. Further small-scale purification was achieved by sequential coprecipitation with barium chromate (for the removal of barium, lead and radium), ferric hydroxide (for the removal of actinides, yttrium and radium daughters) and strontium carbonate (for the removal of chromate ions), before a final nitrate precipitation to remove ingrown Y-90.

Samples were then gamma well counted for chemical recovery of the Sr-85 yield tracer. The typical recovery yield for this analysis is greater than 90%. The Y-90 daughter was allowed to grow in for a minimum of 3 weeks before a further ferric hydroxide coprecipitation was performed and the unsupported Y-90 in the dried precipitate was counted on a Berthold LB7700 low background Gas Flow Proportional Counter. Each analytical batch also included a reagent ‘blank’ sample an internal Quality Control sample and a tracer purity check sample.

Strontium-90 in small volume water samples was determined by a propriety methodology using ion exchange purification. The volumes analysed for Sr-90 were determined on the basis of the results obtained for Cs-137 from the same samples and varied between 1 and 100 ml. Prior to loading on ion-exchange resin, Sr-85 was added to all samples as a yield monitor before the water samples were evaporated to dryness and ashed. Purified Sr fractions were stored for two to three weeks to allow equilibrium between Sr-90 and Y-90. The Y-90 was separated from the Sr-90 by hydroxide precipitation using NH_3 and resulting precipitate removed by filtering. Saturated oxalic acid was added to the supernatant and Y precipitated using NH_3. The Y precipitate was collected on filters before all samples were counted using a Risø low-level beta GM multicounter for between 4 and 7 days. After counting, filters were ashed and the Y yield determined using EDTA titration.

3.1.3 Determination of Pu-239, Pu-240 and U-236

The initial steps for sample treatment differed, according to the sample type (i.e., seawater, filter, biota or sediment). Where samples were analysed for Pu-239, Pu-240 and U-236, Pu-242 and U-233 tracers (NPL, UK) were added to the samples to monitor recovery. Ultrapure nitric, hydrochloric and hydrofluoric acids used for sample dissolution and for further analytical steps were prepared by sub-boiling distillation. All glassware used was pretreated by acid-washing with a 35% nitric acid/3% hydrofluoric acid/2% Decon-90 (Campion, 1975). Prepacked anion exchange resin (AG) and extraction chromatography resins (UTEVA) were used to effect separation and purification. After target preparation, the samples were shipped to the Australian National University (ANU) in Canberra for measurement by accelerator mass spectrometry (AMS).

Seawater samples were treated according to the methodology published by Lopez-Lora et al (2018), and which included oxidation state adjustment and co-precipitation of plutonium and uranium on iron hydroxide. Precipitated iron hydroxide was recovered by filtration before redissolution in 8 M nitric acid. Biota samples (1 to 5 g) were placed in PTFE containers and heated in the presence of concentrated nitric acid (25 ml) to oxidise organic matter, before dissolution of the remaining material using an Ultraclave system at approximately 250°C and 50 bar. Following dissolution, plutonium and uranium were co-precipitated on iron hydroxide, and recovered by centrifuging at 4000 rpm before redissolution in 15 ml of 8 M nitric acid. Sediment samples also required oxidation to destroy residual organic matter and dissolution to break down silica, but this process is complicated by the presence of calcium which forms insoluble CaF_2 with hydrofluoric acid.

Sediment samples (5 g) were placed in PTFE containers with nitric acid (30 ml) and hydrofluoric acid (30 ml) and dissolved using an Ultraclave system at approximately 250°C and 50 bar. Any CaF_2 precipitate was removed by centrifugation and thoroughly washed with nitric acid. The remaining solution and added washes were reduced in volume by evaporation at approximately 120 to 150°C, before co-precipitation of plutonium and uranium on iron hydroxide. Precipitated iron hydroxide was recovered by filtration before redissolution in 15 ml of 8 M nitric acid.

Biota and filter samples were treated similarly, given that both matrices are largely organic material. Prior to dissolution in the Ultraclave system, both matrices were pretreated by oxidation of the organic matter with concentrated nitric acid at ~120-150°C in the PTFE vessels used in the Ultraclave system; the treatment was repeated until the volume of material had decreased significantly and fewer NO_2 fumes were observed on heating. The digested material was then dissolved in the Ultraclave system as before. Except for the filter screened by autoradiography, entire filters were digested. For the filter that was screened by autoradiography, only part of the filter was digested with the remaining part kept for other analyses. Gamma spectrometry analysis of the remaining part of the filter showed that most of the Cs-137

(96%) and Am-241 (subsequent result was below the detection limit) activity was contained within the part of the filter that was digested.

Following the different initial treatment of seawater, filter, biota and sediment samples as described above, all 8 M nitric acid sample solutions were then processed in the same manner using anion extraction chromatography columns that had been pre-treated with 8 M nitric acid. All 8 M nitric acid sample solutions were first oxidised with 1 ml 3 M sodium nitrite solution, before loading on to an AG anion exchange resin that retains plutonium, followed by further washings of 8 M nitric acid. The eluate (sample and washings) from each AG column was passed directly through a UTEVA column which retains uranium. The eluate from each UTEVA column was discarded. Each AG column was washed with 9 M hydrochloric acid, before plutonium was eluted with a mixture of 9 M hydrochloric acid containing 1% hydroiodic acid. Eluates were then evaporated to dryness at approximately 120 to 150°C for at least three times with 5ml concentrated nitric acid to remove all iodide and chloride ions. Each UTEVA column was washed with 8 M nitric acid, before uranium was eluted with 0.1 M nitric acid. Any residual uranium was eluted with 18 MΩ water. Combined eluates from each sample were then evaporated to dryness at approximately 120 to 150°C for at least three times with 5ml concentrated nitric acid to remove all chloride ions. AMS target material from separated plutonium and uranium solutions were prepared by adding approximately 2.5 mg of iron in the form of a 10 mg/g iron (III) nitrate solution before the solution was slowly evaporated to dryness in a 5 ml glass vial at approximately 120 to 150°C. When dry, the vials were placed in a muffle furnace and heated to approximately 600°C for 10 hours. After cooling, the iron oxide matrix was transferred to a clean vial, for subsequent analysis by AMS.

Plutonium and uranium isotopic ratios and concentrations were determined by AMS using a 14UD Pelletron accelerator at the Australian National University based on the original methods described in Fifield (2008), Fifield et al. (2010, 2013), Srncik et al. (2014) and Kuwae et al. (2023) but modified as indicated below. The AMS measuring technique used involves extraction of molecular PuO- (UO-) ions from a Cs sputter ion source. The ions are accelerated to ~105 keV and mass-selected by an 83 cm radius injection magnet with a resolution M/DM =300, and then transported towards the positive terminal of the tandem accelerator. The PuO^- molecules are then dissociated in a low-pressure gas stripper, and electrons are removed from the Pu to form positive Pu ions which are further accelerated away from the positive terminal of the tandem accelerator. Pu^{5+} ions are selected by an analysing magnet and passed through a velocity filter (Wien filter) before reaching the gas-ionisation detector. The detector identifies and counts the Pu ions. Switching between different target isotopes is achieved by changing the pre-injection mass-analysing magnet, the terminal voltage of the accelerator, and the Wien filter.

Accelerator mass spectrometry (AMS) has a high level of suppression against U interference. Any uranium-containing molecular ions that are injected into the accelerator along with PuO^- are dissociated in the gas stripper in the high voltage terminal. The mass difference between the uranium and plutonium atomic ions then ensures that the uranium ions are rejected by the post-acceleration analysing magnet. The different isotopes of uranium – U-233 (yield monitor), U-234, U-235 U-236 and U-238 – and plutonium – Pu-239, Pu-240 and Pu-242 (yield monitor) – were counted sequentially for varying count times, depending on the observed count rate.

In the case of plutonium measurements, a Trek 10/40A-HS high voltage amplifier was used to “bounce” the accelerating voltage so that beams of Pu-242, Pu-240 and Pu-239 O^- ions with the same magnetic rigidity are sequentially injected into the magnet. The selected PuO^- ions were then focussed and injected into the 14UD accelerator, which is operated at ~4 MV. A low-pressure gas stripper in the high-voltage terminal at the centre of the accelerator dissociates the ~4 MeV molecular ions and removes outer electrons from the Pu atoms. The positively charged atoms are then re-accelerated and Pu^{5+} ions of energy ~24 MeV were selected by the high-energy analysing magnet. The strength of the focussing lens,

and the terminal voltage of the accelerator, are also “bounced” so that Pu isotopes enter the analysing magnet with equivalent magnetic rigidities.

Relative count rates for each isotope were determined using a propane-filled ionisation chamber. The signal from the detector is recorded with a PIXIE-4 digital pulse processor (XIA LLC) interfaced to a custom version of the NEC AccelNET control system. This provides reference voltages that control the Trek amplifier, focussing lens, accelerator terminal potential and the electric field of the Wien filter (located downstream of the analysing magnet) to coordinate isotope sequencing. The switching time between isotopes is 1.5 s. Measurement times were typically 2.5 s for Pu-242, 15 s for Pu-240 and 10 s for Pu-239, with at least 25 cycles of the sequence, and concluding with a Pu-242 measurement, made for each sample. Reproducibility was checked using a reference material (Dittmann et al. 2019) with accurately known Pu isotopic ratios measured periodically. The reproducibility of this standard over the course of the sample measurements was better than 4% and the Pu detection limit for the system was ~10^5 atoms (Fifield et al., 2010).

Uranium samples were measured using a time-of-flight detector with a 6 m flight path (Fifield et al., 2013). Measurement times for uranium were typically 60 s for U-233, and 300 s for U-236, with at least two cycles of the sequence, and concluding with a U-233 measurement. The reproducibility of uranium measurements was determined to be 7% using the Vienna-KkU standard (Steier et al., 2008).

Atom concentrations of Pu-239, Pu-240 and U-236 were deduced from the known masses of the Pu-242 and U-233 spikes added to each sample following the appropriate blank corrections.

3.1.4 Determination of trace elements

Trace elements (including U) in selected samples were determined in the laboratory by ICP-MS (Agilent ICP-MS 8900 QQQ) from 50 ml of 0.45 µm filtered seawater samples acidified with 5% ultrapure HNO_3 and in sediments and biota by ultraclave digestion of freeze-dried samples with 10% ultrapure HNO_3 or HF. The accuracy of the measurements was controlled using the standard reference materials; CLASS 5 and TM-SEA, to control seawater measurements; NCS Zc73007, CRM73325, 2702-Inorg. Marine Sed. to control measurements of sediments.

3.1.5 Autoradiography

Digital autoradiography imaging was used to identify potential inhomogeneous radioactivity distributions and radioactive particles in the filter that showed the highest activity concentrations of gamma emitters. The air-dried filter was fixed on a white cardboard sheet and wrapped with commercial cling film to avoid sample displacement and cross contamination. The sample was then exposed to a photosensitive phosphor imaging plate (Molecular Dynamics, Amersham Pharmacia Biotech) inside a sealed exposure cassette, which was placed between lead sheets in a dark room to reduce external interferences. Exposure time was 14 days. The photo-stimulated luminescence (PSL) signals (autoradiography images or autoradiograms) were obtained by scanning the exposed plates on a portable imaging plate scanner (HD-CR 35 NDT, Dürr NDT, Germany) with a 50 µm pixel size resolution. Autoradiography images were analysed using an imaging software (ImageJ 1.52h; open source, http://imagej.nih.gov/ih).

3.2 Data handling

Unless otherwise stated, data is reported as individual values with associated uncertainties (1 sigma). Where data values are reported as detection limits, the full detection limit value is used. Inventories, activity ratios and atom ratios based on individual measurements are reported with their propagated uncertainties (1 sigma). Activity concentrations for particulate fractions (>0.45 μm) have been calculated back to the volume of water filtered for gamma emitters or the volume of water analysed for U and Pu isotopes. Activity concentrations for sediments are given as dry weight (d.w.) and for biota as fresh weight (f.w.).

Sediment distribution coefficients (K_d) were derived by:

K_d = Activity concentration in sediment (Bq/kg d.w.)/Activity concentration in seawater (Bq/l)

4 Results of investigations at the site of the sunken nuclear submarine Komsomolets

4.1 Oceanography

A total of five CTD salinity and temperature profiles were taken over the site where Komsomolets lies on the seafloor (Figure 4.1). Atlantic water is observed in the upper 400 m where salinities are greater than 35‰. Below circa 600 m there is little variation in salinity, but a local salinity minimum (34.91‰) was observed at about 1000 m in the intermediate layer. The temperature profiles decreased with depth, until 100 m above the bottom where the recorded water temperature was constant, indicating a thoroughly mixed bottom layer. This agrees with the salinity and temperature observations for a hydrographic transect taken north of Komsomolets for May and June in the same year (Mork et al., 2022).

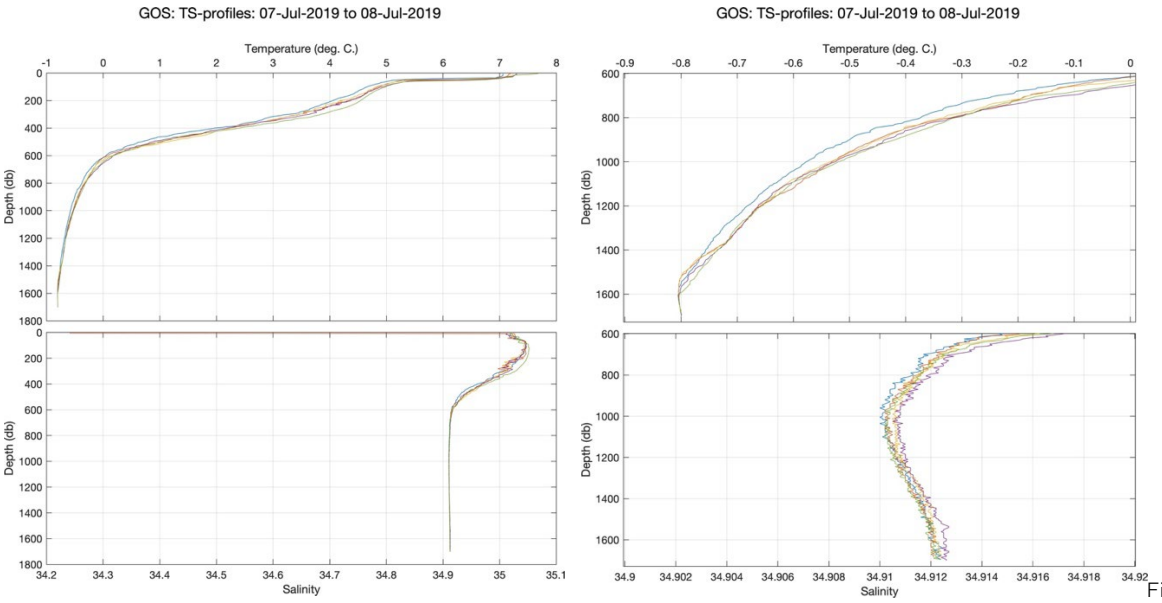

Figure 4.1. Temperature and salinity profiles taken over the site where Komsomolets lies on the seafloor. The right-hand figures show the profiles between 600 m and the seafloor.

4.2 Sonar and visual inspection

4.2.1 High-resolution side scan sonar survey of Komsomolets

From the high-resolution side scan sonar survey, Komsomolets was observed lying upright, with the bow of the submarine pointing almost due North and an estimated 3 m of the lower hull buried in the seafloor. No obvious damage could be observed to the stern section, but there were clear indications of damage to the forward section and to the upper deck over the torpedo compartment (Figure 4.2). The location where the escape chamber was previously attached in the sail of the submarine was also clear. The high-resolution side scan sonar also revealed an obvious deformation in the sediment around the hull of Komsomolets which was particularly obvious around the forward section of the submarine, suggesting that the submarine struck the seafloor bow first (Figure 4.3).

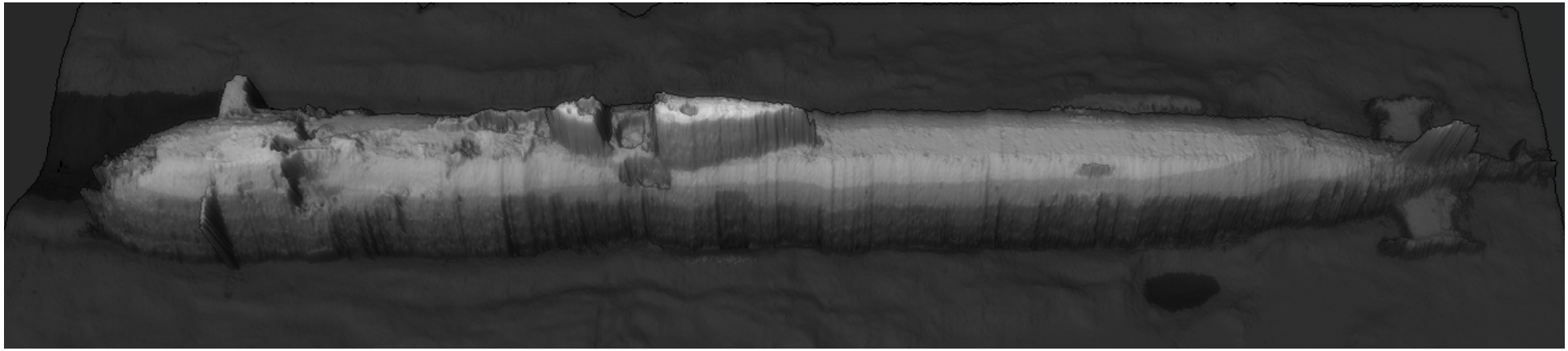

Figure 4.2. 3D side view high-resolution side scan sonar image of Komsomolets on the seafloor.

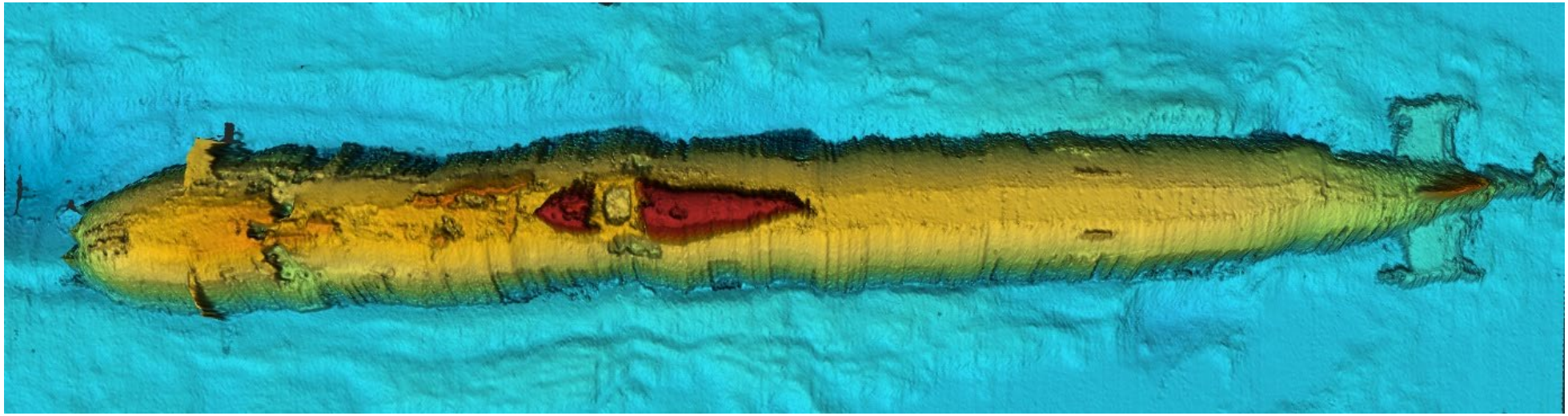

Figure 4.3. Overhead false colour high-resolution side scan sonar image showing the deformation in the sediment around the hull of Komsomolets. False colour scheme simply shows differences in depth.

4.2.2 Video survey of Komsomolets

The video surveillance of Komsomolets confirmed the initial overview from the sonar survey, in that there was little in the way of obvious signs of damage to the external hull of the stern section of the submarine, but clear signs of damage to the forward section. In general, there was little or no evidence of corrosion to the external surfaces, which probably reflects the use of titanium in the construction of the hulls of the submarine. The entire outer hull of the submarine was covered with a sparse layer of marine biota growth, but individual deck tiles and hull markings could be clearly seen (Figure 4.4). The only obvious damage to the stern section was an area of missing deck tiles on the starboard side below the closed rear entrance hatch that leads to compartment seven (Figure 4.5) as well as a smaller area on the starboard side near the main propeller (Figure 4.6). Although the rear entrance hatch was closed, it is known that this hatch was opened during previous Russian investigations in the 1990s. The missing deck tiles over compartment seven matches the eyewitness reports of deck tiles over the stern starboard ballast tank peeling off into the water just after the submarine surfaced at the time of the accident (Romanov, 2006). It has been suggested that loss of the deck tiles was due to hot gases from the fire being pumped into the starboard ballast tank following the failure of the high-pressure air system pipework in compartment seven due to the ongoing fire (Romanov, 2006). Romanov (2006) estimated that temperatures in compartment seven may have reached around 800 to 900°C after high-pressured air was forced into the compartment following the command to blow the main ballast tanks after the fire was discovered. That deck tiles near the main propeller were also missing may lend some support to the suggestion that hot gases from compartment seven were also forced through the starboard stern tube gland cooling system damaging the Kingston valve at this point and eventually providing a pathway for the flooding of the submarine once the fire died out and the pressure dropped in compartment seven (Romanov, 2006).

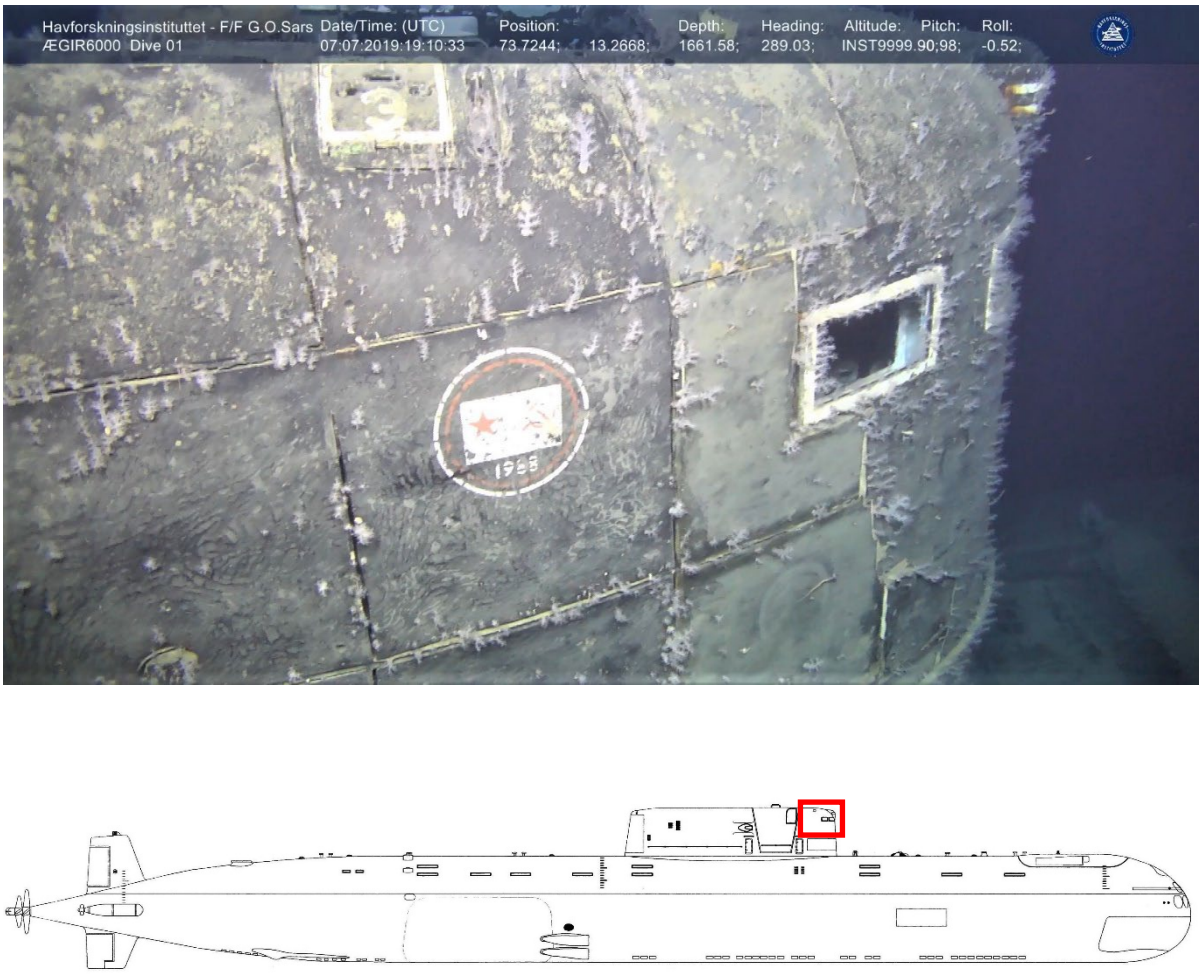

Figure 4.4. Details of deck tiles and hull markings on the starboard side of the sail of Komsomolets with only a sparse covering of marine biota growth over the outer hull. The insignia dated 1988 relates to the assignment of the tactical number K-278 to the submarine (Photo: IMR). Red frame on the plan drawing of Komsomolets shows the relative position of the image above.

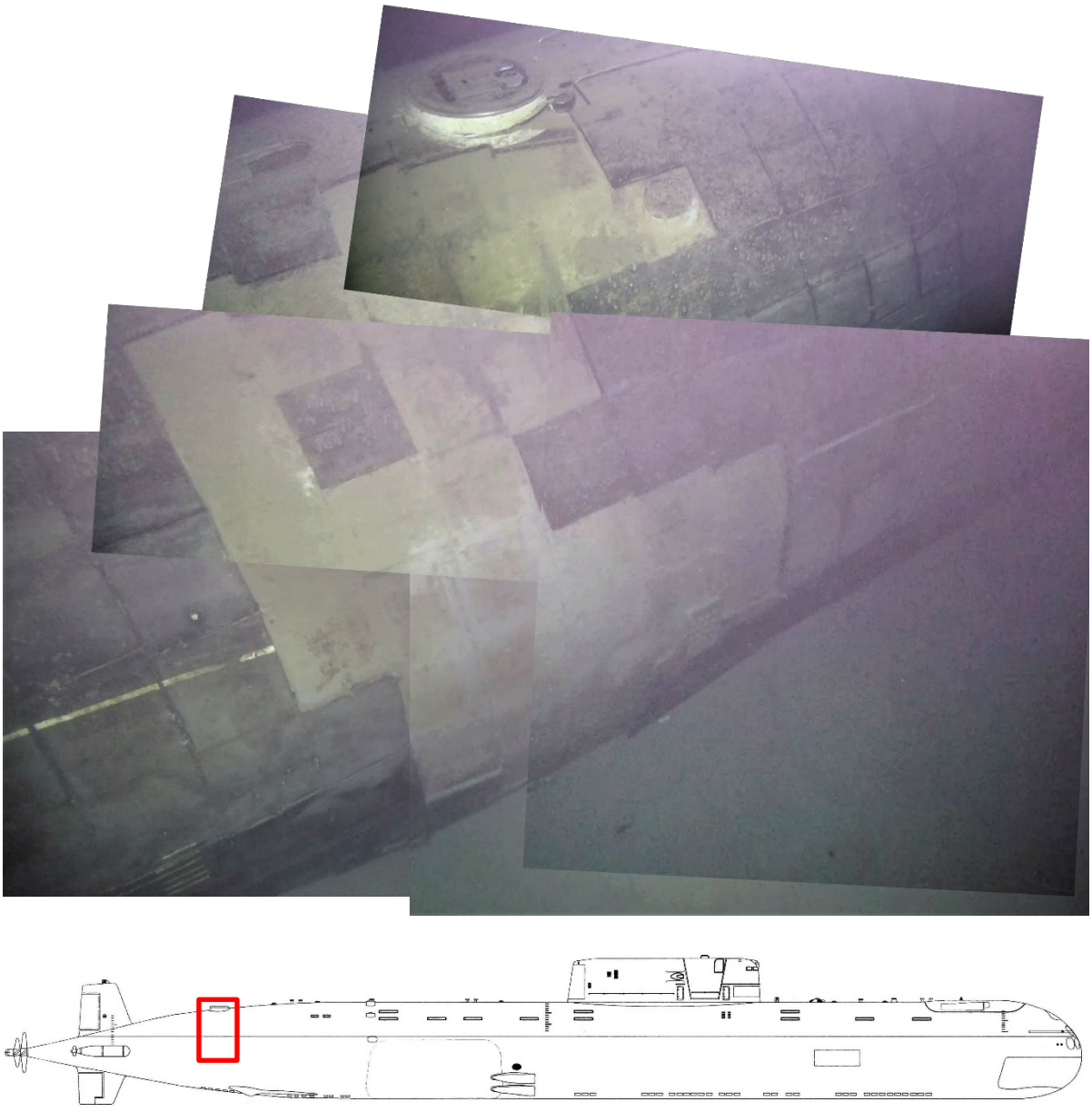

Figure 4.5. Missing deck tiles on the starboard side of Komsomolets below the closed rear entry hatch that leads to compartment seven where the fire occurred (Photo composite: DSA/IMR). Red frame on the plan drawing of Komsomolets shows the relative position of the image above.

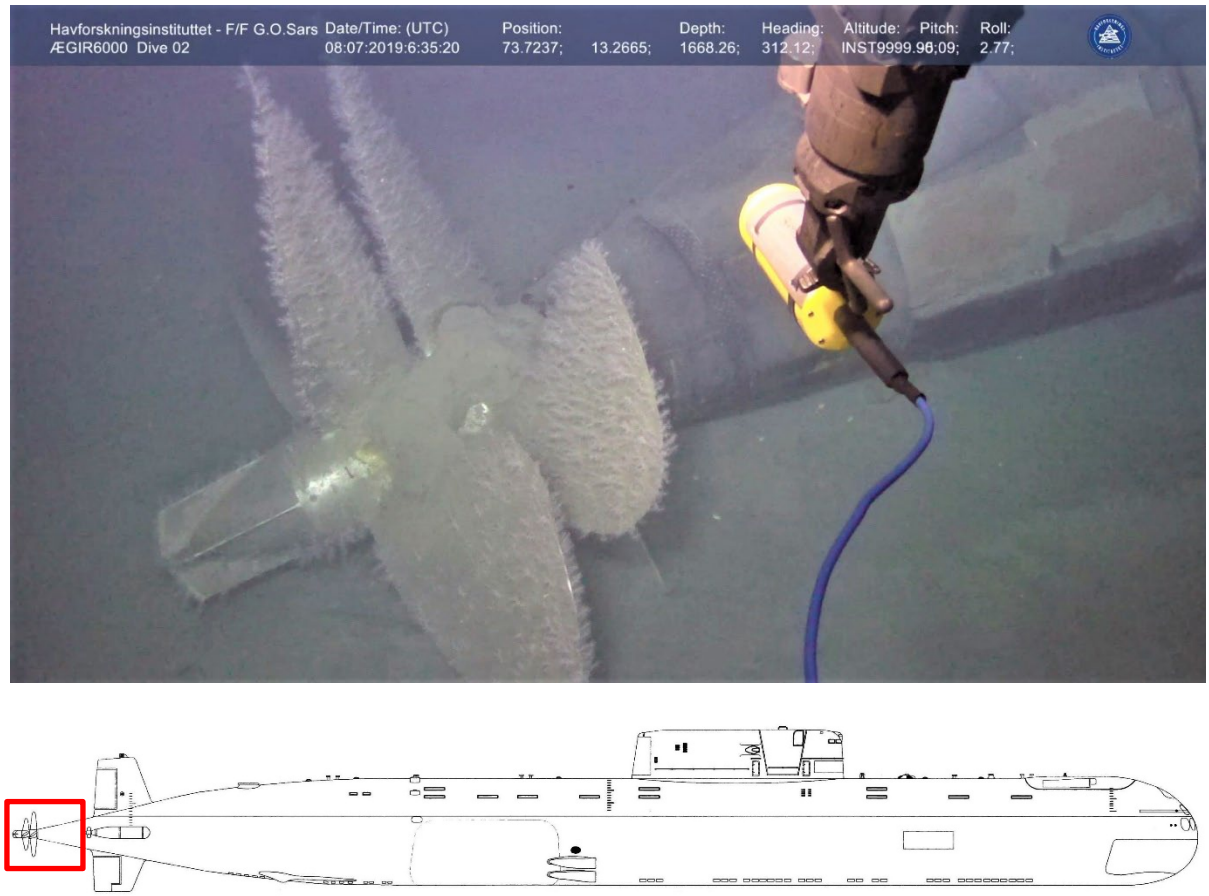

Figure 4.6. Missing deck tiles (top right) on the starboard side of Komsomolets close to the main propeller. The lack of any clear corrosion of the outer structure can be seen from the condition of the main propeller (Photo: IMR). Red frame on the plan drawing of Komsomolets shows the relative position of the image above.

From the video surveillance, the location in the sail where the escape chamber was previously attached to the submarine was clear (Figure 4.7). There appears to be no obvious opening through the attachment coaming which connected the escape chamber to the submarine. Instead, it appears that the base of the coaming has been covered by particulate material (Figure 4.8). However, according to the sole survivor from the escape chamber, the hatch at the base of the attachment coaming was not closed, as there was not time to detach the ladder that was used to climb into the escape chamber when the submarine was sinking (Romanov, 2016). The normal procedure to release the escape chamber would be to detach the entry ladder first, then close the hatch to the submarine at the base of the attachment coaming and then the lower hatch of the escape chamber itself (Romanov, 2016).

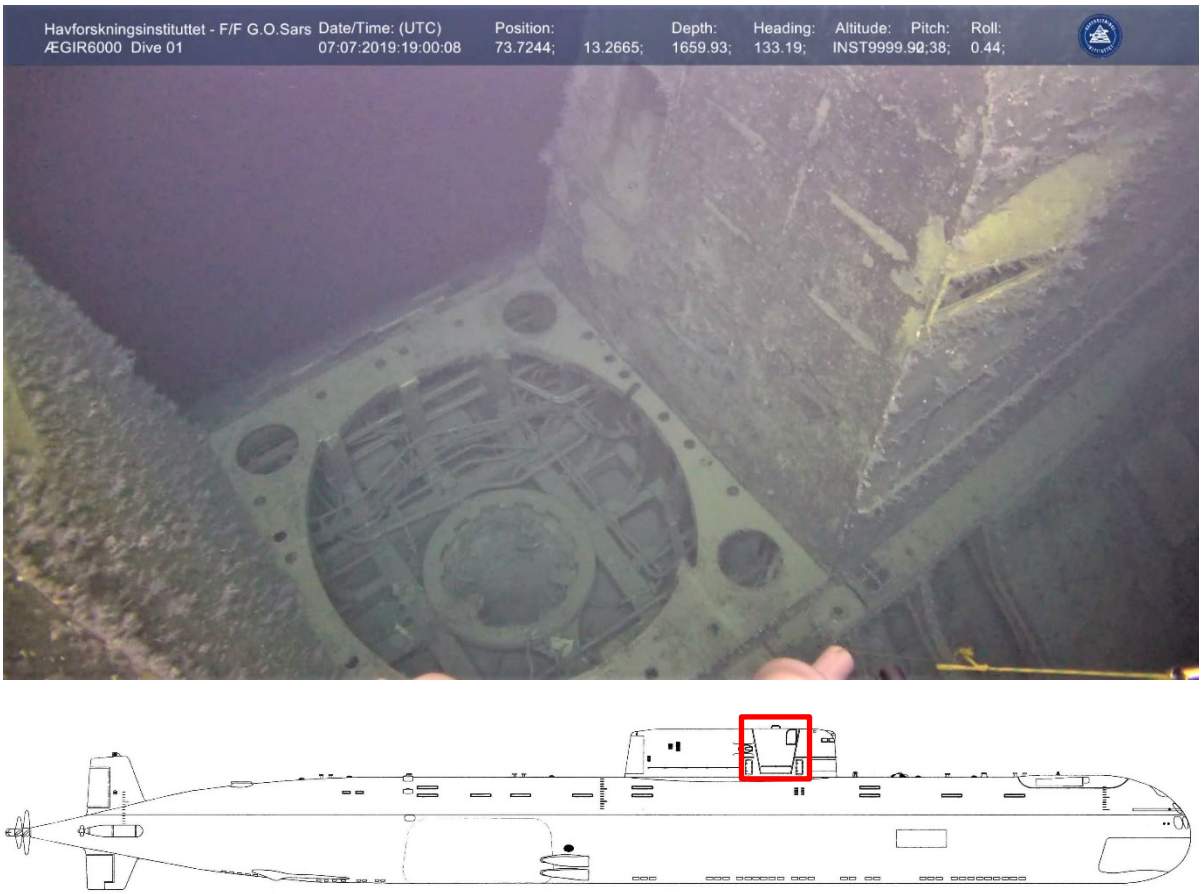

Figure 4.7. Location within the sail where escape chamber was held to the submarine (Photo: IMR). Red frame on the plan drawing of Komsomolets shows the relative position of the image above.

Figure 4.8. View down into the attachment coaming which connected the escape chamber to the submarine. Note the accumulation of particulate material across the base of the coaming (Photo: IMR).

Forward of the sail of Komsomolets, significant damage could be seen to the outer deck which extends along the length of the forward section. Below the sail, two high-pressure air cylinders could be seen that would have been mounted between the outer and inner hulls (Figure 4.9). In addition, the emergency buoy could be seen lying on the upper deck to one side of its original housing. (Figure 4.9). Beyond the emergency buoy, further structural damage could be seen to the outer hull along the upper deck (Figure 4.10). The forward outer entrance hatch and coaming that led to the torpedo compartment were missing (Figure 4.11), but it was not possible to determine the condition of the forward inner entrance hatch. According to testimony from one of the survivors, when the command was given to abandon the submarine the forward lower entrance hatch was opened (Romanov, 2006). We can assume that the forward outer entrance hatch was also open when the submarine sank as other eyewitness accounts recalled that water was entering compartment three from the back of compartment two immediately after the submarine went under (Romanov, 2006). This would indicate that there is an open pathway connecting the marine environment to compartment three via the forward entrance hatchway. According to Romanov (2006), it is likely that transverse bulkheads between compartments were broken as the submarine sank due to the water pressure, which if so, may have created open pathways between compartment three and the rear compartments. Other pathways between compartments may exist through the hydraulic and other system tube lines that ran through the transverse bulkheads and along length of the submarine, and which by all accounts were not shut when the fire was discovered (Romanov, 2006).

The outer hull plates along the port and starboard sides of the submarine below the forward entrance hatch have been deformed so that the aft edge of the hull plates have been forced inwards (Figure 4.12). A wide and horizontal jagged opening in the outer and inner hulls can be seen across the entire upper deck over the torpedo compartment (Figure 4.13). This opening was partially filled with various material during the 1994 Russian investigation (Figure 4.14). Obvious deformation damage can be seen to the outer hull down both the port and starboard sides of the submarine that extend from the jagged opening in the upper deck (Figure 4.15). Beyond the jagged opening in the upper deck, the port and starboard sides of the torpedo compartment are still covered by the coverings that were also installed in 1994 (Figure 4.16 and 4.17). These coverings likely cover the cracks in the outer and inner hulls along the sides of the torpedo compartment that were reported by Yablokov et al. (1993). Furthermore, it was possible to see several titanium plates on the upper deck over the torpedo compartment that were placed over smaller openings in 1994 (Figure 4.18).

The outer hull is cracked open on both the port and starboard sides of the torpedo compartment directly under each of the dive planes (Figure 4.19). At the bow of the submarine, the plugs installed over the six torpedo tubes in 1994 can still be seen (Figure 4.20), but in some cases these plugs do not form a complete seal over the opening to the torpedo tubes (Figure 4.21). The lower outer hull plates at the bow show significant damage and have been pushed out and over the upper outer hull plates (Figure 4.21), which adds further support to the likelihood that Komsomolets hit the seafloor bow first.

There was little in the way of debris on the seafloor around the submarine even where significant damage had occurred to the outer hull, although it is known that some artifacts were recovered during the Russian investigations to Komsomolets in the 1990s. The lack of debris might support the case for an explosion within the forward section before the submarine hit the seafloor, as what little debris is present is clearly related to some of the damage that can be seen to the outer hull (Figure 4.22).

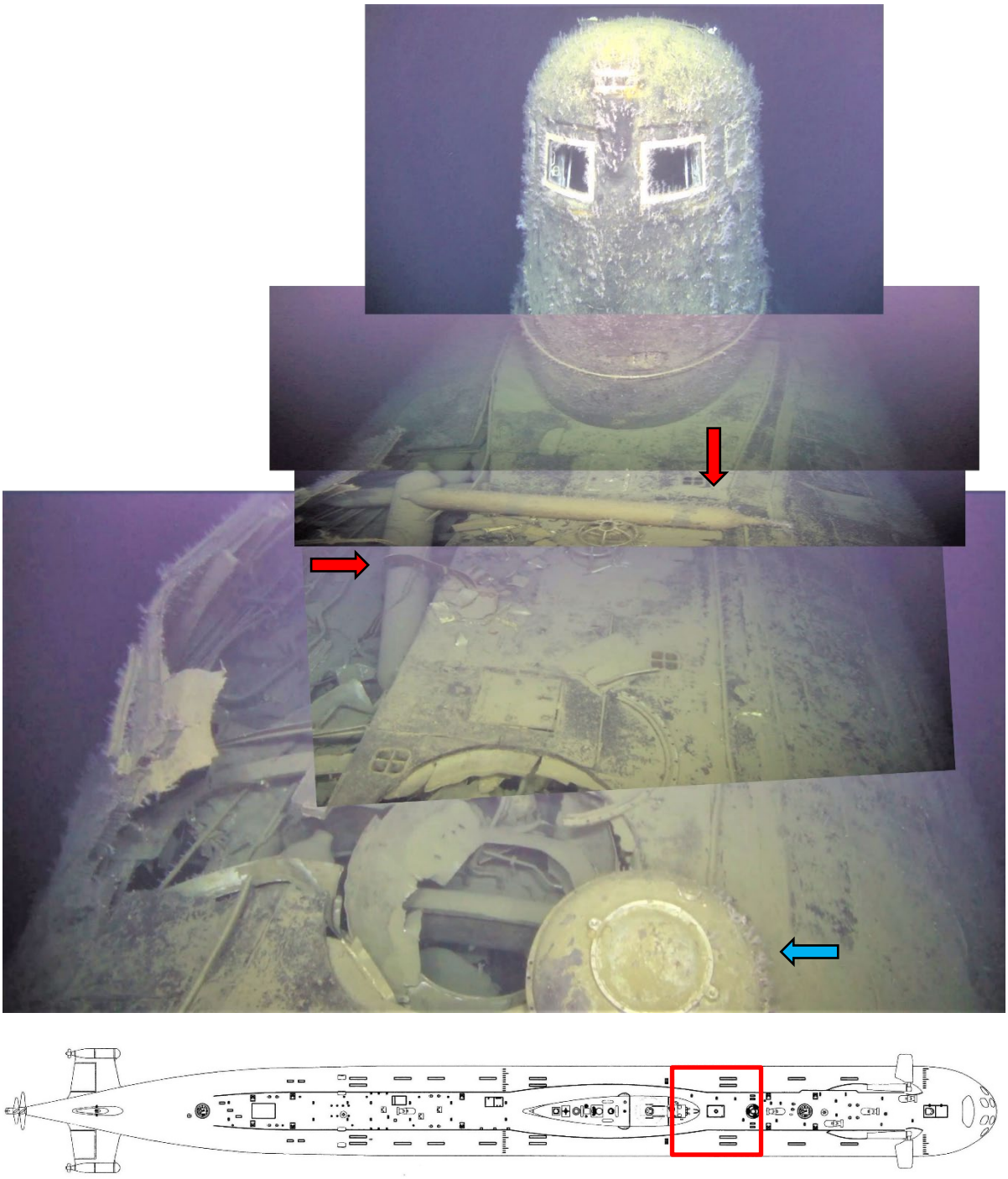

Figure 4.9. View of the damage to the forward outer deck below the sail of Komsomolets. Two high pressure air cylinders can be seen (red arrows) as well as the emergency buoy (blue arrow) (Photo composite: DSA/IMR). Red frame on the plan drawing of Komsomolets shows the relative position of the image above.

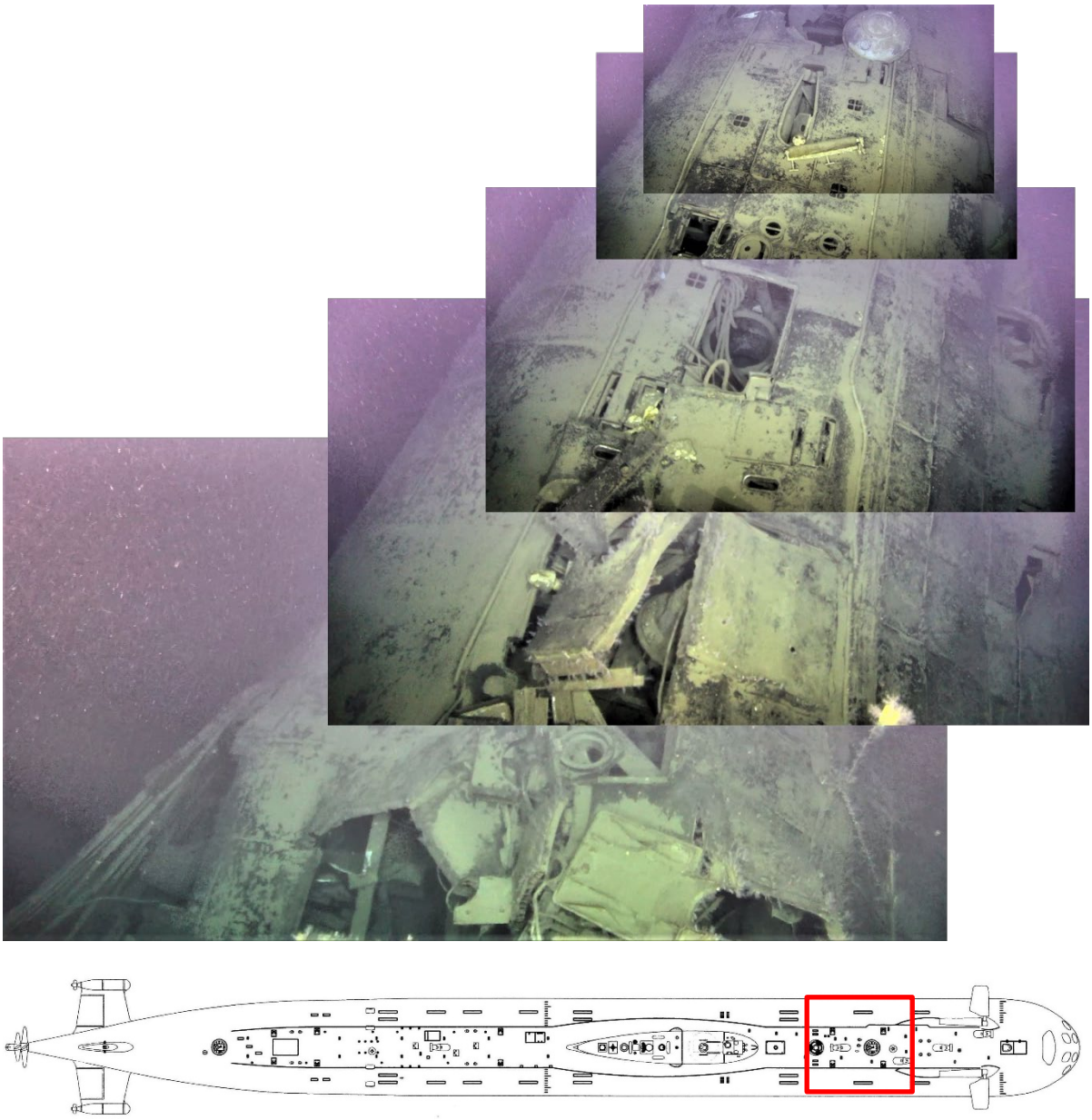

Figure 4.10. View of the damage to the forward outer deck from the emergency buoy to the torpedo compartment. (Photo composite: DSA/IMR). Red frame on the plan drawing of Komsomolets shows the relative position of the image above.

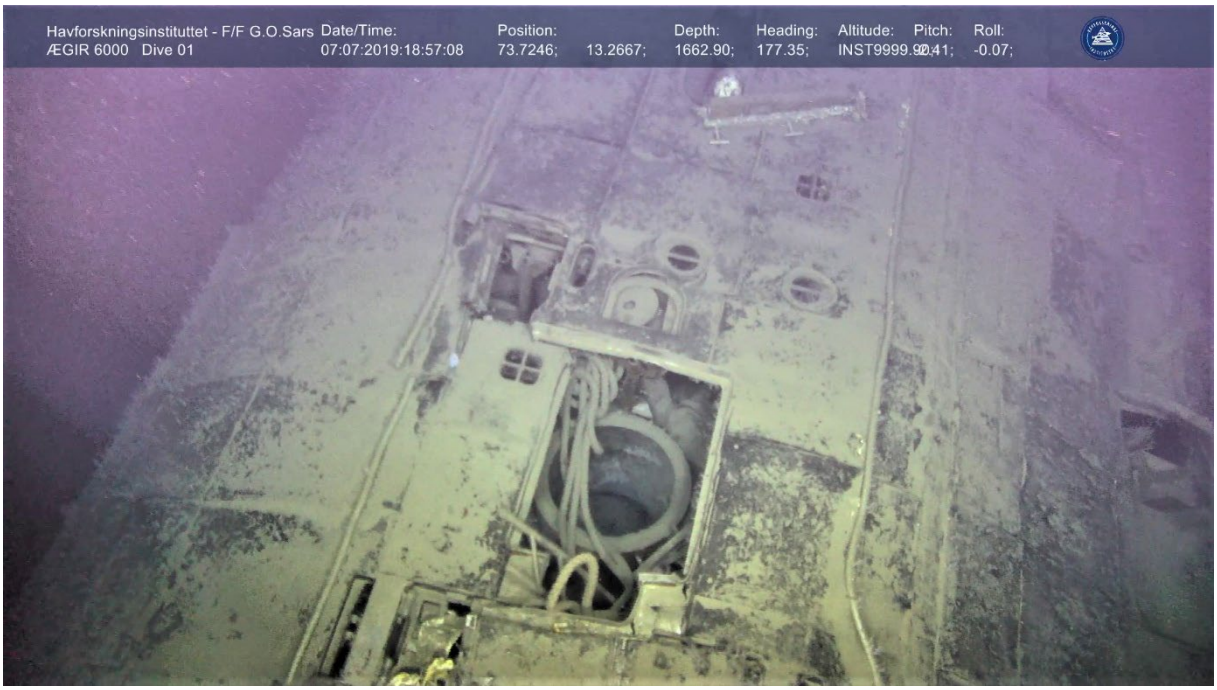

Figure 4.11. Close up view of the forward entrance hatch that led to the torpedo compartment. The outer hatch and coaming were missing, but it was not possible to determine whether the inner hatch was open or closed (Photo: IMR).

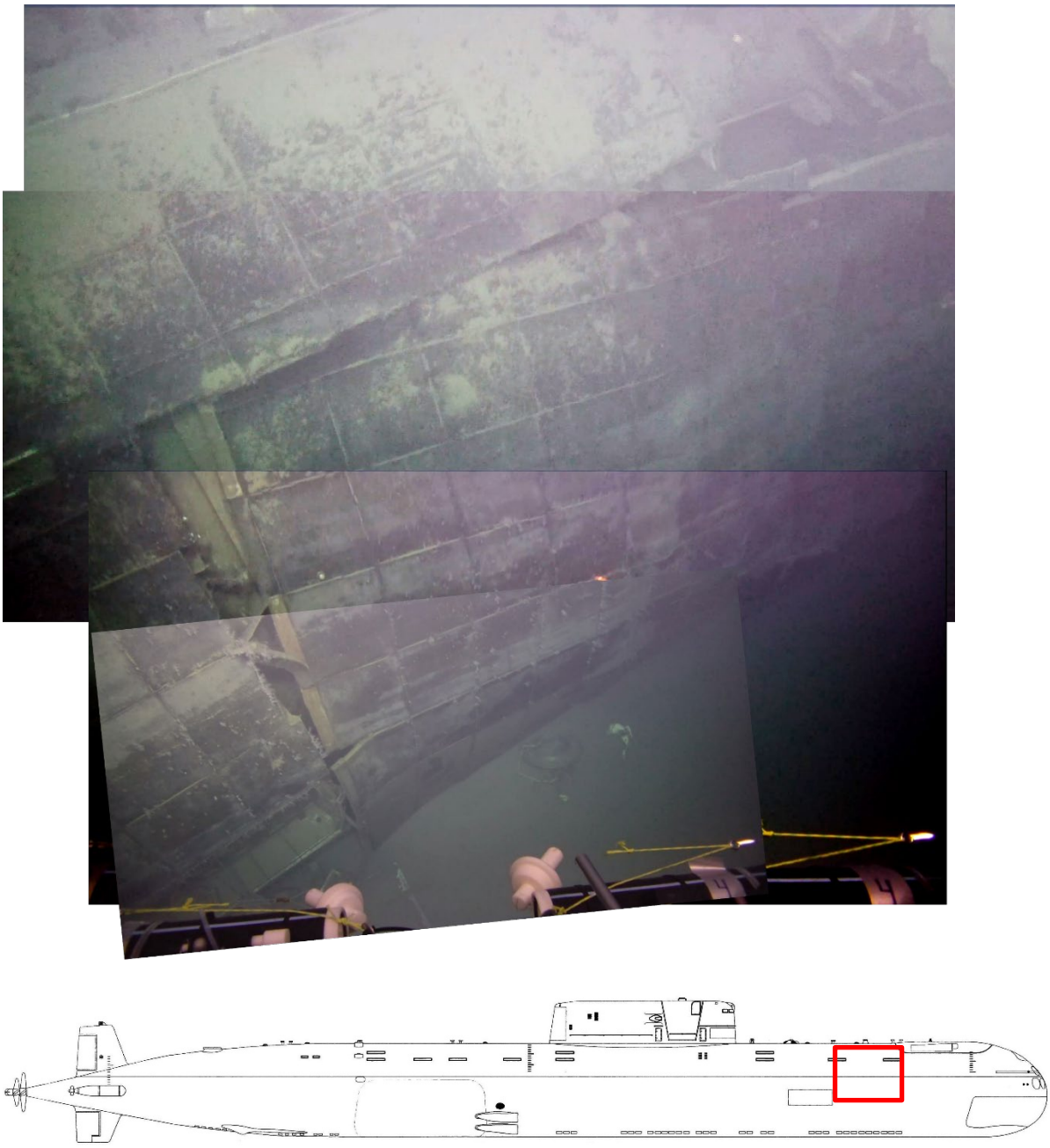

Figure 4.12. View of the damage to the outer deck on the starboard side adjacent to the torpedo compartment (Photo composite: DSA/IMR). Red frame on the plan drawing of Komsomolets shows the relative position of the image above.

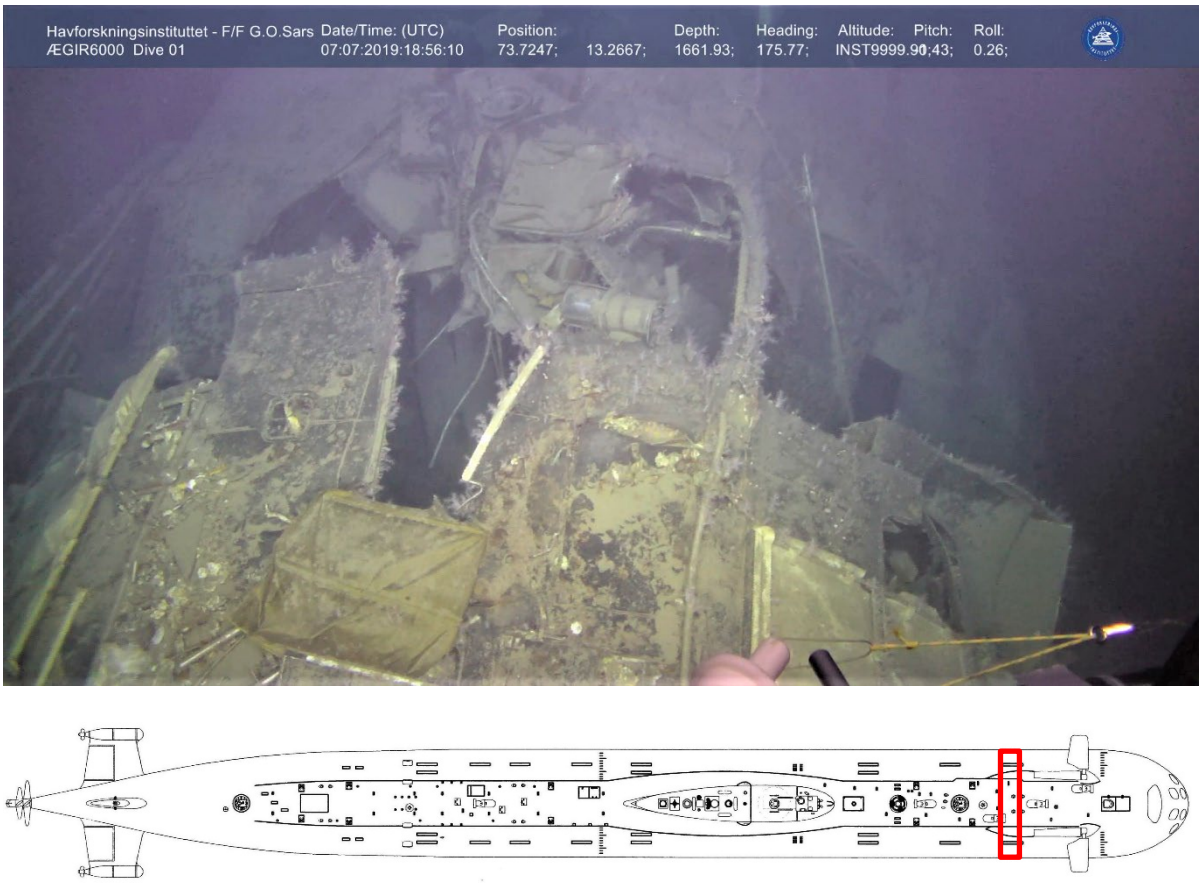

Figure 4.13. View (from the bow of the submarine) of the extensive damage to the outer and inner hulls over the torpedo compartment. The wide and horizontal jagged opening extends across the entire upper deck (Photo: IMR). Red frame on the plan drawing of Komsomolets shows the relative position of the image above.

Figure 4.14. View down into the opening in the outer and inner hulls seen in Figure 4.13. The blue and yellow objects are part of the material that was packed into the torpedo compartment during the Russian investigation to Komsomolets in 1994. The yellow instrument in the ROV's manipulator arm is a Geiger counter (Photo: IMR).

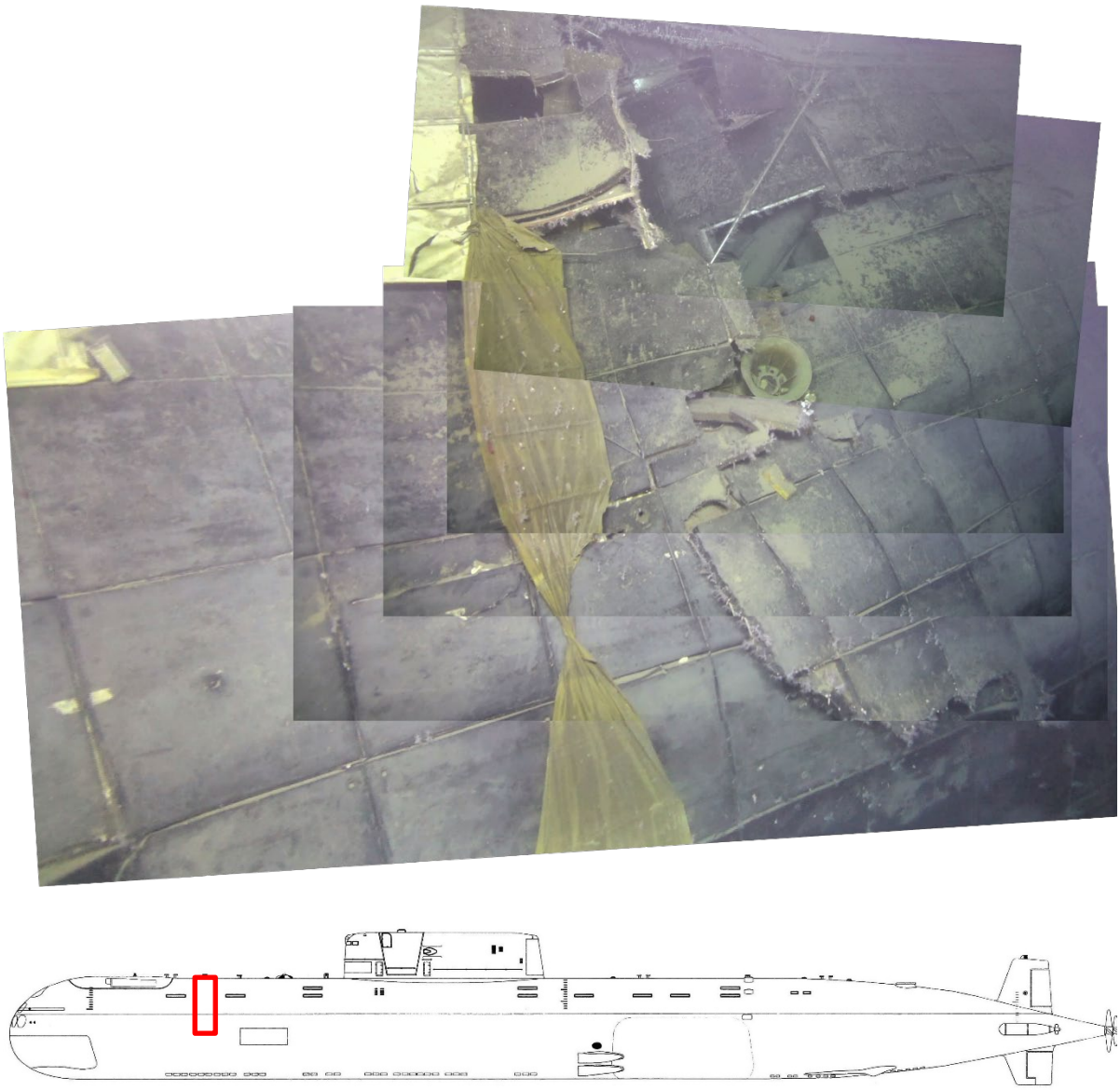

Figure 4.15. Damage to the outer hull on the port side below the opening in the upper deck shown in Figure 4.13. (Photo composite: DSA/IMR). Red frame on the plan drawing of Komsomolets shows the relative position of the image above.

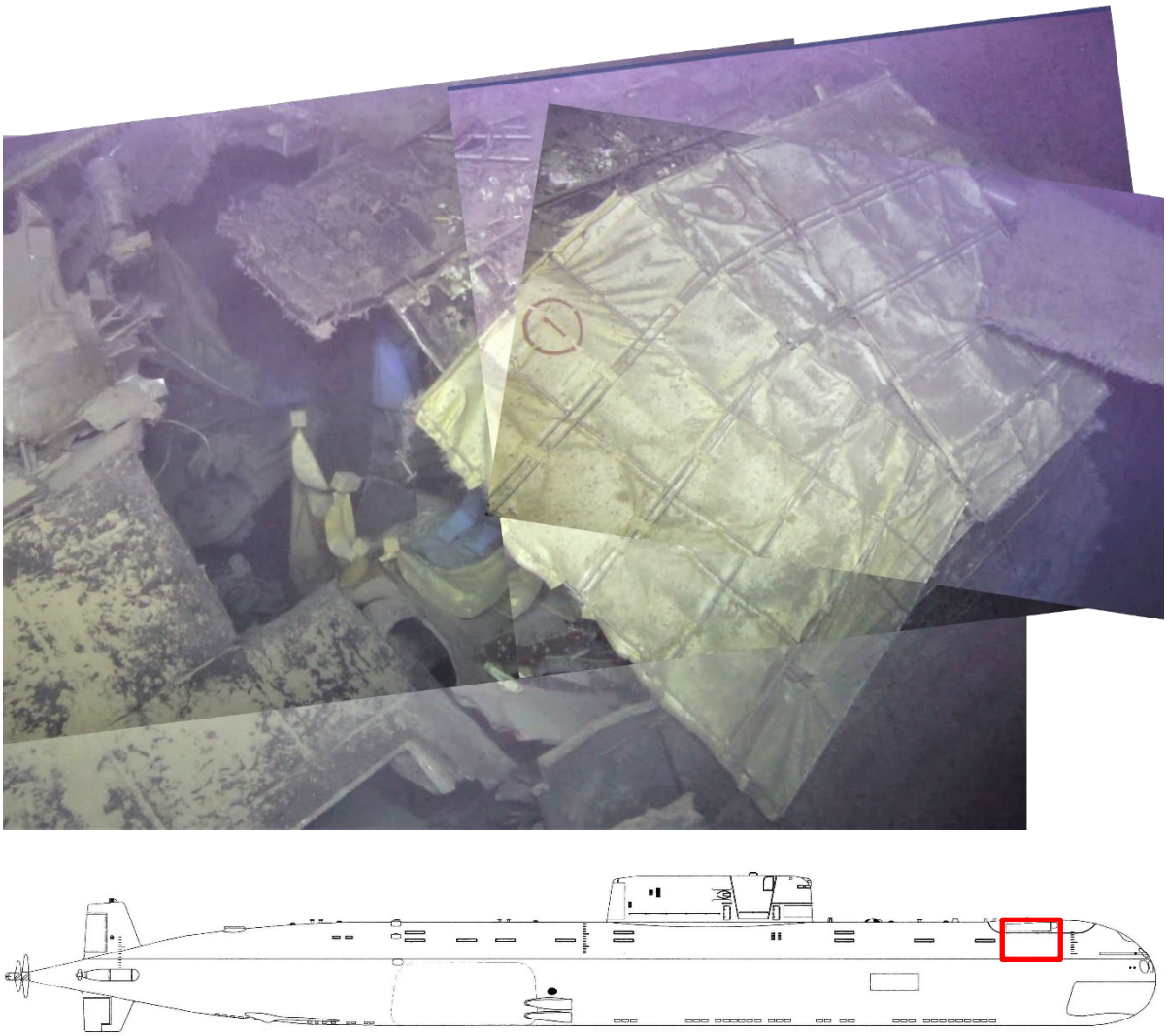

Figure 4.16. View of the coverings installed over the starboard side of the torpedo compartment by the Russian investigation to Komsomolets in 1994 (Photo composite: DSA/IMR). Red frame on the plan drawing of Komsomolets shows the relative position of the image above.

Figure 4.17. View of the coverings installed over the port side of the torpedo compartment by the Russian investigation to Komsomolets in 1994 (Photo composite: DSA/IMR). Red frame on the plan drawing of Komsomolets shows the relative position of the image above.

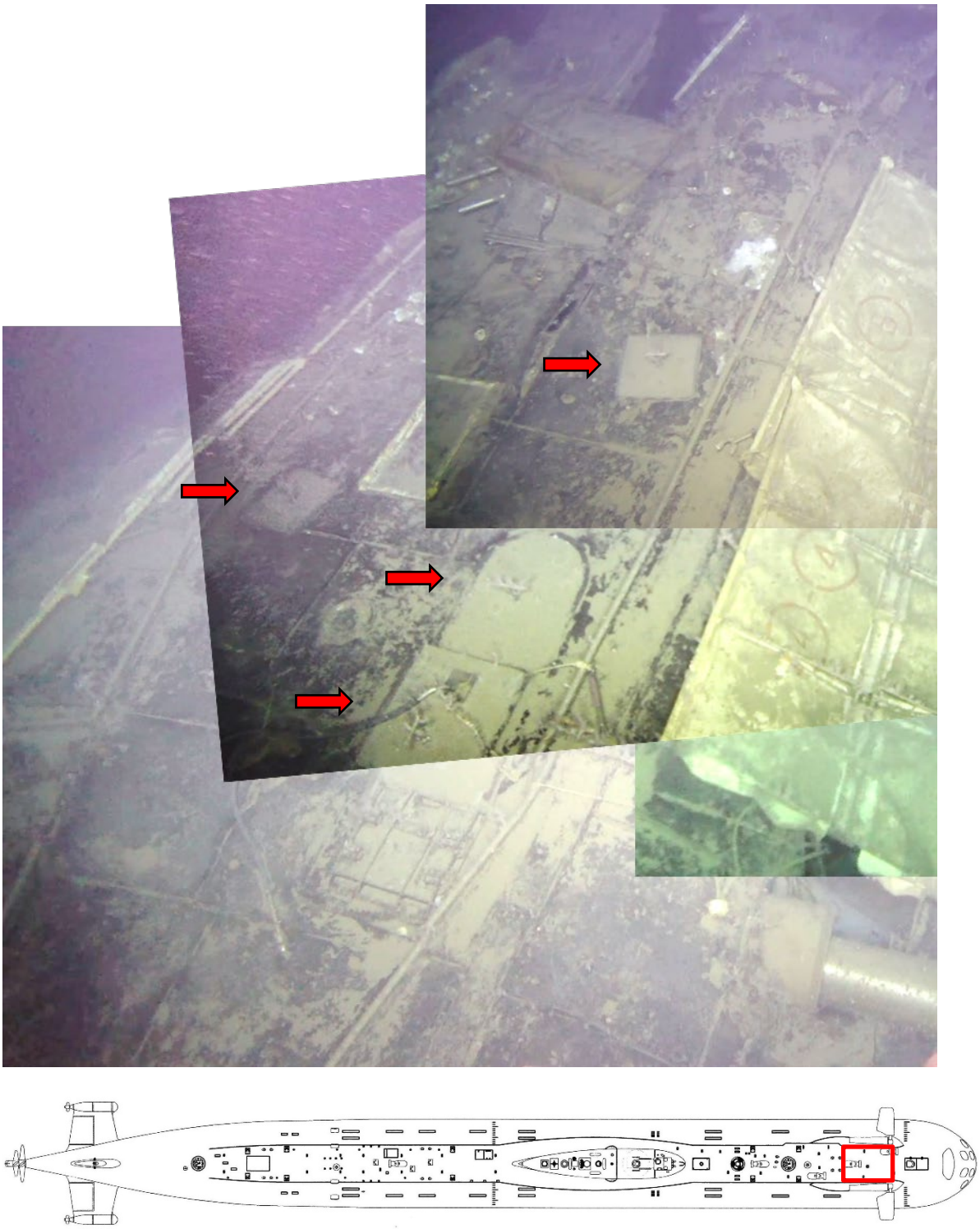

Figure 4.18. View (from the bow of the submarine) of the titanium plates (red arrows) on the upper deck over the torpedo compartment that were installed over smaller openings by the Russian investigation to Komsomolets in 1994 (Photo composite: DSA/IMR). The handles on the plates that the MIR submersible used to position the plates can clearly be seen. Red frame on the plan drawing of Komsomolets shows the relative position of the image above.

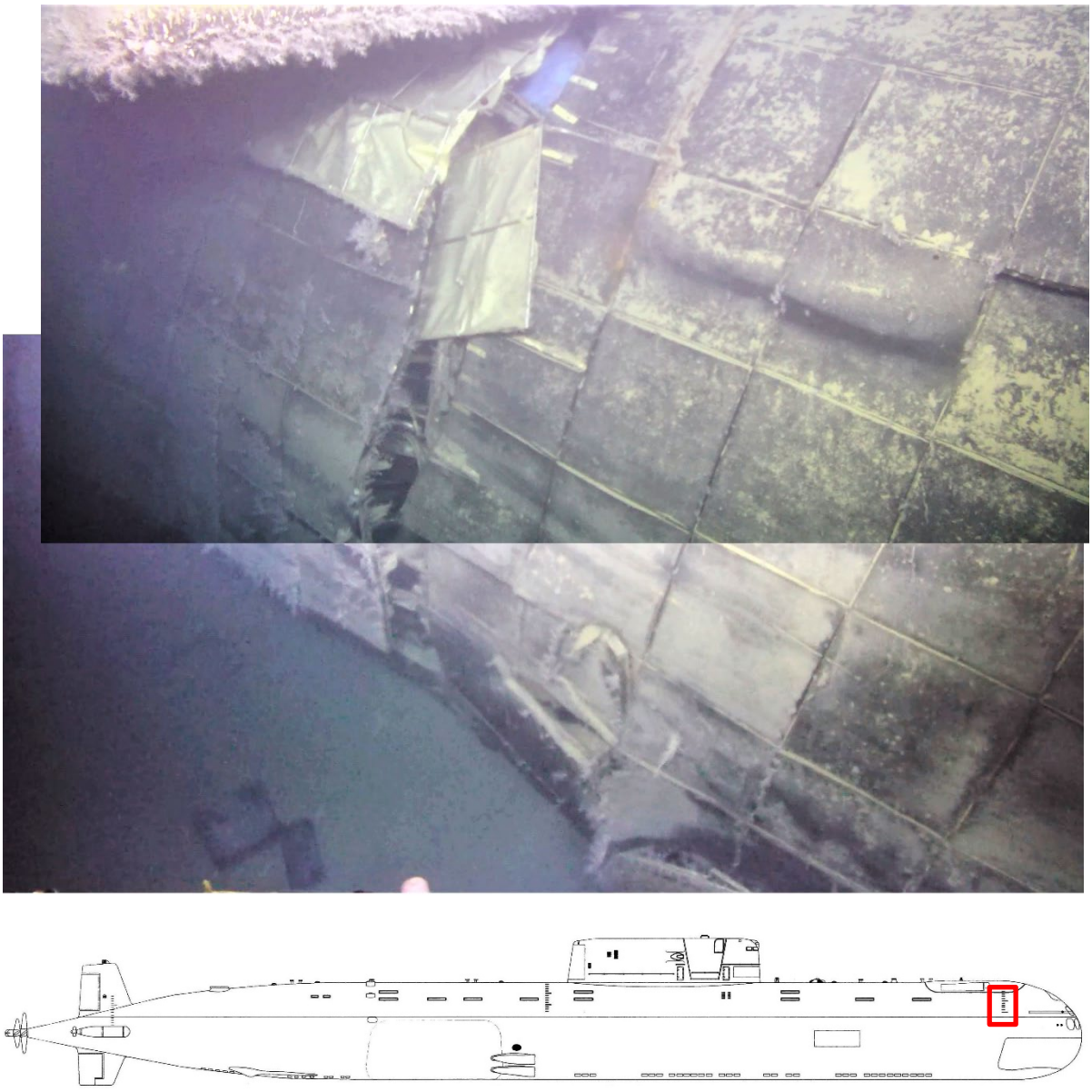

Figure 4.19. View (from the bow of the submarine) of damage to the outer hull below the starboard dive plane (Photo composite: DSA/IMR). Red frame on the plan drawing of Komsomolets shows the relative position of the image above.

Figure 4.20. View of the bow of Komsomolets showing the plugs installed over the six torpedo tubes by the Russian investigation to Komsomolets in 1994 and the damage to the lower outer hull (Photo composite: DSA/IMR). Red frame on the plan drawing of Komsomolets shows the relative position of the image above.

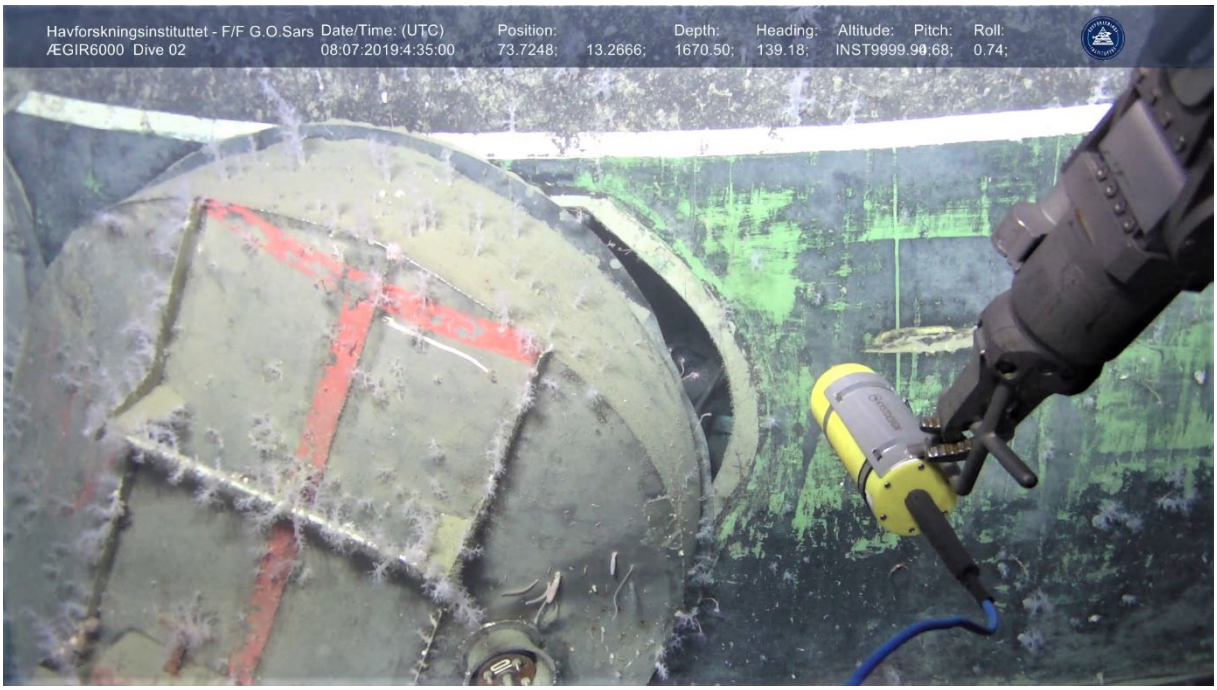

Figure 4.21. Close up view of one of the plugs installed over a torpedo tube by the Russian investigation to Komsomolets in 1994, showing that the torpedo tube in this instance is not entirely covered. The yellow instrument in the ROV's manipulator arm is a Geiger counter (Photo: IMR).

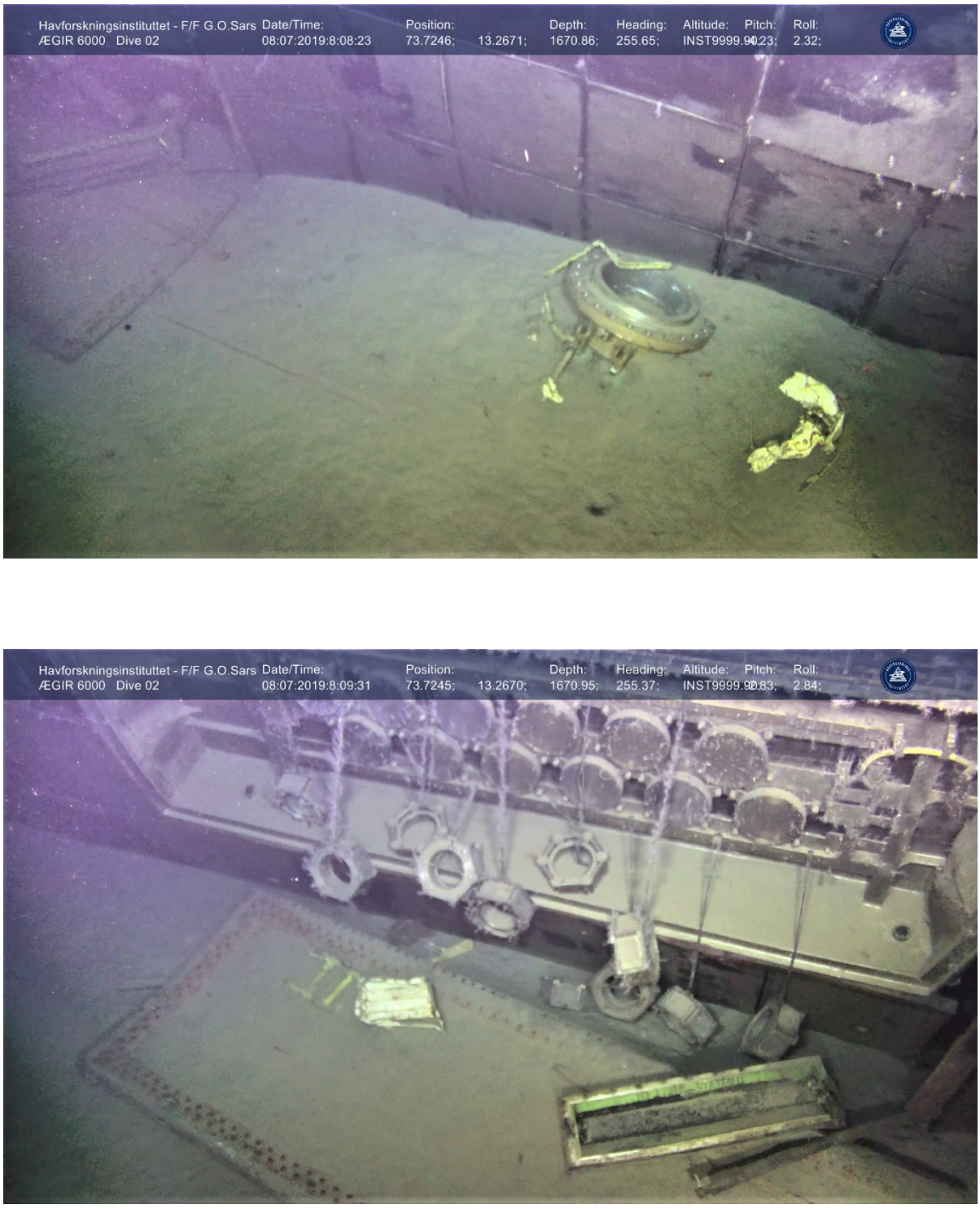

Figure 4.22. Debris on the seafloor next to the submarine. Upper photo shows what appears to be part of the forward outer entrance hatch lying below the original position of the hatch on the upper deck. Lower photo shows an open panel on the seafloor directly below where it was originally attached to the outer hull on the starboard side. The purpose of the fittings in this hatch is not known. (Photos: IMR).

4.2.3 Video survey of the ventilation pipe where releases from the reactor have been reported previously

Releases of radionuclides from Komsomolets have been detected previously by in situ measurements in a ventilation pipe that forms an open connection between compartment five, aft of the reactor compartment, and the open sea (Nejdanov, 1993; Gladkov et al., 1994; Kazennov, 2010). This ventilation pipe was located on top and at the back of the sail, aft of the last antenna bay (Figure 4.23). Initial visual observations of the ventilation pipe during the first dive of the ROV did not reveal anything unexpected, although there was an obvious accumulation of particulate material on the upper hull surfaces of this section of the sail and around the ventilation pipe (Figure 4.23). However, during the subsequent three dives with the ROV an obvious visual release could be seen coming out of the ventilation pipe that appeared to vary in intensity (Figure 4.24). From the available published information on the various Russian investigations to Komsomolets, there has not been any mention of such a visual release from the ventilation pipe, however such a visual release can be briefly seen from video footage taken by one of the MIR submersibles during a previous Russian investigation. In addition to the visual release from the ventilation pipe, a similar release was observed on some occasions emerging from the metal grill immediately forward of the ventilation pipe (Figure 4.25) and at times from both the ventilation pipe and the metal grill simultaneously (Figure 4.26). Releases of any kind from this metal grill have not been reported by any previous Russian investigation. Based on available schematics of Komsomolets, it is possible that the pipe under the metal grill is the air inlet for the diesel generator in compartment three, immediately forward of the reactor compartment. However, it is not known whether there is any connection or opening between the ventilation pipe and the pipe covered by the metal grill either by design or as a result of the accident and/or subsequent corrosion that would allow releases to pass from one pipe to the other. As is likely the case for the ventilation pipe, the air inlet pipe for the diesel generator would have been open when Komsomolets sank as it was reported that the diesel generator in compartment three was in operation at the time of sinking (Romanov, 2006). No obvious visual releases were observed emerging from any other opening around the submarine during any of the dives with the ROV. When visual releases were observed, these tended to drift slowly towards the bow of the submarine (i.e. northwards).

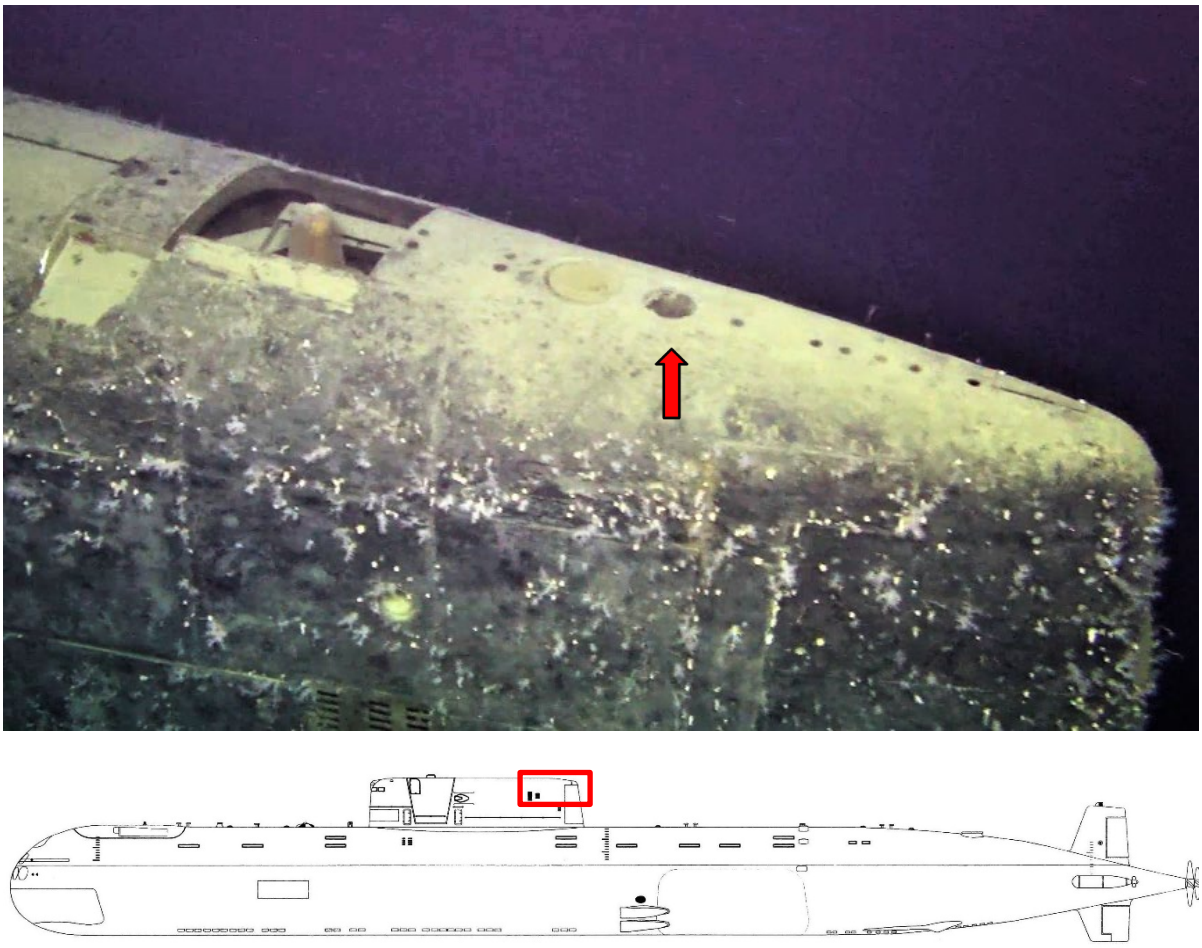

Figure 4.23. Port side view of the top of the rear section of the sail, showing the location of the ventilation pipe (red arrow) where releases of radionuclides from the reactor have been reported by previous Russian expeditons. The square open bay to the left of the ventilation pipe houses one of the communication antenna (Anais type), the top of which can clearly be seen (Photo: IMR). Red frame on the plan drawing of Komsomolets shows the relative position of the image above.

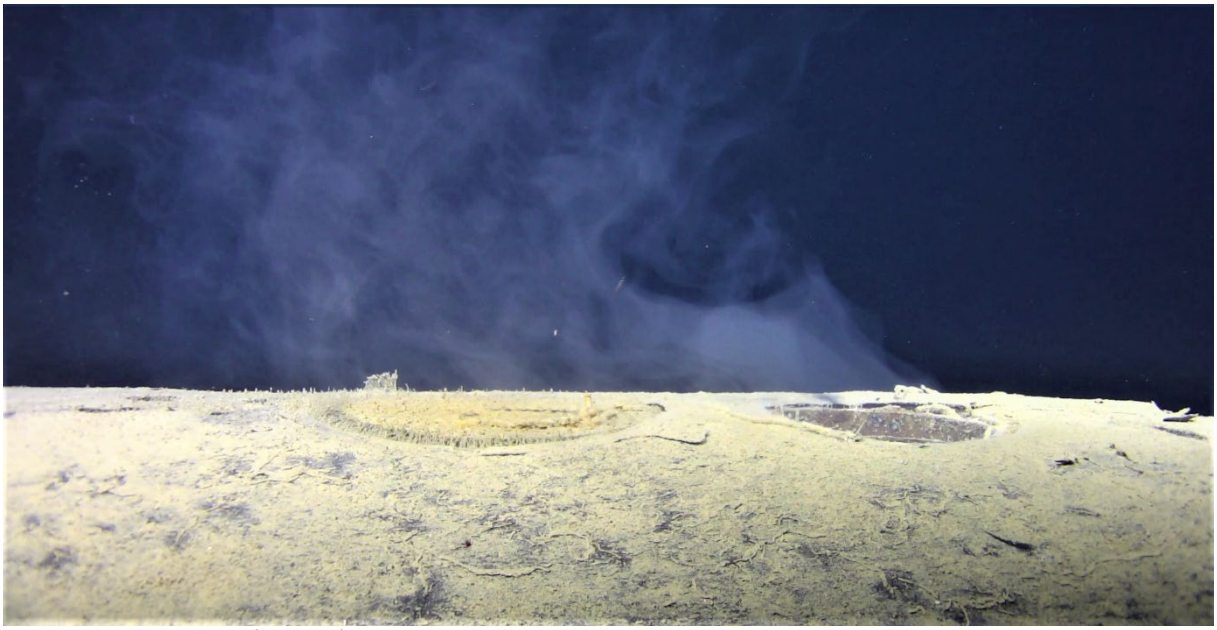

Figure 4.24. Close up view (port side) of the visual release coming out of the ventilation pipe and the particulate material accumulated on the hull surface at this location (Photo: IMR).

Figure 4.25. Close up view (port side) of the visual release coming out of the metal grill forward of the ventilation pipe. At this time, there was no visual release emerging from the ventilation pipe (Photo: IMR).

Figure 4.26. Close up view (port side) of the visual release coming out of the ventilation pipe and the metal grill at the same time (Photo: IMR).

4.3 Radionuclides and trace elements in seawater

4.3.1 Cesium-137 (Cs-137)

The results for the analysis of filtered large volume seawater samples for Cs-137 are given in Table 4.1. The activity concentration of Cs-137 in surface seawater collected over Komsomolets was 1.0 ± 0.4 Bq/m^3 which was similar to values for surface water for previous and subsequent monitoring years up to 2021 (Figure 4.27) and is typical for current levels of Cs-137 in the wider Norwegian Sea (Skjerdal et al., 2020; RAME, unpublished). Such values reflect the current low contribution of known sources of Cs-137 to surface waters in the North-East Atlantic from the European reprocessing plants at Sellafield (UK) and Cap la Hague (France) as well as contributions from the Chernobyl accident and global fallout. The activity concentration of Cs-137 in the large volume bottom seawater collected approximately 3 m directly over the ventilation pipe was 5.9 ± 0.3 Bq/m^3. This is around 5 times higher than the average activity concentration for bottom seawater sampled around Komsomolets since 1995 (1.2 ± 0.5 Bq/m^3), when samples were collected from surface ships alone, but lower than the values reported for 1991 to 1993 (Figure 4.27). Prior to 2015 it was not known with any precision as to where bottom samples were collected in relation to the submarine. From 2015 onwards, bottom samples have been collected using an acoustic transponder that allows samples to be taken within 20 m of the submarine at known locations, but it is likely that the bottom water samples taken in 2019 were the first time that such large water volume samples were taken at a height of around 3 m directly over the ventilation pipe.

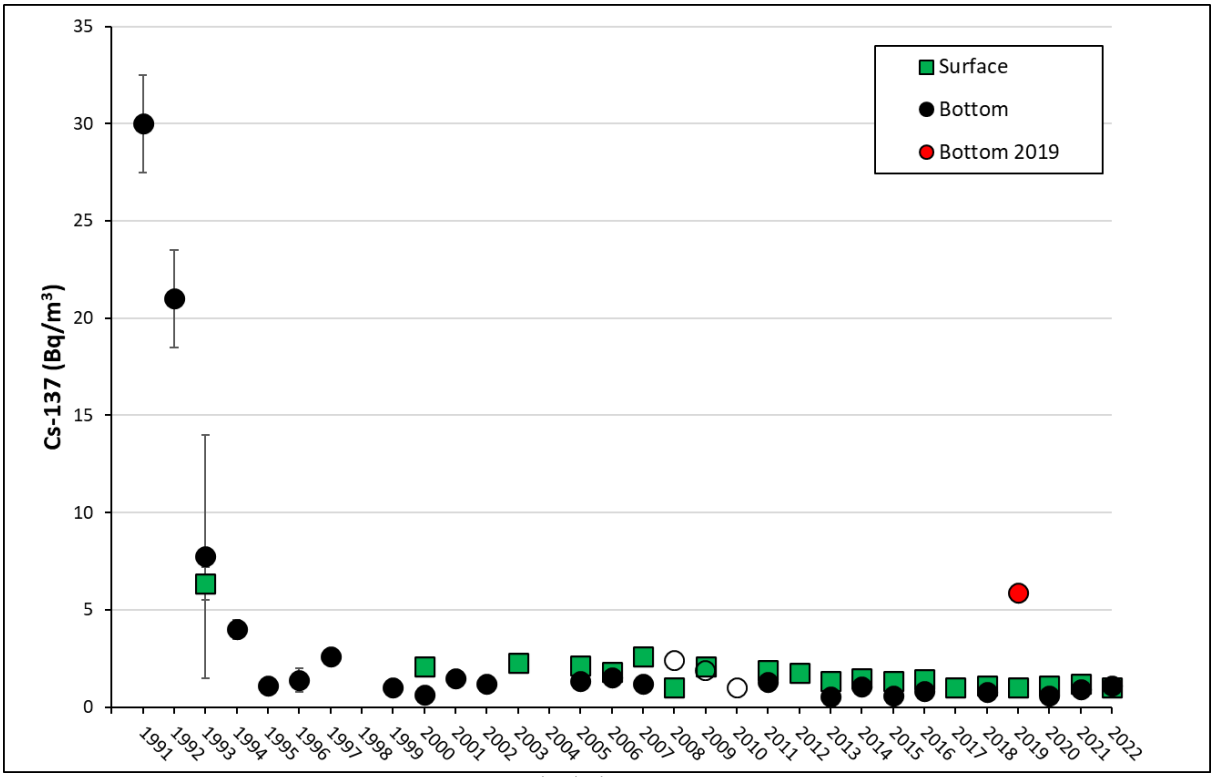

Figure 4.27 Time series of Cs-137 activity concentrations (Bq/m^3) in surface and bottom seawater samples collected by Norwegian monitoring at the site of Komsomolets since 1991. Data values for individual years represent individual measurements except for 1993 and 1996 (mean values; n=2). Vertical error bars for individual measurements are measurement uncertainties while vertical error bars for mean values represent the associated standard deviation. Open symbols represent values below detection limits. Uncertainties on individual measurements were typically less than 10%. The observed activity concentration in the bottom seawater sample collected around 3 m directly over the ventilation pipe in 2019 is included as the red dot. Overview of data for 1991 to 2015 published previously in Gwynn et al. (2018). Data for 2016 to 2018 and 2020 to 2022 from the Norwegian national monitoring programme (unpublished).

Results for the analysis of the dissolved (<0.45 µm) and particulate fractions (>0.45 µm) from the small volume seawater samples for Cs-137 are given in Table 4.2. The initial set of small volume samples of seawater sampled by the ROV during the first dive consisted of a sample taken directly from the ventilation pipe, at around 1 m and 5 m directly over the ventilation pipe as well as on the port and starboard sides of the reactor compartment. No visual release coming from either the ventilation pipe or the metal grill was observed when these samples were collected. Direct gamma spectroscopy analysis of these filtered seawater samples gave activity concentration detection limits for Cs-137 of <60 Bq/m^3. After pre-concentration, the filtered seawater samples taken 5 m directly over the ventilation pipe and the starboard side of the reactor compartment gave improved detection limit results for Cs-137 of <5.9 and <2.4 Bq/m^3 respectively. Pre-concentration of the filtered seawater sample taken on the port side of the reactor compartment gave an activity concentration result of 11.7 ± 1.1 Bq/m^3. The remaining two filtered seawater samples collected during the first dive of the ROV were not pre-concentrated for further Cs-137 analysis as these samples were prioritised for other analyses. Activity concentrations of Cs-137 in the particulate fractions from the small volume samples (Table 4.2) collected during first dive were above the detection limit for the sample collected 1 m over the ventilation pipe (520 ± 130 Bq/m^3) and the sample collected around 1 m from port side of the reactor compartment (270 ± 60 Bq/m^3), but no other man-made gamma emitters were identified in these samples.

On the second ROV dive two further seawater samples were collected directly from the ventilation pipe, 6.5 and 11 hours after the first ventilation pipe sample was taken. When the first of these samples were collected, no visual release could be seen emerging from the ventilation pipe, but a visual release was observed when the second sample was collected. The activity concentration of Cs-137 in the 6.5 hour filtered seawater sample was 0.08 ± 0.02 kBq/m^3, while for the 11-hour filtered seawater sample the activity concentration of Cs-137 had increased by a factor of 1000 to 92.6 ± 2.6 kBq/m^3. Activity concentrations of Cs-137 in the particulate fractions of the same samples were of a similar order of magnitude at 0.63 ± 0.16 kBq/m^3 and 0.95 ± 0.05 kBq/m^3, respectively.

For the third ROV dive, seawater samples were collected above the metal grill, directly from the ventilation pipe and at a height of 40 cm above the ventilation pipe. Visual releases could be seen from the ventilation pipe and/or the metal grill throughout the entirety of the third dive whenever the ROV was in position to observe the top of the rear section of the sail. The samples taken 40 cm above the ventilation pipe were collected within the plume of the ongoing visual release. The activity concentration of Cs-137 in the filtered seawater sample collected above the metal grill was 792 ± 22 kBq/m^3, the highest value detected in any of the seawater samples collected by the ROV. The activity concentration of Cs-137 in the filtered seawater sample collected directly from the ventilation pipe (23.1 hours after the first sample was collected) was 86.9 ± 2.5 kBq/m^3, which was similar to the 11-hour filtered seawater sample that was collected from the ventilation pipe during the second dive. Just prior to the collection of the sample from the ventilation pipe at 23.1 hours, a seawater sample was collected 40 cm above the ventilation pipe. The activity concentration of Cs-137 in this filtered seawater sample was a factor of 10 lower than that observed in the sample taken directly from the ventilation pipe a few minutes later. A second sample collected 40 cm above the ventilation pipe on the third dive at 24.5 hours, showed a lower Cs-137 activity concentration of 420 ± 50 Bq/m^3.

The activity concentration of Cs-137 in the particulate fraction for the sample collected above the metal grill was also elevated at 78.4 ± 2.5 kBq/m^3. In the particulate fraction from this sample, Eu-152 (3.2 ± 0.1 kBq/m^3), Eu-154 (1.19 ± 0.04 kBq/m^3) and Am-241 (0.36 ± 0.02 kBq/m^3) were also detected. Autoradiography of the particulate material on the filter from this sample showed hotspots of radioactivity (Figure 4.28), but no radioactive particles could be detected when the filter was split, and the parts reanalysed separately by gamma spectrometry. It should be noted some particulate material from the metal grill was resuspended and taken up by the syringe sampler when this sample was

collected. This might explain the higher activity concentrations observed in both the dissolved and the particulate fraction for this sample. Activity concentrations of Cs-137 in the particulate fractions from the samples collected 40 cm above the ventilation pipe at 23 hours (86 ± 6 Bq/m^3) and directly from the ventilation pipe at 23.1 hours (2100 ± 90 Bq/m^3) were approximately 1 to 2% of the activity concentrations in the dissolved fractions of these samples. The activity concentration of Cs-137 in the particulate fraction for the sample collected 40 cm above the ventilation pipe at 24.5 hours (256 ± 70 Bq/m^3) was an order of magnitude higher than the previous sample taken at this location at 23.1 hours.

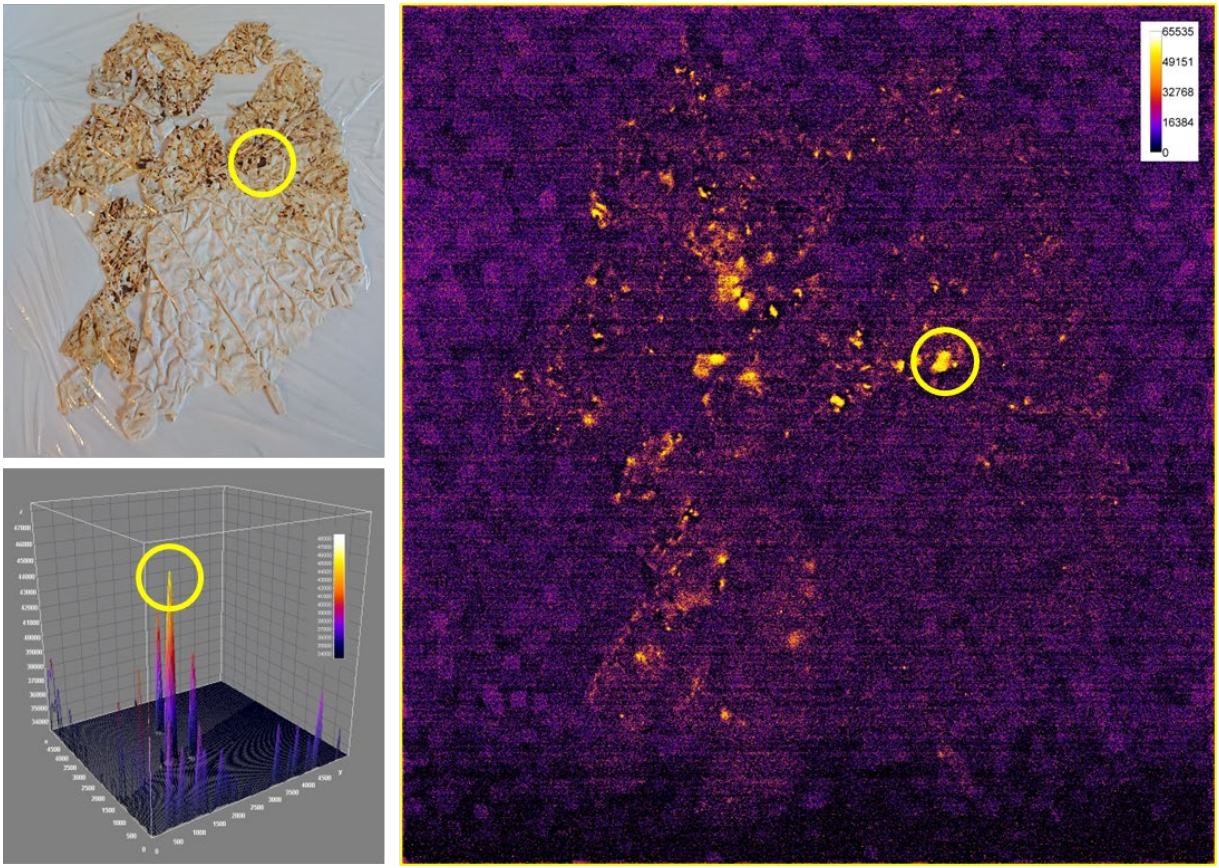

Figure 4.28. Autoradiography of the particulate material on the filter used with the small volume sample collected above the metal grill by the ROV. Photo of dried filter mounted on cardboard and wrapped under cling film (upper left), 3D surface plot of photostimulated luminescence (PSL) signal (lower left) and 2D representation of PSL (right). The yellow circles indicate position of the most active part of the sample. Colour scales represent photostimulated luminescence (PSL) signal intensity.

On the fourth ROV dive, seawater samples were collected directly from the ventilation pipe, next to the ventilation pipe and again at a height of 40 cm above the ventilation pipe. As was the case for the third dive, visual releases could be seen from the ventilation pipe and/or the metal grill throughout the entirety of the fourth dive whenever the ROV was in position to observe the top of the rear section of the sail. Likewise, the samples taken 40 cm above the ventilation pipe were again collected within the plume of the ongoing visual release. The filtered seawater samples collected directly from the ventilation pipe on dive 4 at 33.9 and 34.9 hours showed activity concentrations of Cs-137 of 29.7 ± 0.9 kBq/m^3 and 72.1 ± 2.0 kBq/m^3, which were similar in magnitude to the samples collected directly from the ventilation pipe at 11 hours (dive 2) and 23.1 hours (dive 3). After each of these samples were collected, a sample of seawater was also collected 40 cm over the ventilation pipe. Activity concentrations of Cs-137 in these filtered seawater samples again showed values that were a factor of 10 lower than the respective matching sample that was taken directly from the ventilation pipe. The last filtered seawater sample from the fourth dive, which was taken next to the ventilation pipe and 35.3 hours after the first sample had been taken during the first dive, showed an activity concentration of 14.0 ± 0.4 kBq/m^3.

The activity concentration of Cs-137 in the particulate fractions of the samples that were taken directly from the ventilation pipe during the fourth dive at 33.9 hours (2.3 ± 0.2 kBq/m^3) and 34.9 hours (11.1 ± 0.3 kBq/m^3) showed an increasing trend compared to the previous sample taken directly from the ventilation pipe at 23.1 hours. For the final sample collected next to the ventilation pipe at 35.3 hours, the Cs-137 activity concentration in the particulate fraction in was somewhat lower at 0.72 ± 0.02 kBq/m^3. The Cs-137 activity concentrations in the particulate fractions for the two samples collected 40 cm above the ventilation pipe during the fourth dive were lower still at 0.29 ± 0.08 kBq/m^3 (34 hours) and 0.35 ± 0.09 kBq/m^3 (35 hours).

An overview of the temporal evolution of Cs-137 activity concentrations in the dissolved and particulate fractions of samples collected either directly from or next to the ventilation pipe over the duration of the sampling campaign in 2019 is shown in Figure 4.29.

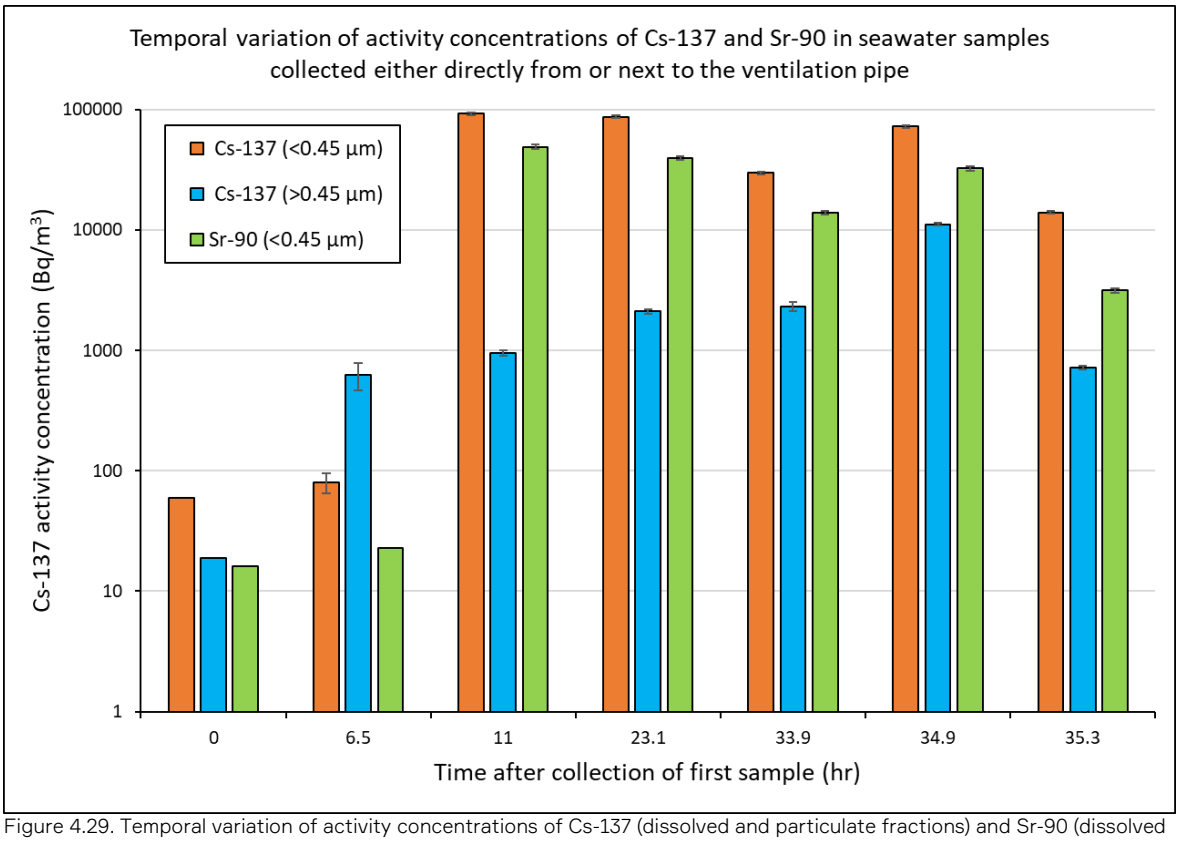

Figure 4.29. Temporal variation of activity concentrations of Cs-137 (dissolved and particulate fractions) and Sr-90 (dissolved fraction only) in seawater samples collected either directly from or next to the ventilation pipe (sample from 35.3 hr only) over the duration of the sampling campaign in 2019. All activity concentrations of Cs-137 and Sr-90 in the first sample collected (0 hr) were below the detection limit. No visual release was observed when the 0 hr and 6.5 hr samples were collected. Visual releases were observed when all other samples in the figure above were collected. Note use of logarithmic scale on the y axis. Error bars represent the measurement uncertainties for samples where activity concentrations were above the detection limit.

The range of Cs-137 activity concentrations in filtered seawater samples collected from or near the ventilation pipe and metal grill when visual releases were observed were within the range of values reported by the Russian investigations between 1993 and 2007 (Hollister, 1993a; Gladkov et al., 1994; Kazennov, 2010). These values are up to 800 000 times higher than typical background values for Cs-137 in seawater from the Norwegian Sea. Activity concentration ratios of Cs-137 between the dissolved (<0.45 µm) and particulate fractions (>0.45 µm) in the small volume samples collected by the ROV varied from 6 to 85, indicating that Cs-137 is released to the marine environment mainly in a dissolved form although a significant colloidal contribution cannot be ruled out. That such elevated levels of Cs-137 have been detected in releases from the reactor in Komsomolets over a period of 30 years, might suggest that the nuclear fuel assemblies have been damaged and that nuclear fuel is in direct contact with seawater.

It is clear from the analytical results that the release of Cs-137 from the submarine can vary over time and there appears to be a direct connection between the release of elevated activity concentrations of Cs-137 and the visual release observed emerging from the ventilation pipe and/or metal grill. In 2019, when no visual release was observed the activity concentration of Cs-137 in filtered seawater from the ventilation pipe was of the order of less than 10^1 Bq/m^3, which then increased to an order of 10^4 Bq/m^3 when visual releases were observed. Seawater collected directly from the ventilation pipe was taken at a depth of 20 to 30 cm inside the pipe which might explain why the sample taken 6.5 hours after the first sample showed an activity concentration above the detection limit despite the lack of any sign of a visual release. It is possible that this sample was taken as activity concentrations of Cs-137 within the ventilation pipe itself began to increase prior to the start of a period of elevated releases to the external environment.

Comparing the results for dissolved and particulate fractions from each sample, it is clear that Cs-137 is mainly present in the dissolved fraction, although a significant amount of Cs-137 is associated with particulate material. This may account for the observations of higher Cs-137 activity concentrations in the particulate fractions compared to the dissolved fractions of two samples collected during dive 1.

When reviewing the video footage from the ROV when the large water sample was collected approximately 3 m directly over the ventilation pipe, no visible release was observed from either the ventilation pipe or the metal grill during the first cast, but a visible release from the ventilation pipe was observed when the second cast was collected. The large water sample was collected in between the two samples that were taken directly from the ventilation pipe on dive 2. Water from both casts was pooled onboard before sub-samples were taken for different analyses. If we assume firstly that there was no release of Cs-137 from the ventilation pipe during the first cast, secondly that the volumes collected from the first and second casts were identical and thirdly that the average activity concentration of Cs-137 observed since 1995 (1.2 ± 0.5 Bq/m^3) represents a typical value for bottom water, we can derive a theoretical value of 10.6 Bq/m^3 for the seawater collected during the second cast.

Overall, the results indicate that releases of Cs-137 are rapidly diluted resulting in a clear gradient in activity concentrations in the immediate area around the release point (Figure 4.30). The one seawater sample taken next to the opening to the ventilation pipe showed an activity concentration of Cs-137 that was a factor of 10 lower than the sample taken directly from the ventilation pipe shortly beforehand. Furthermore, the samples taken 40 cm above the ventilation pipe whilst visual releases were observed, showed activity concentrations of Cs-137 that were a further factor of 10 to 100 lower than the sample collected next to the ventilation pipe (Figure 4.30).

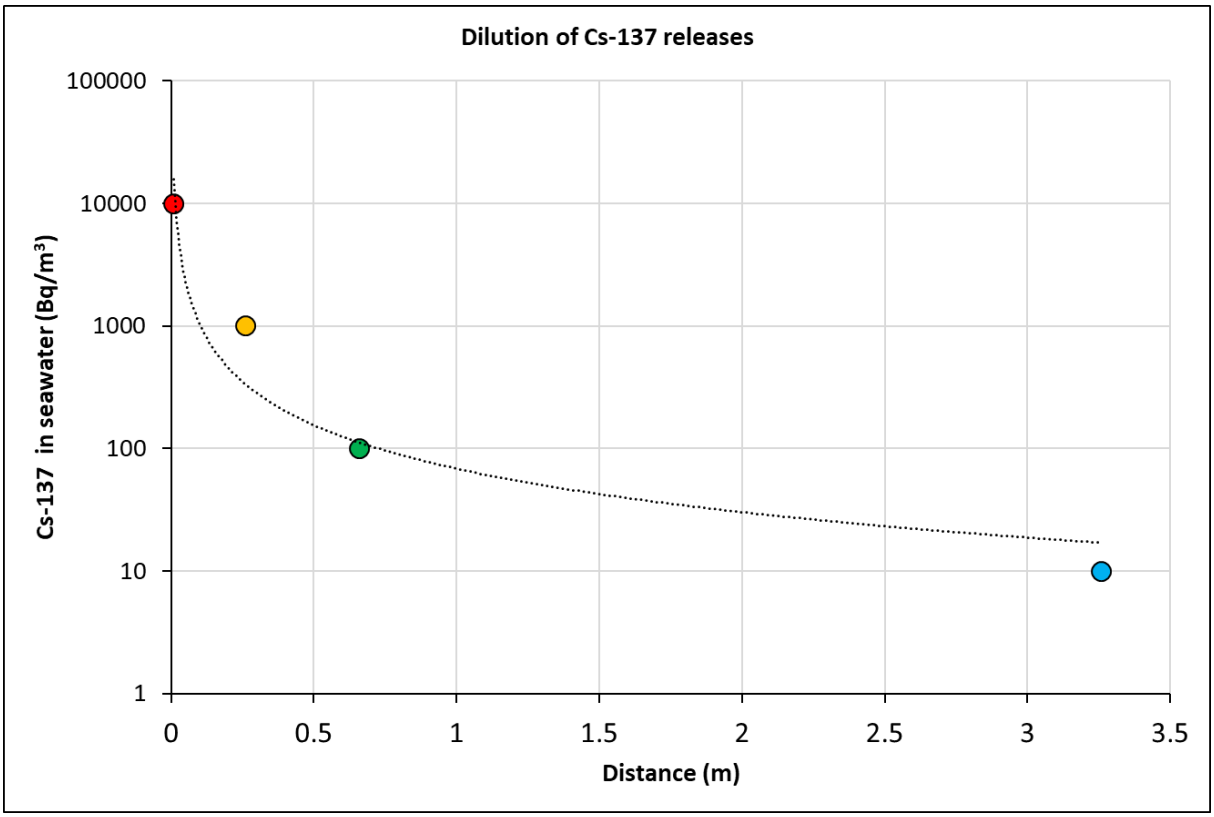

Figure 4.30. Estimated rate of dilution of Cs-137 releases based on the magnitude of Cs-137 activity concentrations (Bq/m^3) in filtered seawater at different distances from the release point. The red dot represents samples taken directly from ventilation pipe at an assumed depth of 25 cm within the pipe. The orange dot represents the sample taken next to the ventilation pipe (assumed distance of 1 cm). The green dot represents samples taken 40 cm over ventilation pipe. The blue dot represents the large volume sample taken 3 m over the ventilation pipe, with a magnitude based on the theoretical value derived for second cast. For use in the figure above, the first data point is set to 0 m, and all other data points shifted by 25 cm to take into account the assumed sampling depth inside the ventilation pipe.

Although the elevated activity concentrations of Cs-137 in the sample that was collected from above the metal grill could be explained by the resuspension and inclusion of some of the particulate material from the metal grill when this sample was collected, an alternative hypothesis could be that releases from the metal grill represent a different pathway from the reactor compared to the pathway leading to the ventilation pipe. However, since no sample was taken from the ventilation pipe at the same time as the sample that was collected near the metal grill, this difference could also simply reflect the inherent variation in activity released over time.

Table 4.1. Activity concentrations of Cs-137 and Sr-90 (Bq/m^3) in filtered (<1 µm) large volume surface and bottom seawater samples[a].

Depth	Cs-137 (Bq/m^3)	Sr-90 (Bq/m^3)
Surface	1.0 ± 0.4	-[b]
Bottom[c]	5.9 ± 0.3	2.0 ± 0.2

a – 75 l for Cs-137 and 50 l for Sr-90

b - Sample was lost during the analytical process.

c - Samples were taken approximately 3 m directly over the ventilation pipe. Samples represent water collected from 2 separate casts. Visual releases were observed during the second cast, but not the first cast.

Table 4.2. Activity concentrations of Cs-137 and Sr-90 (Bq/m^3) in dissolved fractions (<0.45 µm) and Cs-137 activity concentrations (Bq/m^3) in the particulate fraction (>0.45 µm) of small volume seawater samples collected by the ROV[a].

Dive No.	Sample description	Time interval (hr)[b]	Visual release observed	Cs-137 (Bq/m^3)[c] <0.45 µm	Cs-137 (Bq/m^3)[d] >0.45 µm	Sr-90 (Bq/m^3) <0.45 µm
1	From the ventilation pipe	0	N	<60	<19	<16
	1 m over the ventilation pipe	0.1	N	<60	520 ± 130	<16
	5 m over the ventilation pipe	0.2	N	<5.9[e]	<14	<26
	~1 m from starboard side of RC[f]	0.4	N	<2.4[e]	<7	<20
	~1 m from port side of RC[f]	0.5	N	11.7 ± 1.1[e]	270 ± 60	<13
2	From the ventilation pipe	6.5	N	80 ± 15	630 ± 160	<23
	From the ventilation pipe	11	Y	92600 ± 2600	950 ± 50	49000 ± 2000
3	Above metal grill[g]	16.5	Y	791700 ± 22000	78400 ± 2470	398000 ± 15000
	40 cm above ventilation pipe	23	Y	7700 ± 200	86 ± 6	3580 ± 135
	From the ventilation pipe	23.1	Y	86900 ± 2500	2100 ± 90	39500 ± 1500
	40 cm above ventilation pipe	24.5	Y	420 ± 50	256 ± 70	174 ± 14
4	From the ventilation pipe	33.9	Y	29700 ± 900	2320 ± 200	13900 ± 500
	40 cm above ventilation pipe	34	Y	1060 ± 60	290 ± 80	480 ± 25
	From the ventilation pipe	34.9	Y	72100 ± 2000	11100 ± 290	32400 ± 1200
	40 cm above ventilation pipe	35	Y	6000 ± 200	350 ± 90	2240 ± 85
	Next to ventilation pipe	35.3	Y	14000 ± 400	720 ± 20	3150 ± 135

a – The volumes collected for these samples were between 0.6 and 2.1 l.

b - Time interval after the first sample was taken.

c - Analysed by direct gamma spectroscopy analysis of seawater sample unless otherwise stated.

d - Activity concentrations for particulate fractions (>0.45 µm) are calculated back to the original volume of seawater that was filtered.

e - Pre-concentrated with AMP before gamma spectroscopy analysis of precipitate.

f - Reactor compartment.

g - Note, some of the particulate material from the metal grill was resuspended and taken up the syringe sampler when this sample was collected.

4.3.2 Strontium-90 (Sr-90)

Results for the analysis of large and small volume seawater samples for Sr-90 are given in Tables 4.1 and 4.2, respectively. Unfortunately, the sample of filtered surface seawater collected over Komsomolets was lost during the analysis procedure, but typical values for Sr-90 in surface water for previous and subsequent monitoring up to 2021 have been around 1 Bq/m^3, which is typical for current levels of Sr-90 in the wider Norwegian Sea (Skjerdal et al., 2020). The activity concentration of Sr-90 in filtered bottom seawater collected approximately 3 m directly over the ventilation pipe was 2.0 ± 0.2 Bq/m^3 (Table 4.1). This is around 3 times higher than the average activity concentration for bottom seawater sampled around Komsomolets since 2004 (0.6 ± 0.4 Bq/m^3), when samples were collected from surface ships alone (Figure 4.31).

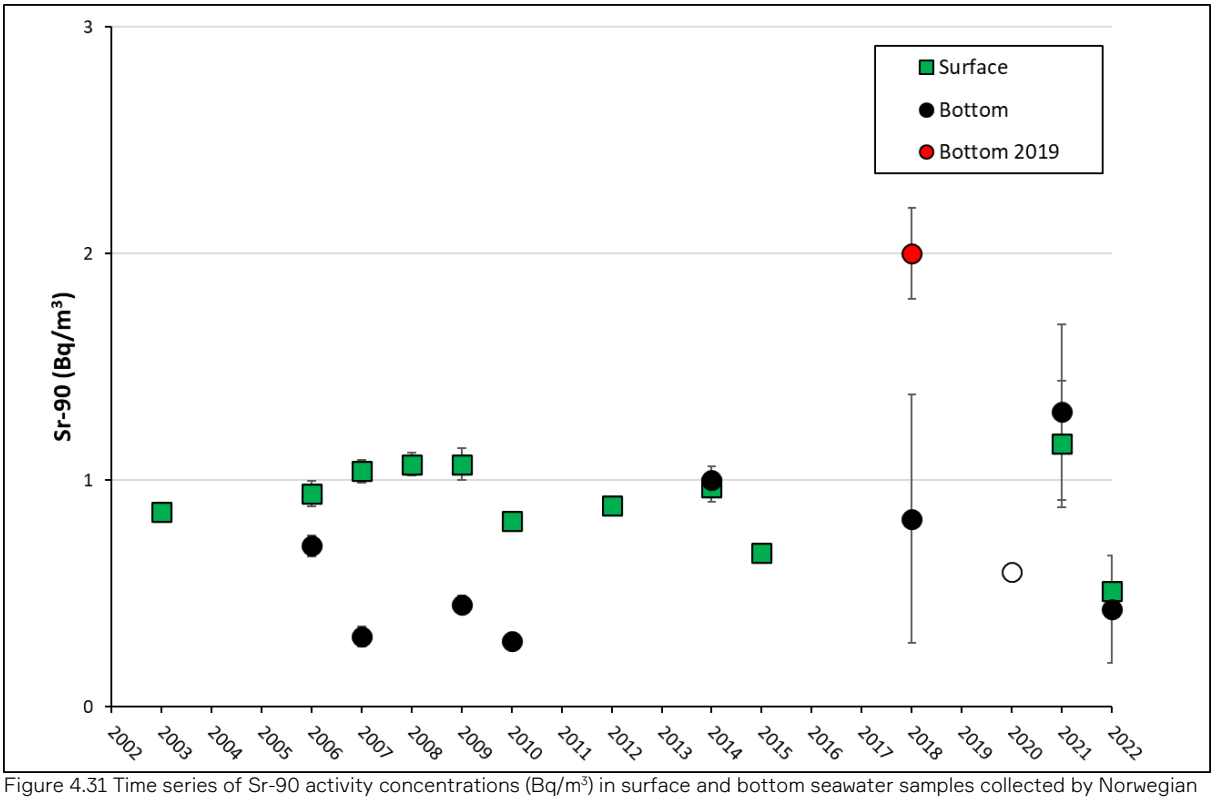

Figure 4.31 Time series of Sr-90 activity concentrations (Bq/m^3) in surface and bottom seawater samples collected by Norwegian monitoring at the site of Komsomolets since 2004. Data values for individual years represent individual measurements. Open symbols represent values below detection limits. Uncertainties on individual measurements were typically around 10%. The observed activity concentration in the bottom seawater sample collected around 3 m directly over the ventilation pipe in 2019 is included as the red dot. Data for 1991 to 2015 from Gwynn et al. (2018). Data for 2016 to 2018 and 2020 to 2022 from the Norwegian national monitoring programme (unpublished).

We can expect that Sr-90 would be as soluble in seawater as Cs-137. Therefore, using the same assumptions as for Cs-137 to take into account that visual releases were observed during the second cast to collect the large volume seawater samples, we can derive a theoretical value of 3 Bq/m^3 for Sr-90 in seawater collected during the second cast.

For the small volume seawater samples collected by the ROV, activity concentrations of Sr-90 followed the same trends as observed for Cs-137. For seawater samples which were collected when no visual release was observed from either the ventilation pipe and/or the metal grill, activity concentrations of Sr-90 were below detection limits (<13 to <23 Bq/m^3). This was the case for the five small seawater samples collected on dive 1 and for the first sample collected on dive 2. When visual releases were observed emerging from the ventilation pipe, all seawater samples showed levels of Sr-90 above the detection limit, with the magnitude of the observed activity concentration dependent on the sampling location. Samples

of seawater collected directly from the ventilation pipe showed activity concentrations of Sr-90 between 13.9 ± 0.5 to 49 ± 2 kBq/m^3, whereas the one sample of seawater collected near the ventilation pipe showed an activity concentration of Sr-90 of 3.2 ± 0.1 kBq/m^3. An overview of the temporal evolution of Sr-90 activity concentrations in the dissolved fraction of samples collected either directly from or next to the ventilation pipe over the duration of the sampling campaign in 2019 is shown in Figure 4.27. Samples of seawater collected 40 cm over the ventilation pipe when visual releases were observed showed activity concentrations of Sr-90 between 0.17 ± 0.01 to 3.6 ± 0.1 kBq/m^3. As was the case for Cs-137, the highest activity concentration of Sr-90 (398 ± 15 kBq/m^3), was observed in the sample of seawater that was collected near the metal grill. These values are up to 400 000 times higher than typical background values for Sr-90 in seawater from the Norwegian Sea (Skjerdal et al., 2017; RAME unpublished). However, the results for Sr-90 in the large and small volume seawater samples again indicate that the releases from the reactor are rapidly diluted in the immediate area around the release point.

4.3.3 Activity concentration ratios of Cs-137/Sr-90

The activity concentration ratio of Cs-137 to Sr-90 in the large volume water sample based on the observed measurements was 3. For the small volume water samples this ratio was typically around 2.2 (including the sample collected above the metal grill) for all samples sampled between 11 and 35 hours but was somewhat higher (4.4) for the last sample that was collected (Table 4.3). These dissolved fraction ratios are higher than the predicted activity concentration ratio of Cs-137 to Sr-90 in the reactor which has been estimated as approximately 1:1 (Gladkov et al., 1994; Høibråten et al. 1997). However, a Soviet study that investigated the effect of exposing nuclear fuel assemblies to seawater, that were similar in design to those we might expect to have been used in the reactor of Komsomolets, reported that Cs-137 selectively leached from the exposed nuclear fuel matrices at a rate that was approximately 3 times greater than for Sr-90 (Zhuravkov et al., 1992). Such selective leaching may account for the higher observed activity concentration ratios in the dissolved fraction of the large and small volume samples than predicted based on the estimated radionuclide inventory. It might be anticipated that ratios of Cs-137 to Sr-90 in the particulate fraction of the small volume samples would be higher than the dissolved fractions due to the likely greater association of Cs-137 with particulate material than Sr-90. However, This provides further evidence that the nuclear fuel is in direct contact with seawater. Furthermore, Zhurakov et al (1992) concluded that the activity concentration ratio of Cs-137 to Sr-90 in seawater would only match that in the nuclear fuel when the fuel underwent corrosion induced destruction. As such, future monitoring of the activity concentration ratios of Cs-137 to Sr-90 in such samples may provide insights into the deterioration of the nuclear fuel within the reactor.

Table 4.3. Activity concentration ratios of Cs-137 and Sr-90 in the dissolved fractions (<0.45 µm) of small volume seawater samples collected by the ROV.

Dive No.	Sample description	Time interval (hr)[a]	Visual release observed	Cs-137/Sr-90
1	From the ventilation pipe	0	N	NA
	1 m over the ventilation pipe	0.1	N	NA
	5 m over the ventilation pipe	0.2	N	NA
	~1 m from starboard side of RC[b]	0.4	N	NA
	~1 m from port side of RC[b]	0.5	N	NA
2	From the ventilation pipe	6.5	N	NA
	From the ventilation pipe	11	Y	1.9 ± 0.1

3	Above metal grill[c]	16.5	Y	2.0 ± 0.1
	40 cm above ventilation pipe	23	Y	2.2 ± 0.2
	From the ventilation pipe	23.1	Y	2.2 ± 0.1
	40 cm above ventilation pipe	24.5	Y	2.4 ± 0.6
4	From the ventilation pipe	33.9	Y	2.1 ± 0.2
	40 cm above ventilation pipe	34	Y	2.2 ± 0.3
	From the ventilation pipe	34.9	Y	2.2 ± 0.1
	40 cm above ventilation pipe	35	Y	2.7 ± 0.2
	Next to ventilation pipe	35.3	Y	4.4 ± 0.3

a - Time interval after the first sample was taken.

b - Reactor compartment.

c - Note, some of the particulate material from the metal grill was resuspended and taken up by the syringe sampler when this sample was collected.

4.3.4 Plutonium isotopes (Pu-239 and Pu-240)

Results for the analysis of large volume seawater samples for plutonium isotopes are given in Table 4.4. The combined activity concentration of Pu-239 and Pu-240 in 0.45 µm filtered surface seawater collected over Komsomolets was 2.5 ± 0.3 mBq/m^3 which was comparable to values for surface water for previous and subsequent monitoring years up to 2021 (Figure 4.30) and is typical for current levels of Pu-239,240 in the wider Norwegian Sea (Skjerdal et al., 2020; RAME, unpublished). The combined activity concentration of Pu-239 and Pu-240 in 10 kDa filtered surface seawater was similar to the <0.45 µm sample, indicating that only a minor fraction of plutonium isotopes was associated with colloids. These levels reflect the current low contribution of known sources of these plutonium isotopes to surface waters in the North-East Atlantic from European reprocessing plants at Sellafield (UK) and la Hague (France) as well as fallout from the Chernobyl accident. The combined activity concentration of Pu-239 and Pu-240 in 0.45 µm filtered bottom seawater collected approximately 3 m directly over the ventilation pipe was 10.7 ± 0.5 mBq/m^3. Unlike the situation that was observed for Cs-137 and Sr-90, this value was comparable to Pu-239,240 activity concentrations for bottom water for previous and subsequent monitoring years up to 2021 (Figure 4.30). Again, the combined activity concentration of Pu-239 and Pu-240 in 10 kDa filtered bottom water sample was similar to the <0.45 µm sample. Due to the differences in solubility of Pu-239 and Pu-240 compared to Cs-137 and Sr-90 it does not make sense to derive a theoretical value for these plutonium isotopes in seawater collected during the second cast when visual releases were observed coming from the ventilation pipe. Higher activity concentrations of Pu-239 and Pu-240 in bottom water compared to surface water likely reflect the scavenging and export of plutonium isotopes from surface waters by organic and inorganic particulate material and the subsequent dissolution of such material and release these plutonium isotopes in deeper waters (e.g., Livingston & Anderson, 1983; Nyffeler et al., 1996). The combined activity concentrations of Pu-239 and Pu-240 in 0.45 µm filtered bottom seawater collected at two locations near the torpedo compartment were similar to the value for 0.45 µm filtered bottom seawater collected approximately 3 m directly over the ventilation pipe.

Results for the analysis of the dissolved and particulate fractions from the small volume seawater samples for plutonium isotopes are given in Table 4.5. Analysis for Pu-239 and Pu-240 was only performed for small volume samples that were collected when visual releases were observed from the ventilation pipe. Of these samples, activity concentrations of Pu-239 and Pu-240 were both above the detection limit in only two of the filtered seawater samples, one of these being the sample collected

above the metal grill and which showed the highest activity concentrations for Cs-137 and Sr-90. The combined activity concentration of Pu-239 and Pu-240 in filtered seawater from the sample collected above the metal grill was 775 ± 51 mBq/m^3, which is 64 times higher than the average activity concentration for Pu-239,240 in bottom water sampled around Komsomolets since 1993 (Figure 4.32). Again, when interpreting this result, it should be remembered that some of the particulate material from the metal grill was resuspended and taken up by the syringe sampler when this sample was collected. Importantly, we do not know what the effect of the recovery of these samples from 1700 m to the surface might have had on the dissolution or precipitation of such radionuclides. Although the sample collected above the metal grill was filtered onboard there is also a need to consider the impact of storage on the other samples prior to their filtration in the laboratory. In the other sample, which was collected 40 cm above the ventilation pipe, the combined activity concentration of Pu-239 and Pu-240 in filtered seawater was 26 ± 9 mBq/m^3, 2.1 times higher than the average activity concentration for Pu-239,240 in bottom water sampled around Komsomolets since 1993. In the other eight samples that were analysed for Pu-239 and Pu-240, activity concentrations of Pu-239 were above the detection limit in five samples, with values for Pu-239 alone in two samples higher than the range of activity concentrations for the sum of Pu-239 and Pu-240 in bottom water sampled around Komsomolets since 1993.

Activity concentrations of Pu-240 in the particulate fractions from five of the ten small volume samples that were analysed were below the detection limits, including all four samples that were collected 40 cm above the ventilation pipe. Again, the highest combined activity concentration for Pu-239 and Pu-240 in any particulate fraction was from the sample collected above the metal grill at 54500 ± 1500 mBq/m^3, which was 2 orders of magnitude higher than any other particulate fraction where activity concentrations for both Pu-239 and Pu-240 were above the detection limit. As mentioned previously, this result probably reflects the inclusion of particulate material from the metal grill as this sample was collected. Combined activity concentrations of Pu-239 and Pu-240 in the particulate fractions from the remaining four samples ranged from 138 ± 31 to 570 ± 41 mBq/m^3. For the particulate fractions from the five samples where activity concentrations of Pu-240 were below the detection limit, activity concentrations of Pu-239 ranged from 6 ± 3 to 14 ± 3 mBq/m^3. As activity concentrations of Pu-239 in the particulate fractions of samples showed a sharp decrease in magnitude between samples taken within and 40 cm above the ventilation pipe, this might indicate that plutonium associated with particulate material undergoes relatively rapid vertical settling.

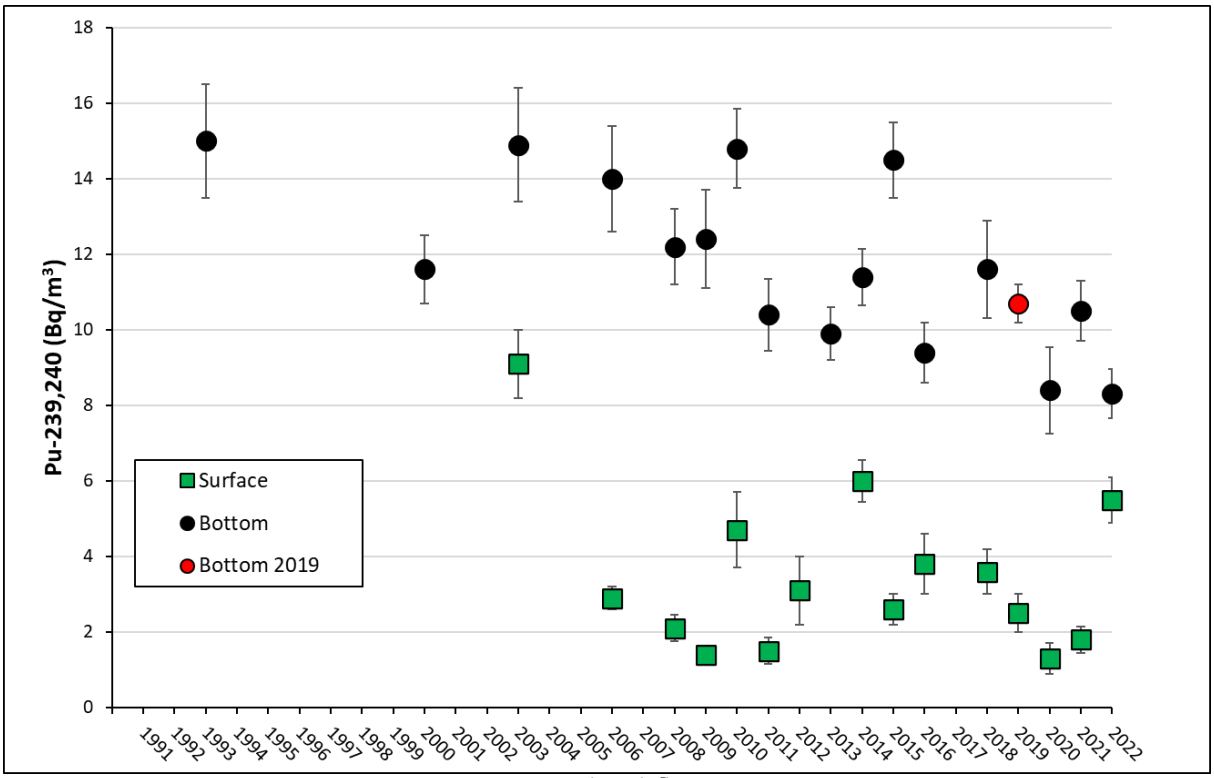

Figure 4.32. Time series of Pu-239,240 activity concentrations (mBq/m³) in surface and bottom seawater samples collected by Norwegian monitoring at the site of Komsomolets since 1992. Data values for individual years represent individual measurements. Uncertainties on individual measurements were typically less than 10%. The observed combined activity concentration of Pu-239 and Pu-240 in the bottom seawater sample collected around 3 m directly over the ventilation pipe in 2019 is included as the red dot. Data for 1991 to 2015 from Gwynn et al. (2018). Data for 2016 to 2018 and 2020 to 2022 from the Norwegian national monitoring programme (unpublished).

Table 4.4. Combined Pu-239 and Pu-240 activity concentrations (mBq/m³) and Pu-240/Pu-239 atom ratios in filtered large volume surface and bottom seawater samples[a].

Depth	Size fraction	Pu-239 and Pu-240 (mBq/m³)	Pu-240/Pu-239
Surface	<0.45 µm	2.5 ± 0.3	0.144 ± 0.041
	<10 kDa	2.0 ± 0.2	0.254 ± 0.062
Bottom (~3 m over ventilation pipe)[b]	<0.45 µm	10.7 ± 0.5	0.185 ± 0.029
	<10 kDa	10.8 ± 0.9	0.168 ± 0.046
Bottom (beside port dive plane)	<0.45 µm	8.6 ± 0.9	0.187 ± 0.044
Bottom (beside portside opening in TC[c])	<0.45 µm	10.8 ± 0.9	0.180 ± 0.033

a – The volume collected for these samples was 40 l.

b - Sample represents water collected from 2 separate casts. Visual releases were observed during the second cast, but not the first cast.

c - Torpedo compartment. Figure 2.2. shows this sample being collected.

Table 4.5. Activity concentrations of Pu-239 and Pu-240 (mBq/m^3) and Pu-240/Pu-239 atom ratios in dissolved (<0.45 μm) and particulate (>0.45 μm) fractions of small volume seawater samples collected by the ROV[a].

Dive No.	Sample description	Time interval (hr)[b]	<0.45 μm			>0.45 μm		
			Pu-239 (mBq/m^3)	Pu-240 (mBq/m^3)	Pu-240/Pu-239	Pu-239 (mBq/m^3)[c]	Pu-240 (mBq/m^3)[c]	Pu-240/Pu-239
2	From the ventilation pipe	11	<14	<17	-	150 ± 21	177 ± 40	0.322 ± 0.084
3	Above metal grill[d]	16.5	516 ± 34	259 ± 39	0.137 ± 0.022	37200 ± 1310[e]	17300 ± 700[e]	0.127 ± 0.004[e]
	40 cm above ventilation pipe	23	7.6 ± 1.8	<14	-	14 ± 3	<21	-
	From the ventilation pipe	23.1	<21	<18	-	96 ± 14	42 ± 28	0.119 ± 0.081
	40 cm above ventilation pipe	24.5	2.2 ± 1.3	<14	-	6 ± 3	<29	-
4	From the ventilation pipe	33.9	<25	<24	-	373 ± 25	197 ± 33	0.143 ± 0.025
	40 cm above ventilation pipe	34	14 ± 2	<17	-	6 ± 2	<12	-
	From the ventilation pipe	34.9	20 ± 9	<19	-	123 ± 101	72 ± 19	0.158 ± 0.044
	40 cm above ventilation pipe	35	11 ± 2	15 ± 9	0.37 ± 0.24	7 ± 2	<20	-
	Next to ventilation pipe	35.3	57 ± 7	<49	-	13 ± 5	<26	-

a – The volumes collected for these samples were between 0.6 and 2.1 l. None of samples collected during Dive 1 were analysed for Pu-239 and Pu-240.

b - Time interval after the first sample was taken. Visual releases were observed when all these samples were collected.

c - Activity concentrations for particulate fractions (>0.45 μm) are calculated back to the original volume of seawater that was filtered.

d - Note, some of the particulate material from the metal grill was resuspended and taken up by the syringe sampler when this sample was collected.

e – Note, only part of the filter from this sample was digested for plutonium isotope analysis, but further gamma spectroscopy analysis of the part of the filter that was not digested showed that most of the Cs-137 (96%) and Am-241 (result was below the detection limit) activity was contained within the part of the filter that was digested.

4.3.5 Atom ratios of Pu-240/Pu-239

Atom ratios for Pu-240/Pu-239 in large and small volume seawater samples are given in Tables 4.4 and 4.5, respectively. The Pu-240/Pu-239 atom ratios for filtered surface seawater were 0.144 ± 0.041 for the <0.45 µm fraction and 0.254 ± 0.062 for the <10 kDa fraction. Activity concentrations of Pu-239,240 and atom ratios of Pu-240/Pu-239 in surface waters of the Norwegian Sea would be expected to be influenced by the main sources of these plutonium isotopes, namely global fallout, discharges from the nuclear reprocessing facilities at Sellafield (UK) and la Hague (France), and Chornobyl deposition. The atom ratios for surface water fall either side of the reported global fallout value (0.180 ± 0.014) for northern regions (Kelley et al., 1999) and the range of reported values (0.184 ± 0.003 to 0.242 ± 0.004) for an Irish Sea seawater reference material (IAEA-381) from 1993 (Lee et al., 2001; Eigl et al., 2013; Cao et al., 2016), but are lower than the value (0.34 ± 0.03) reported for effluent from la Hague (Oughton et al. 1999) and a value (0.38 ± 0.07) for Chornobyl deposition (Lindahl et al., 2010). Further interpretation of the atom ratios for these surface water samples is difficult.

The Pu-240/Pu-239 atom ratios for all the large volume bottom filtered seawater samples were similar to each other and the reported global fallout value (0.180 ± 0.014) for northern regions (Kelley et al., 1999). The atom ratios for these samples show no influence of potential sources of these plutonium isotopes from either the reactor or the two nuclear warheads within the torpedo compartment. Based on estimated total inventories for Pu-239 and Pu-240 (Gladkov et al., 1994; Høibråten et al., 1997), the atom ratio for Pu-240/Pu-239 in the reactor is 0.105, which is somewhat lower than the value (0.13) that has been estimated for Russian submarine pressurised water reactors (Sivintsev, 1995). However, it can be expected that atom ratios for Pu-240/Pu-239 may vary between individual fuel rods due to any differences in enrichment and burnup (Moghaddam et al., 2011). Pu-240/Pu-239 atom ratios for weapons grade plutonium have been reported as being typically less than 0.07 (e.g., Choppin et al., 1995; Momoshima et al., 1997; Oughton et al., 2000; Geckeis et al., 2019).

The atom ratio of Pu-240/Pu-239 for the small volume filtered seawater sample collected above the metal grid was 0.137 ± 0.022, which is closer to the aforementioned reactor ratios than the value for global fallout. The atom ratio of Pu-240/Pu-239 in the other small volume filtered seawater sample where activity concentrations of both Pu-239 and Pu-240 were above the detection limit is difficult to interpret due to its high associated uncertainty. The atom ratio of Pu-240/Pu-239 in the particulate fractions from the sample collected above the metal grid (0.127 ± 0.004) and from one sample collected from the ventilation pipe (0.119 ± 0.081) also showed good agreement to estimated reactor ratios, while a further two atom ratios in the particulate fractions from samples collected from the ventilation pipe were lower than the reported value for global fallout. The particulate fraction from the remaining sample collected from the ventilation pipe showed a Pu-240/Pu-239 atom ratio that was far higher than the value reported for global fallout, which is difficult to explain in the context of releases from the reactor but might reflect variations in enrichment and burnup of individual fuel rods (Moghaddam et al., 2011). Overall, the atom ratios of Pu-240/Pu-239 in filtered seawater and particulate fractions from these samples would suggest that that the source of the elevated activity concentrations of Pu-239 and Pu-240 in these samples is from the spent nuclear fuel in the reactor of Komsomolets.

4.3.6 Uranium-236 (U-236)

Results for the dissolved and particulate fractions from the small volume seawater samples for U-236 are given in Table 4.6. In filtered seawater, the highest U-236 activity concentration was again observed in the sample that was collected above the metal grill at 3.4 ± 1.7 mBq/m^3. U-236 activity concentrations in the other filtered seawater samples ranged from 0.15 ± 0.03 to 1.7 ± 0.3 mBq/m^3 and showed no clear

trend for where these samples were collected. A similar situation was seen for U-236 in particulate fractions, with the highest activity concentration observed in the particulate fraction from the sample that was collected above the metal grill at 4.6 ± 1.2 mBq/m^3. Activity concentrations of U-236 in particulate fractions from other samples ranged from 0.06 ± 0.02 to 2.7 ± 0.4 mBq/m^3. The main sources of U-236 to surface waters in the Norwegian Sea are from global fallout, the European reprocessing plants at Sellafield (UK) and Cap la Hague (France) and previous discharges from the nuclear fuel fabrication plant at Springfields (UK) (e.g., Casacuberta et al., 2014; Christl et al., 2015a). Uranium-236 behaves conservatively in seawater (e.g., Sakaguchi et al., 2012), with no expected inputs from global fallout at depths below 1000 m, except in regions where deep water formation occurs (e.g., Christl et al., 2012; Casacuberta et al., 2014). Activity concentrations in surface water near Sellafield and la Hague have been reported to be between 13 to 19.3 mBq/m^3 (1993) and 0.2 mBq/m^3 (2009), respectively, with lower values of 0.014 mBq/m^3 in surface waters of the northern part of the open North Sea and 0.014 to 0.026 mBq/m^3 in surface waters at the entrance of the Barents Sea (Lee et al., 2008; Eigl et al., 2013; Christl et al., 2015b; Casacuberta et al., 2018). For further comparison, activity concentrations of U-236 in surface water from the South Atlantic (which should only reflect the influence of global fallout) have been reported to be as low as 0.005 mBq/m^3 in 2010 (Casacuberta et al., 2014). Compared to the aforementioned value for the North Sea, the activity concentration of U-236 in the sample that was collected above the metal grill was 243 times higher. In view of these other known sources of U-236, it is clear that the source of the elevated activity concentrations of U-236 observed in the small volume samples is from the spent nuclear fuel in the reactor of Komsomolets. Activity concentration ratios of U-236 between filtered seawater and particulate fractions in the small volume samples collected by the ROV were greater than one in all but two cases, which reflects the conservative behaviour of U-236 in seawater. Of the two exceptions, notably one of these was the sample that was collected above the metal grill, which may indicate the presence of U-236 in the particulate material that was resuspended from the metal grill and taken up by the syringe sampler when this samples was collected.

4.3.7 Atom ratios of U-236/Pu-239

Atom ratios for U-236/Pu-239 in the small volume seawater samples are given in Table 4.6. Due to the very different biogeochemical behaviour of U-236 and Pu-239 in the marine environment, it can be difficult to relate observational ratios of these radionuclides directly to known source terms. Atom ratios for U-236/Pu-239 for global fallout have been reported to range from 0.14 to 1.4 (Wendel et al., 2013; Röllin et al., 2020), but global fallout ratios would not be expected to be preserved in bottom water at the depth where Komsomolets lies. Atom ratios of U-236/Pu-239 of 1.3 to 2.3 have been reported for surface seawater near Sellafield from 1993 (Lee et al., 2008; Eigl et al., 2013). Higher values (5.8 ± 2.4 to 14 ± 8) have been reported in the top 250 m at two locations in the central Arctic Ocean in 2011, whereas a lower U-236/Pu-239 atom ratio of 1.2 ± 0.2 was reported at 1800 m from one of these locations (Chamizo et al., 2015). This range of U-236/Pu-239 atom ratios in seawater reflects the intrinsic differences in solubility and vertical transport of U-236 and plutonium isotopes within the water column. The available atom ratios of U-236/Pu-239 in filtered seawater were all greater than one and ranged from 6.4 ± 3.2 to 85 ± 40. Where atom ratios of U-236/Pu-239 were available for matching dissolved and particulate fractions, the atom ratios for particulate fractions were lower except for the sample collected next to the ventilation pipe (35.3 hours). A comparison of Pu-240/Pu-239 versus U-236/Pu-239 atom ratios for dissolved and particulate fractions from the small volume seawater samples against suitable endmember values provides further evidence that releases of plutonium isotopes and U-236 are occurring from the reactor of Komsomolets (Figure 4.33).

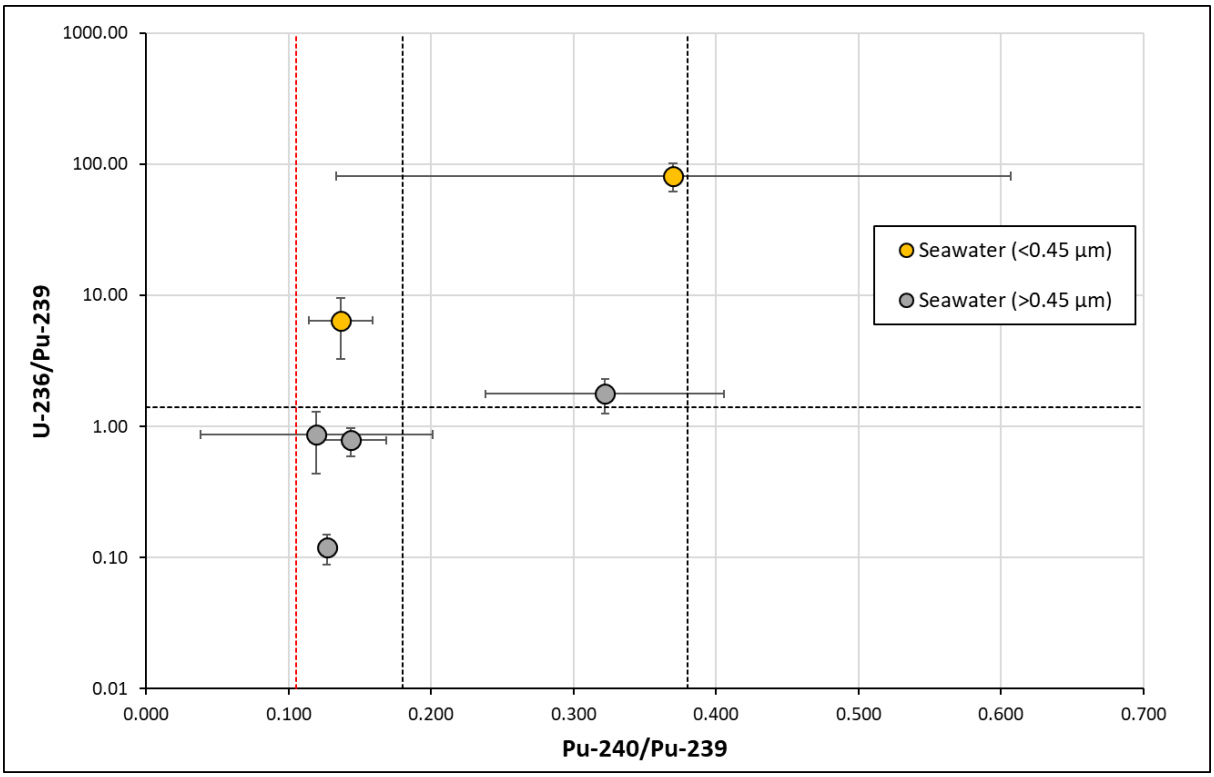

Figure 4.33. Plot showing relationship between atom ratios of U-236/Pu-239 and Pu-240/Pu-239 for all dissolved (<0.45 µm) and particulate (>0.45 µm) fractions from small volume filtered seawater samples where it was possible to determine both ratios. Error bars show propagated uncertainties (1 sigma). The black horizontal dashed line shows the reported U-236/Pu-239 atom ratio for seawater at 1800 m in the central Arctic Ocean (Chamizo et al., 2015). The red vertical dashed line shows the Pu-240/Pu-239 atom ratio derived from the estimated Pu-239 and Pu-240 reactor inventories for Komsomolets (Gladkov et al., 1994; Høibråten et al., 2008). The black vertical dashed lines show the maximum (Chornobyl deposition) and minimum (global fallout) of the range of Pu-240/Pu-239 atom ratios for other sources of these plutonium isotopes to the Norwegian Sea.

Table 4.6. Activity concentrations of U-236 (mBq/m^3) and U-236/Pu-239 atom ratios in dissolved (<0.45 μm) and particulate (>0.45 μm) fractions of small volume seawater samples collected by the ROV[a].

Dive No.	Sample description	Time interval (hr)[b]	<0.45 μm		>0.45 μm	
			U-236 (mBq/m^3)	U-236/Pu-239	U-236 (mBq/m^3)[c]	U-236/Pu-239
2	From the ventilation pipe	11	0.79 ± 0.29	-[d]	0.27 ± 0.07	1.8 ± 0.5
3	Above metal grill[e]	16.5	3.4 ± 1.7	6.4 ± 3.2	4.6 ± 1.2[f]	0.12 ± 0.03[g]
	40 cm above ventilation pipe	23	NM[g]	-	0.07 ± 0.03	4.5 ± 2.3
	From the ventilation pipe	23.1	0.65 ± 0.23	-[d]	0.09 ± 0.04	0.87 ± 0.43
	40 cm above ventilation pipe	24.5	NM[g]	-	0.10 ± 0.04	17 ± 11
4	From the ventilation pipe	33.9	0.40 ± 0.09	-[d]	0.30 ± 0.07	0.78 ± 0.19
	40 cm above ventilation pipe	34	0.15 ± 0.03	11 ± 3	0.06 ± 0.02	10 ± 5
	From the ventilation pipe	34.9	1.7 ± 0.3	85 ± 40	<0.12	-
	40 cm above ventilation pipe	35	0.92 ± 0.10	81 ± 20	0.09 ± 0.02	11 ± 3
	Next to ventilation pipe	35.3	0.44 ± 0.08	7.4 ± 1.7	2.7 ± 0.4	204 ± 80

a - The volumes collected for these samples were between 0.6 and 2.1 l. None of samples collected during Dive 1 were analysed for U-236 and Pu-239.

b - Time interval after the first sample was taken. Visual releases were observed when all these samples were collected.

c - Activity concentrations for particulate fractions (>0.45 μm) are calculated back to the original volume of seawater that was filtered.

d – No atom ratio possible as result for Pu-239 was below the detection limit.

e - Note, some of the particulate material from the metal grill was resuspended and taken up by the syringe sampler when this sample was collected.

f – Note, only part of the filter from this sample was digested for plutonium isotope analysis, but further gamma spectroscopy analysis of the part of the filter that was not digested showed that most of the Cs-137 (96%) and Am-241 (result was below the detection limit) activity was contained within the part of the filter that was digested.

g – Not measured.

4.3.8 Trace elements

Trace element data can provide useful site-specific insights into the behaviour and occurrence of their radioactive counterparts allowing for more accurate predictions of the consequences of any hypothetical releases from Komsomolets.

The concentration of trace elements in seawater were generally similar in the large surface seawater sample compared to the three large bottom seawater samples that were collected 3 m over the ventilation pipe and at two locations on the port side close to the torpedo compartment (Table 4.7). The concentration of trace elements in 0.45 µm and 10 kDa filtered samples were quite similar demonstrating that the dissolved trace metals in the large volume samples were present mainly as low molecular mass species.

The dissolved fractions of the small volume seawater samples collected by the ROV that were analysed for trace elements had all been collected when visual releases were observed. The concentration of several trace elements in the samples that were collected directly from the ventilation pipe, next to the ventilation pipe and above the metal grill were elevated compared to the large volume water samples and in particular for Al, Mn, Ni, Cu, Zn, Cd and Ba (Table 4.8). Overall, these results likely indicate ongoing corrosion processes within the submarine. The concentration of the same trace elements in the small volume samples collected 40 cm above the ventilation pipe when visual releases were observed were typically lower (Table 4.8). Data for uranium in large and small seawater samples is not shown, but there was no difference in the concentration of uranium in any of the samples that were analysed.

Compared to quality standards for coastal seawater set by the Norwegian Environment Agency, the elevated levels of Ni, Cu, Zn and Cd in some of the small volume samples would be classified as giving rise to chronic, acute or extensive toxic effects to ecosystems (Miljødirektoratet, 2016).

Taking the results for trace elements in the large and small seawater samples together, these observations follow the same trends as for the activity concentrations of Cs-137, Sr-90 and plutonium isotopes in the same samples, showing rapid dilution of elevated levels in releases in the surrounding bottom water.

Table 4.7. Concentration of selected trace elements (µg/l) in large volume seawater samples.

	Al	Mn	Fe	Ni	Cu	Zn	Cd	Sn	Ba	W	Pb
Surface											
<0.45 µm	29 ± 48%	0.23 ± 10%	4.0 ± 92%	0.69 ± 79%	1.7 ± 59%	10 ± 18%	0.0068 ± 28%	<0.030	5.8 ± 1%	0.068 ± 78%	0.030 ± 66%
<10 kDa	18 ± 13%	0.15 ± 16%	1.2 ± 72%	0.36 ± 14%	0.56 ± 16%	8.9 ± 8%	0.0078 ± 10%	<0.030	5.7 ± 2%	0.071 ± 83%	0.022 ± 4%
Bottom (3 m over ventilation pipe)[a]											
Unfiltered	34 ± 49%	0.41 ± 4%	7.6 ± 24%	0.36 ± 10%	1.7 ± 59%	14 ± 4%	0.031 ± 18%	0.073 ± 110%	6.9 ± 3%	0.13 ± 12%	0.13 ± 63%
<0.45 µm	19 ± 22%	0.13 ± 9%	1.1 ± 31%	0.28 ± 12%	0.76 ± 11%	14 ± 9%	0.026 ± 7%	<0.030	6.7 ± 1%	0.088 ± 86%	0.042 ± 15%
<10 kDa	19 ± 10%	0.14 ± 6%	1.7 ± 36%	0.29 ± 13%	0.85 ± 42%	12 ± 11%	0.026 ± 17%	<0.030	6.7 ± 2%	0.078 ± 89%	0.051 ± 2%
Bottom (beside portside opening in TC[b])											
<0.45 µm	17 ± 15%	0.17 ± 4%	0.48 ± 14%	0.24 ± 11%	0.77 ± 4%	12 ± 10%	0.025 ± 6%	<0.030	6.6 ± 1%	0.037 ± 139%	0.088 ± 3%
Bottom (beside port dive plane)											
<0.45 µm	17 ± 0.1%	0.14 ± 0.4%	1.2 ± 20.5%	0.33 ± 18%	1.0 ± 56%	9.5 ± 18%	0.024 ± 5%	<0.030	6.5 ± 0.03%	0.010 ± 12%	0.053 ± 8%

a - Sample represents water collected from two separate casts. Visual releases were observed during the second cast, but not the first cast.

b - Torpedo compartment. Figure 2.2. shows this sample being collected.

Results above are the mean (± %SD) of two measurements (unfiltered) or three measurements (<0.45 µm and <10 kDa). Uncertainties on individual measurements were typically between 2% and 5%.

Table 4.8. Concentration of selected trace elements (µg/l) in dissolved (<0.45 µm) fractions of small volume seawater samples collected by the ROV.

	Al	Mn	Fe	Ni	Cu	Zn	Cd	Sn	Ba	W	Pb
From ventilation pipe (11 hr)[a]	152 ± 3%	30 ± 2%	7.5 ± 2%	40 ± 3%	318 ± 2%	106 ± 2%	2.2 ± 6%	0.13 ± 11%	13 ± 2%	0.024 ± 28%	1.9 ± 2%
Above metal grill[b] (16.5 hr)	187 ± 2%	44 ± 1%	0.71 ± 23%	31 ± 1%	54 ± 1%	21 ± 2%	4.1 ± 3%	0.067 ± 13%	10 ± 2%	0.090 ± 15%	0.076 ± 5%
40 cm above ventilation pipe (23 hr)	45 ± 1%	1.6 ± 3%	1.6 ± 4%	0.68 ± 5%	1.4 ± 2%	21 ± 3%	0.10 ± 18%	0.36 ± 2%	8.1 ± 2%	0.58 ± 3%	0.099 ± 3%
From ventilation pipe (23.1 hr)	137 ± 1%	26 ± 1%	6.1 ± 1%	1.2 ± 5%	0.68 ± 4%	21 ± 2%	0.12 ± 9%	0.056 ± 12%	38 ± 1%	0.032 ± 9%	0.051 ± 9%
From ventilation pipe (33.9 hr)	64 ± 4%	11 ± 3%	8.4 ± 3%	1.1 ± 3%	0.62 ± 7%	22 ± 4%	0.057 ± 17%	0.12 ± 13%	33 ± 2%	0.019 ± 23%	0.048 ± 5%
40 cm above ventilation pipe (34 hr)	21 ± 3%	0.24 ± 5%	<0.4	0.57 ± 7%	17 ± 2%	13 ± 1%	0.050 ± 7%	0.46 ± 4%	7.1 ± 4%	0.091 ± 17%	0.45 ± 2%
From ventilation pipe (34.9 hr)	127 ± 2%	24 ± 1%	2.7 ± 1%	21 ± 1%	287 ± 1%	41 ± 2%	1.8 ± 3%	0.070 ± 10%	9.5 ± 1%	0.021 ± 32%	0.20 ± 4%
40 cm above ventilation pipe (35 hr)	30 ± 2%	0.82 ± 2%	0.35 ± 26%	0.82 ± 6%	3.8 ± 2%	9.6 ± 0.4%	0.038 ± 37%	0.068 ± 16%	6.8 ± 4%	0.12 ± 7%	0.018 ± 19%
Next to ventilation pipe (35.3 hr)	29 ± 4%	54 ± 3%	0.69 ± 7%	15 ± 2%	422 ± 3%	92 ± 3%	0.63 ± 4%	<0.030	12 ± 0.4%	0.16 ± 6%	0.17 ± 3%

a - Time interval after the first sample was taken indicated after description of sampling location. Visual releases were observed when all these samples were collected.

b - Note, some of the particulate material from the metal grill was resuspended and taken up the syringe sampler when this sample was collected.

Values in the table above represent single analytical measurements and their associated uncertainties (%).

4.4 Radionuclides and trace elements in sediments

4.4.1 Cesium-137 (Cs-137)

Activity concentrations of Cs-137 in surface sediments (0 to 1 cm) ranged from 1.4 ± 0.2 to 9.9 ± 0.7 Bq/kg d.w. in push cores collected around Komsomolets with no obvious spatial trend due to proximity to the known release points nor the direction of prevailing bottom currents (Figure 4.34). The mean Cs-137 activity concentration in surface sediments (4.9 ± 2.3 Bq/kg d.w.) collected in 2019 was within the range of activity concentrations reported for surface sediments from previous and subsequent monitoring up to 2021 (Figure 4.35). The mean value for 2019 was also within the range of Cs-137 activity concentrations (<2.2 to 15 ± 3 Bq/kg d.w.) reported for surface sediments collected around Komsomolets during the 1993 Russian investigation with the MIR submersible (Hollister, 1994a). No other gamma emitting anthropogenic radionuclides were detected in any sediment sample.

Vertical profiles of Cs-137 in all push cores collected in 2019 (Figure 4.36) were comparable to profiles from cores obtained from previous and subsequent monitoring up to 2021 (Figure 4.37), with activity concentrations decreasing with depth and to levels below detection limits on average by 6 to 7 cm below the surface. Only three of the sixteen push cores showed sub-surface maxima, with all three of these cores showing higher activity concentrations of Cs-137 in the layer from 1 to 2 cm. One of these samples showed the highest observed Cs-137 activity concentration for sediment of 12.0 ± 0.7 Bq/kg d.w.. Previous Pb-210 dating sediment cores collected around Komsomolets determined that sedimentation rates from these cores were of the order of 0.08 to 0.10 cm/a (Gwynn et al., 2018). This would imply that the year that Komsomolets sank (i.e. 1989) would correspond to a sediment depth of 2 to 3 cm (Gwynn et al., 2018). It is interesting to note that maximum activity concentrations of Cs-137 are consistently observed in the surface layers for those years when cores were taken around Komsomolets. Inventories of Cs-137 in the cores sampled in 2019 ranged from 58 ± 5 to 538 ± 15 Bq/m^2, with on average 72% of the total inventory in the top 10 cm being held within the upper 3 cm.

At the depth where Komsomolets lies, it is difficult to assess the flux of Cs-137 from other sources, which at least for surface waters have declined over the preceding decades. Despite the fact that releases of Cs-137 have likely been occurring since Komsomolets sank in 1989 and that even in 2019, the magnitude of these releases were up to 10^5 Bq/m^3, there seems to be little overall impact on the activity concentrations of Cs-137 in sediments around Komsomolets as a result of the releases over the last 30 years. Sediment distribution coefficients (K_d) for Cs-137 based on the average activity concentration for bottom seawater sampled around Komsomolets since 1995 (1.2 ± 0.6 Bq/m^3) and activity concentrations in the top 1 cm of sediment from all sampled cores were of the same order of magnitude as the recommended IAEA value for Cs in the open ocean of 2 x 10^3 (IAEA, 2004).

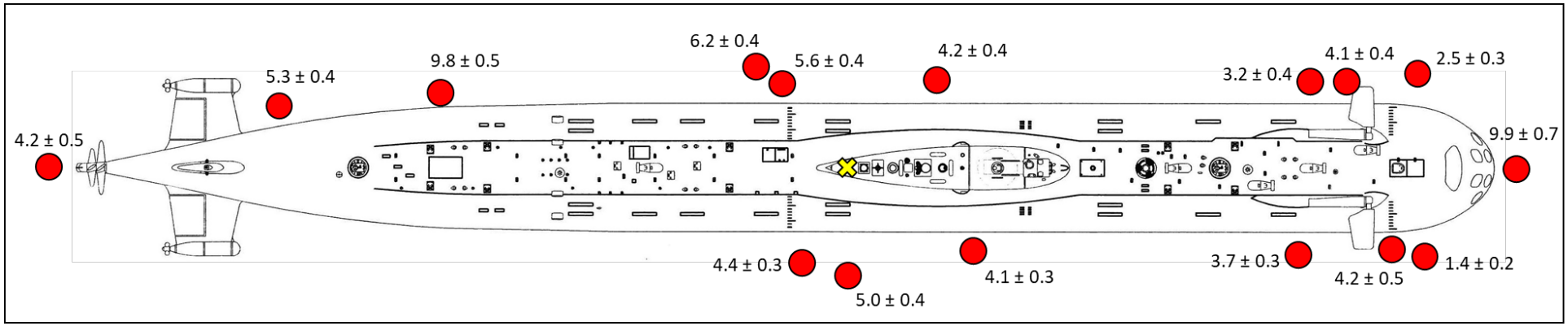

Figure 4.34. Activity concentrations of Cs-137 (Bq/kg d.w.) in surface sediments (0-1 cm) from push cores taken around Komsomolets. The prevailing current direction flows along the submarine from the stern to the bow. Location of the ventilation pipe and metal grill is indicated by the yellow cross.

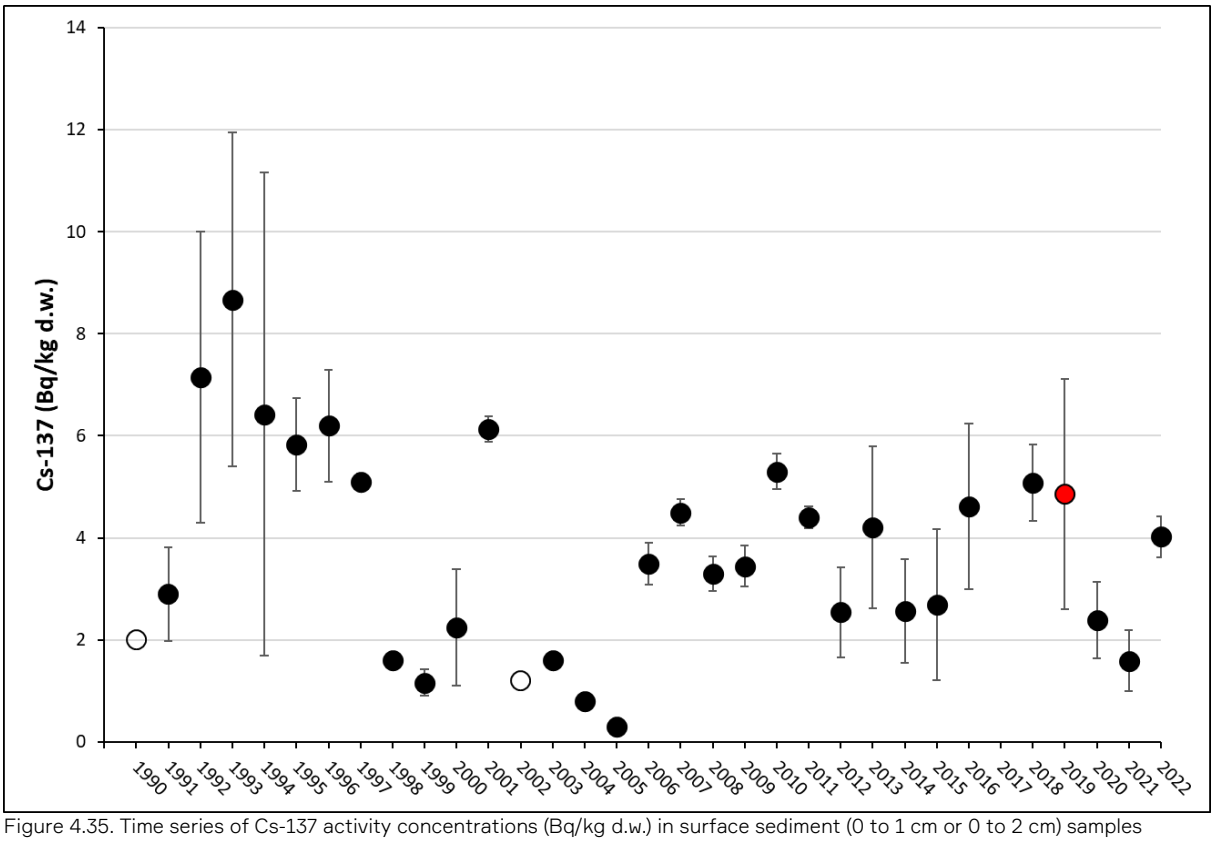

Figure 4.35. Time series of Cs-137 activity concentrations (Bq/kg d.w.) in surface sediment (0 to 1 cm or 0 to 2 cm) samples collected by Norwegian monitoring at the site of Komsomolets since 1990. Data values for individual years represent either individual measurements or mean values. Open symbols represent values below detection limits. Uncertainties on individual measurements were typically less than 10%. The mean activity concentration of Cs-137 in surface sediments collected around Komsomolets in 2019 is included as the red dot. Overview of data from 1990 to 2015 published by Gwynn et al., 2018, but the figure here is updated with additional data for 1991 and 1992 from Bøhmer & Berthelsen, 1992. Data for 2018, 2020 and 2022 from the Norwegian national monitoring programme (unpublished).

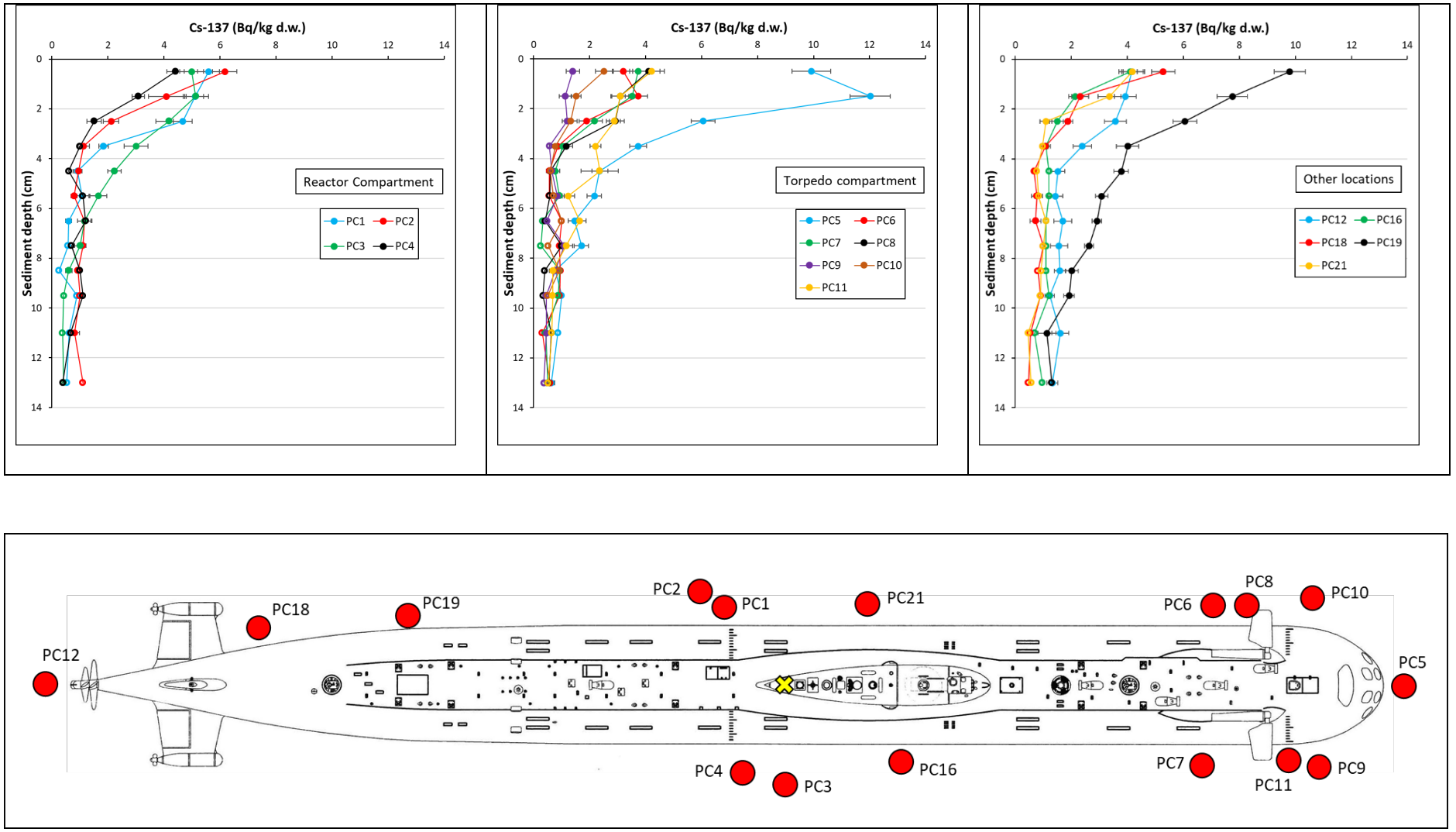

Figure 4.36. Sediment profiles of Cs-137 activity concentrations (Bq/kg d.w.) in push cores taken around Komsomolets. The prevailing current direction flows along the submarine from the stern to the bow. Location of the ventilation pipe and metal grill is indicated by the yellow cross. Open symbols represent data below detection limits. Error bars show measurement uncertainties (1 sigma).

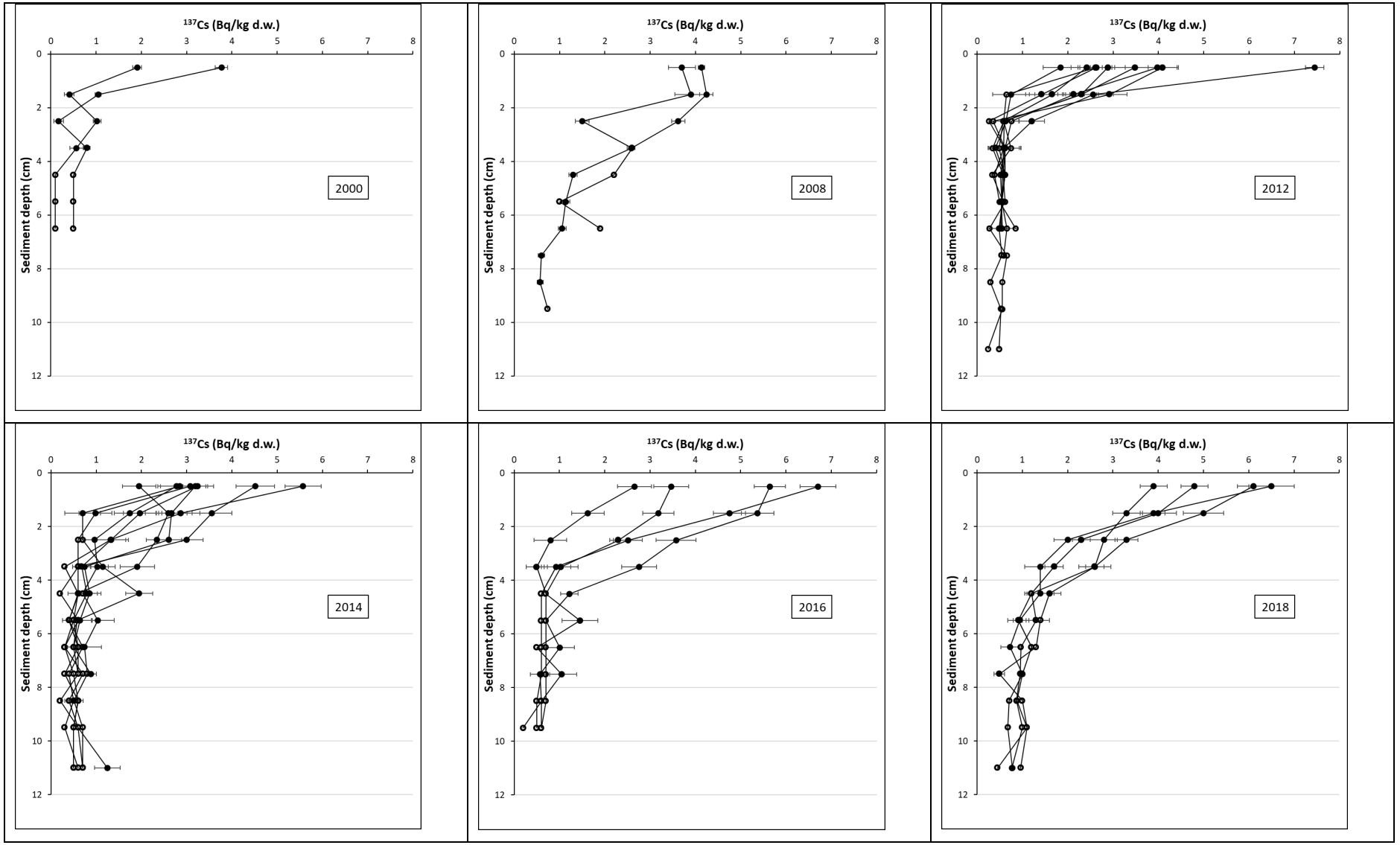

Figure 4.37. Sediment profiles of Cs-137 activity concentrations (Bq/kg d.w.) from cores taken around Komsomolets in other years. Open symbols represent data below detection limits. Data for 2000 to 2014 (Gwynn et al., 2018). Data for 2016 and 2018 from the Norwegian national monitoring programme (unpublished). Error bars show measurement uncertainties (1 sigma).

4.4.2 Plutonium isotopes (Pu-239 and Pu-240)

Combined activity concentrations of Pu-239 and Pu-240 in surface sediments (0 to 1 cm) ranged from 0.07 ± 0.01 to 1.15 ± 0.04 Bq/kg d.w. in push cores collected around Komsomolets with lower values observed at the bow of the submarine (Figure 4.38). Overall, these values are comparable to the range of Pu-239,240 activity concentrations reported for surface sediments around Komsomolets between 1993 and 2013 (0.02 ± 0.01 to 0.51 ± 0.14 Bq/kg d.w.) and for the area in general (0.85 to 1.16 Bq/kg d.w.) (Nies et al., 1999; Gwynn et al., 2018). The lower values observed around the bow could be explained by mixing of surface and deeper sediments when Komsomolets likely hit the seafloor bow first. From the limited data available for the vertical distribution of combined Pu-239 and Pu-240 activity concentrations (Figure 4.39), sub-surface values were within or lower than the range of values observed for surface sediments. Based on these results, there is no evidence of increased activity concentrations of Pu-239 and Pu-240 in the sediment around Komsomolets.

4.4.3 Atom ratios of Pu-240/Pu-239

Atom ratios of Pu-240/Pu-239 in surface sediments (0 to 1 cm) around the torpedo compartment ranged between 0.181 ± 0.022 to 0.260 ± 0.041 and between 0.163 ± 0.014 to 0.189 ± 0.019 at all other locations including either side of the reactor compartment (Figure 4.40). Sub-surface sediment atom ratios of Pu-240/Pu-239 around the torpedo compartment showed no significant deviations from surface values as was typically the case for other locations (Figure 4.41). However, there is a suggestion of decreasing trends with sediment depth in the Pu-240/Pu-239 atom ratios for the two cores taken either side of the reactor compartment (Figure 4.41). For the deepest sediment depth analysed from these two cores, the atom ratios of Pu-240/Pu-239 were 0.152 ± 0.016 (3 to 4 cm; port side) and 0.122 ± 0.032 (7 to 8 cm; starboard side). Overall, the atom ratios of Pu-240/Pu-239 in surface sediment from 2019 are similar to the range of values for sediment samples collected around Komsomolets in the 1990s (0.16 to 0.18) and in 2013 (0.152 to 0.194) (Stepanov et al., 1999; Flo, 2014; Gwynn et al., 2018) and with a value of 0.180 ± 0.014 for global fallout in northern regions (Kelley et al., 1999). There is no indication of any weapons grade plutonium in sediment around the torpedo compartment either at the surface or in the sub-surface samples that were analysed. As mentioned previously, Pu-240/Pu-239 atom ratios for weapons grade plutonium have been reported as being typically less than 0.07 (e.g., Choppin et al., 1995; Momoshima et al., 1997; Oughton et al., 2000; Geckeis et al., 2019). The lower atom ratios of Pu-240/Pu-239 observed deeper in the sediment either side of the reactor compartment would suggest contributions of plutonium from the reactor in Komsomolets, as these values are closer to atom ratios for Pu-240/Pu-239 of 0.105 and 0.13 that are based on estimated reactor inventories of Pu-239 and Pu-240 for Komsomolets (Gladkov et al., 1994; Høibråten et al., 1997) and an estimate for Russian submarine pressurised water reactors (Sivintsev, 1995).

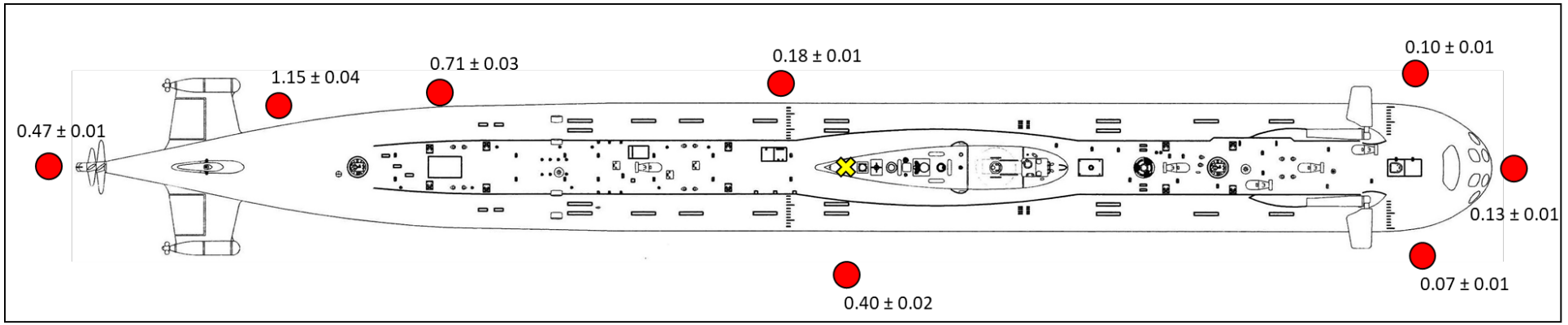

Figure 4.38. Combined activity concentrations of Pu-239 and Pu-240 (Bq/kg d.w.) in surface sediments (0-1 cm) from push cores taken around Komsomolets. The prevailing current direction flows along the submarine from the stern to the bow. Location of the ventilation pipe and metal grill is indicated by the yellow cross.

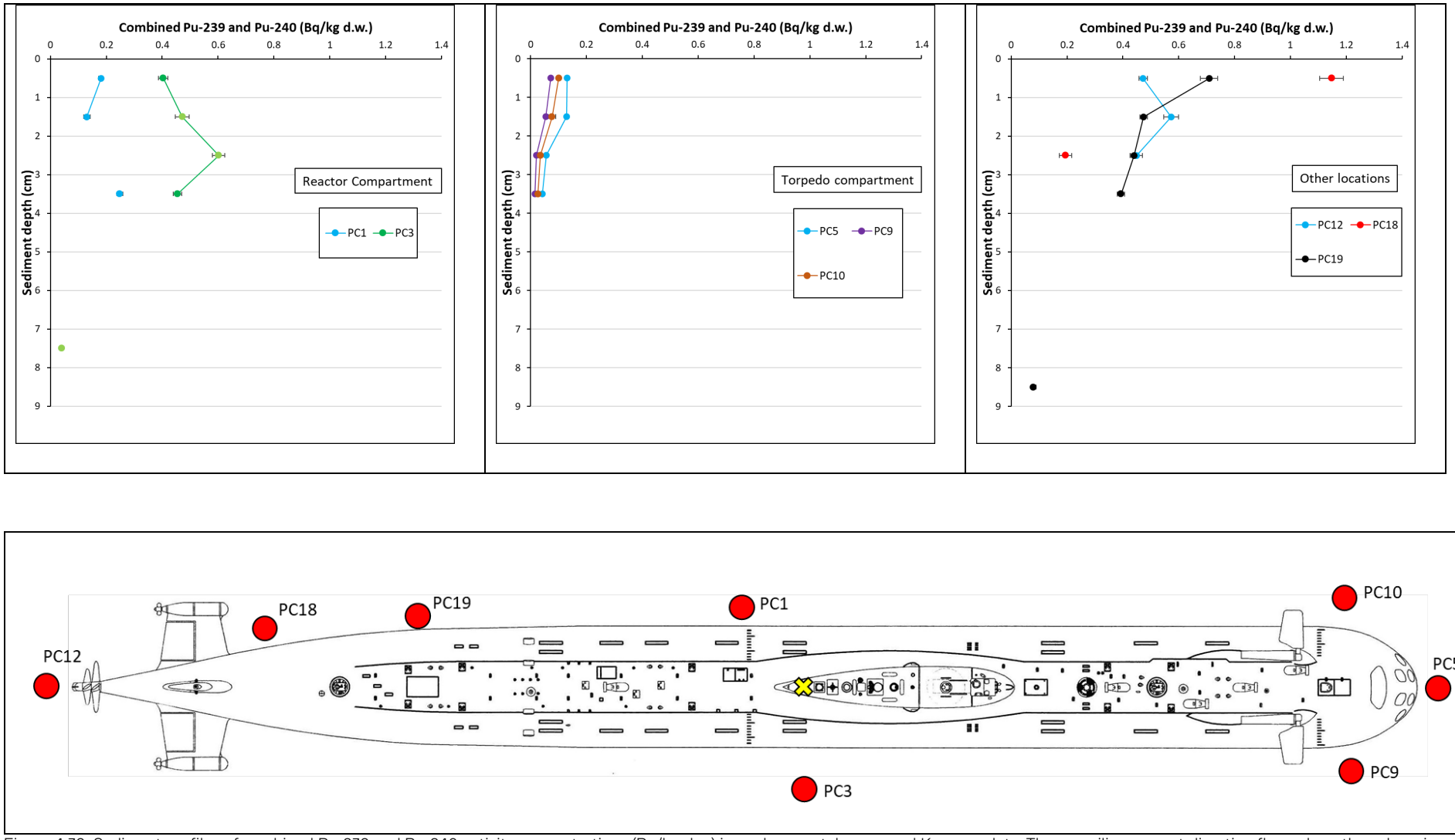

Figure 4.39. Sediment profiles of combined Pu-239 and Pu-240 activity concentrations (Bq/kg d.w.) in push cores taken around Komsomolets. The prevailing current direction flows along the submarine from the stern to the bow. Location of the ventilation pipe and metal grill is indicated by the yellow cross. Error bars show measurement uncertainties (1 sigma).

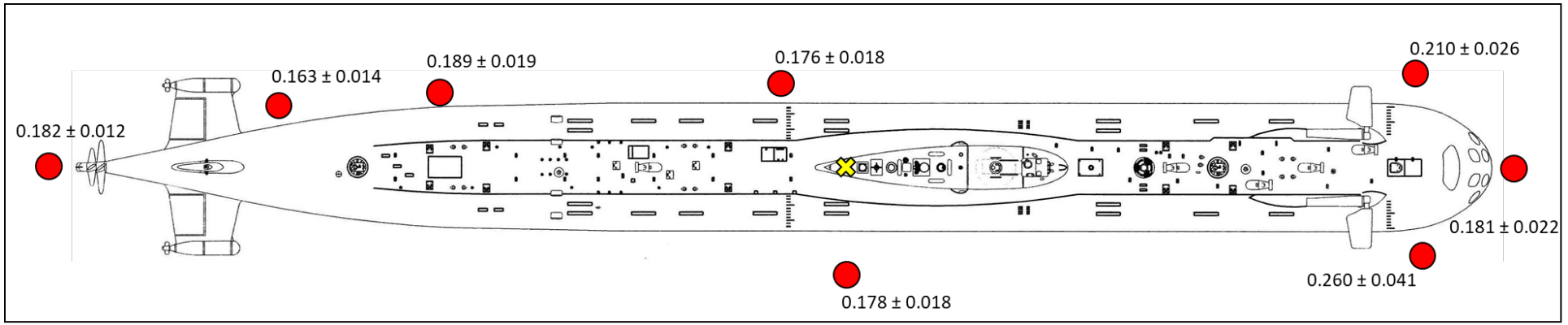

Figure 4.40. Atom ratios of Pu-240/Pu-239 in surface sediments (0-1 cm) from push cores taken around Komsomolets. The prevailing current direction flows along the submarine from the stern to the bow. Location of the ventilation pipe and metal grill is indicated by the yellow cross.

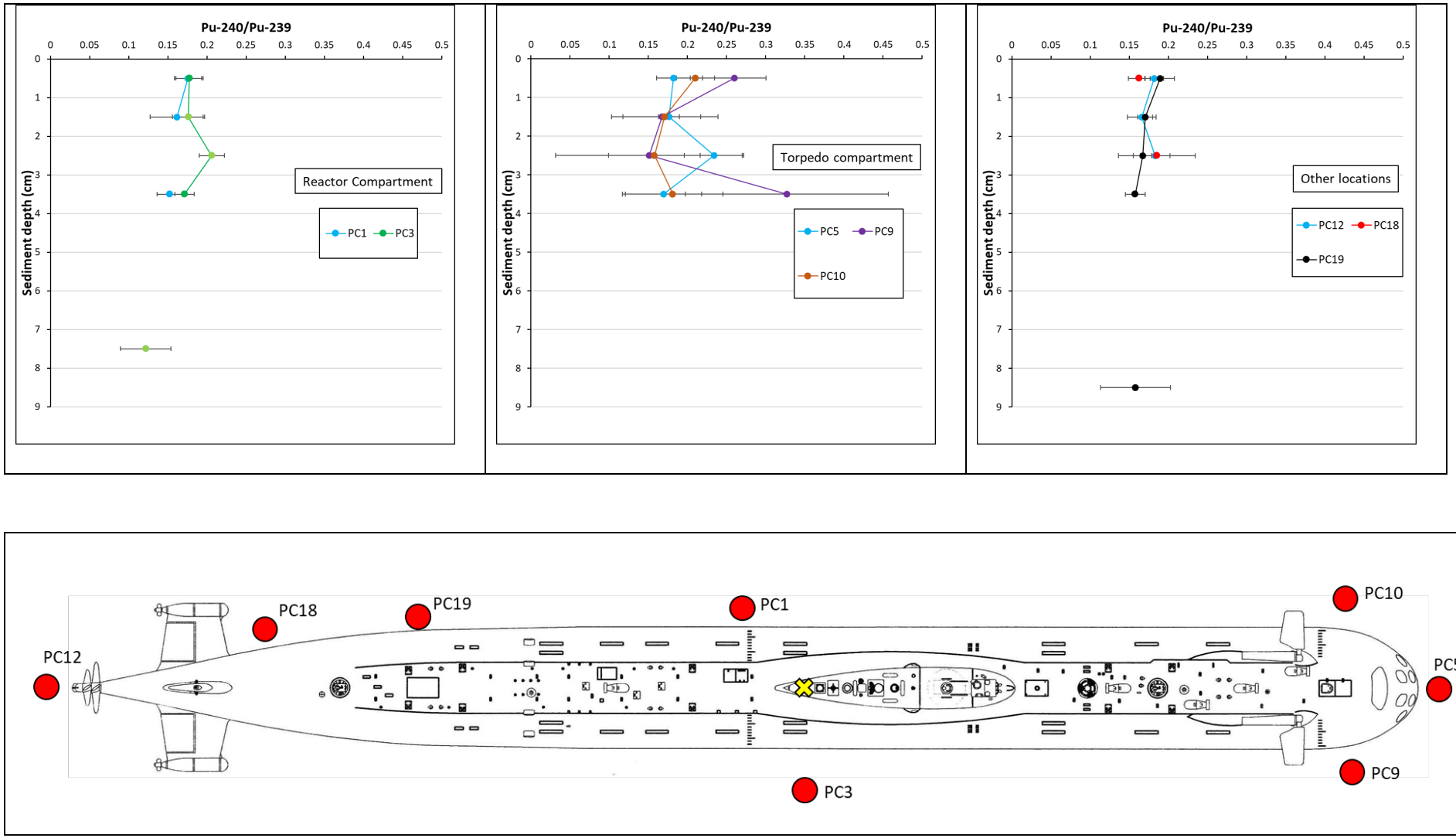

Figure 4.41. Sediment profiles of Pu-240/Pu-239 atom ratios in push cores taken around Komsomolets. The prevailing current direction flows along the submarine from the stern to the bow. Location of the ventilation pipe and metal grill is indicated by the yellow cross. Error bars show propagated measurement uncertainties (1 sigma).

4.4.4 Uranium-236 (U-236)

Activity concentrations of U-236 in surface sediments (0 to 1 cm) ranged from <14 to 132 ± 27 µBq/kg d.w. in push cores collected around Komsomolets with no obvious trend in the spatial distribution of the observed values (Figure 4.42). From the limited data available for the vertical distribution of U-236 activity concentrations, some cores showed higher sub-surface values than surface values (Figure 4.43). For comparison, activity concentrations of U-236 in a sediment reference material (IAEA-385) collected from the Irish Sea in 1993 have been reported to be between 10.3 and 11.2 mBq/kg d.w. (Lee et al., 2008), two orders of magnitude higher than the maximum value observed in sediment around Komsomolets in 2019. Closer to the site of interest, activity concentrations of U-236 in a sediment core collected 168 km Northwest from Komsomolets in 2015 were 6.8 µBq/kg d.w. at the surface (0 to 1 cm), with a sub-surface maximum in the top 10 cm of 11.8 µBq/kg d.w., with similar values for sediment cores at other locations in the Barents Sea (Qiao et al., 2022). The observed activity concentrations of U-236 in the sediment around Komsomolets would confirm that releases of U-236 are occurring from the reactor.

4.4.5 Atom ratios of U-236/Pu-239

Where atom ratios of U-236/Pu-239 were available for surface sediments (0 to 1 cm) these were less than one and ranged between 0.12 ± 0.04 to 0.71 ± 0.23 (Figure 4.44). For two cores where atom ratios of U-236/Pu-239 were available for the top 4 cm of sediment (both located near the torpedo compartment) there appeared to be a clear increase in these ratios with depth, with maximum values of 5.8 ± 2.6 and 14 ± 5 at 3 to 4 cm (Figure 4.45). These values are at least an order of magnitude higher than U-236/Pu-239 atom ratios (0.014 to 0.030) for acid leachates of a radioactive particle recovered from Thule at the site where a US B-52 bomber carrying four nuclear weapons crashed in 1968 (Moreno, 2022). Although no data exists for U-236/Pu-239 ratios for the type of warhead reported to have been part of the armament of Komsomolets, this comparison adds further support to the already available evidence that there has been no release of warhead nuclear material to the sediments around the torpedo compartment of Komsomolets. As previously mentioned, it can be difficult to relate observational ratios of these radionuclides directly to known other source terms due to the very different biogeochemical behaviour of U-236 (more conservative) and Pu-239 (more particle reactive) in the marine environment. However, for comparison a U-236/Pu-239 atom ratio of 0.09 can be derived from data reported for sediment collected from the Irish Sea in 1993 (Lee et al., 2001,2008). The observed increase in atom ratios of U-236/Pu-239 with sediment depth would suggest a greater flux of U-236 to the surrounding sediments in the past. A comparison of Pu-240/Pu-239 versus U-236/Pu-239 atom ratios for sediment samples against suitable endmember values would confirm that releases of Pu-isotopes and U-236 are occurring from the reactor of Komsomolets (Figure 4.46).

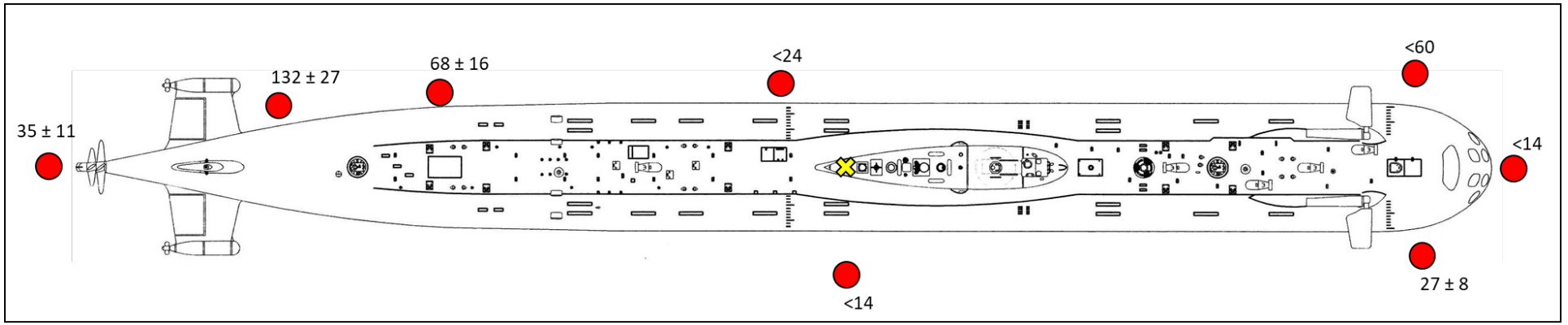

Figure 4.42. Activity concentrations of U-236 (μBq/kg d.w.) in surface sediments (0-1 cm) from push cores taken around Komsomolets. The prevailing current direction flows along the submarine from the stern to the bow. Location of the ventilation pipe and metal grill is indicated by the yellow cross.

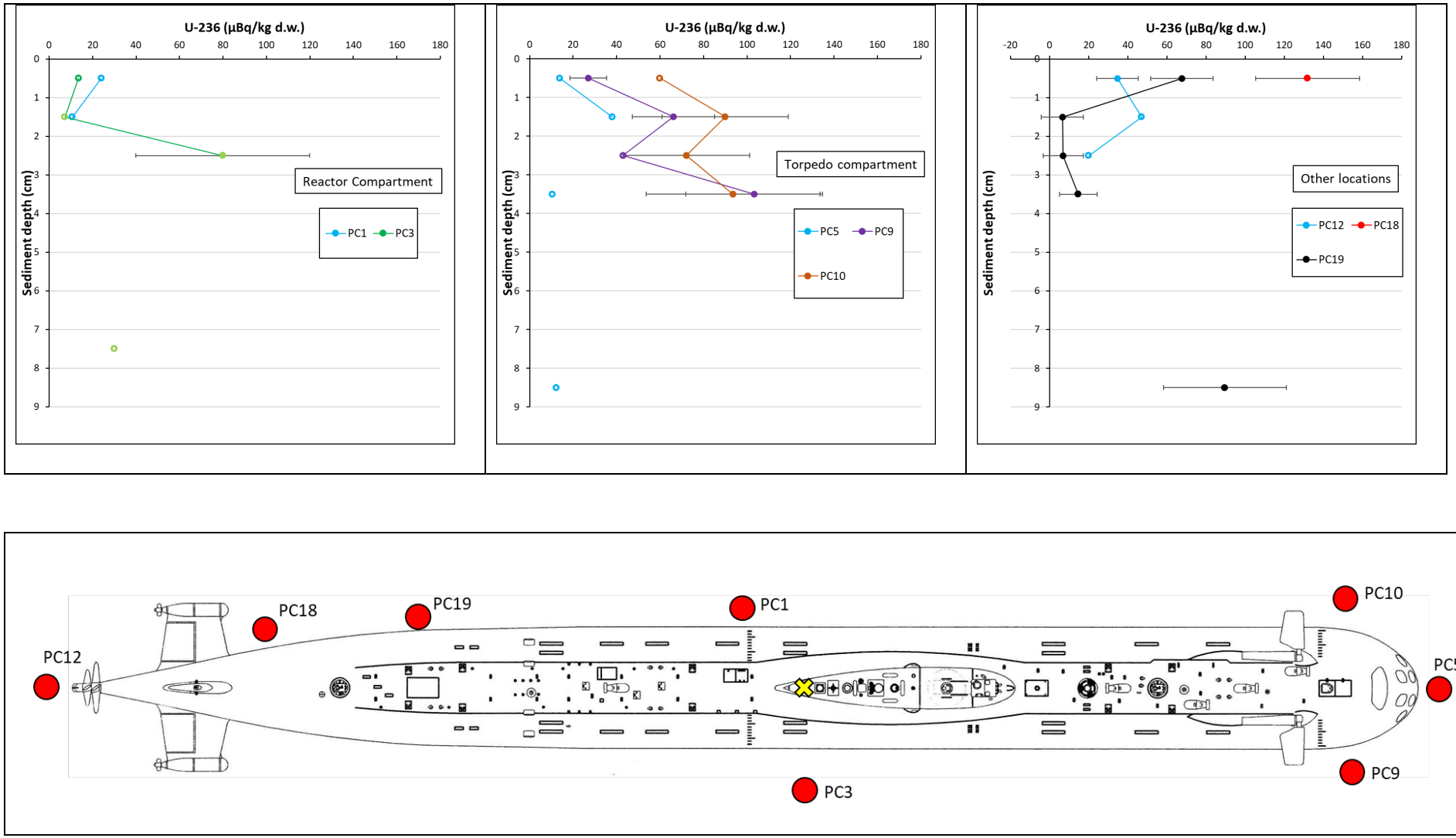

Figure 4.43. Sediment profiles of U-236 activity concentrations (µBq/kg d.w.) in push cores taken around Komsomolets. The prevailing current direction flows along the submarine from the stern to the bow. Location of the ventilation pipe and metal grill is indicated by the yellow cross. Open symbols represent data below detection limits. Error bars show measurement uncertainties (1 sigma).

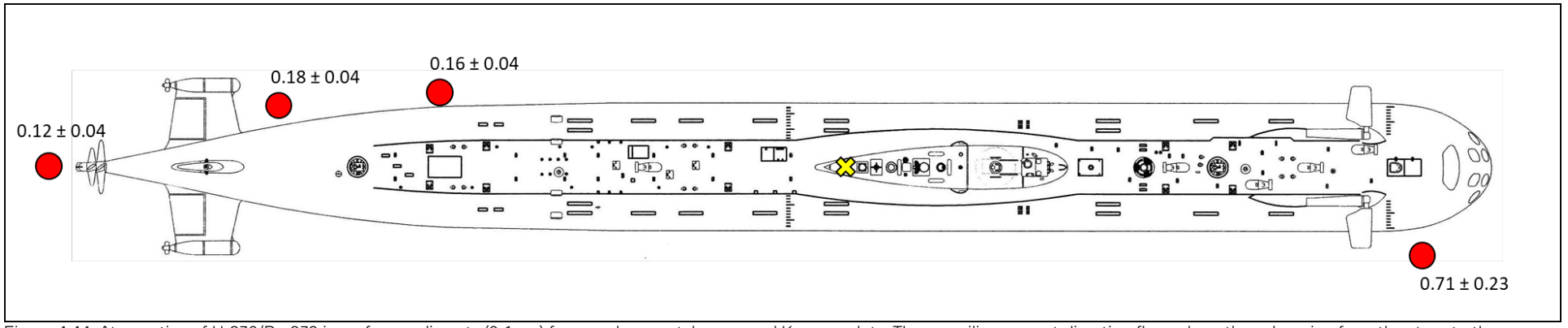

Figure 4.44. Atom ratios of U-236/Pu-239 in surface sediments (0-1 cm) from push cores taken around Komsomolets. The prevailing current direction flows along the submarine from the stern to the bow. Location of the ventilation pipe and metal grill is indicated by the yellow cross.

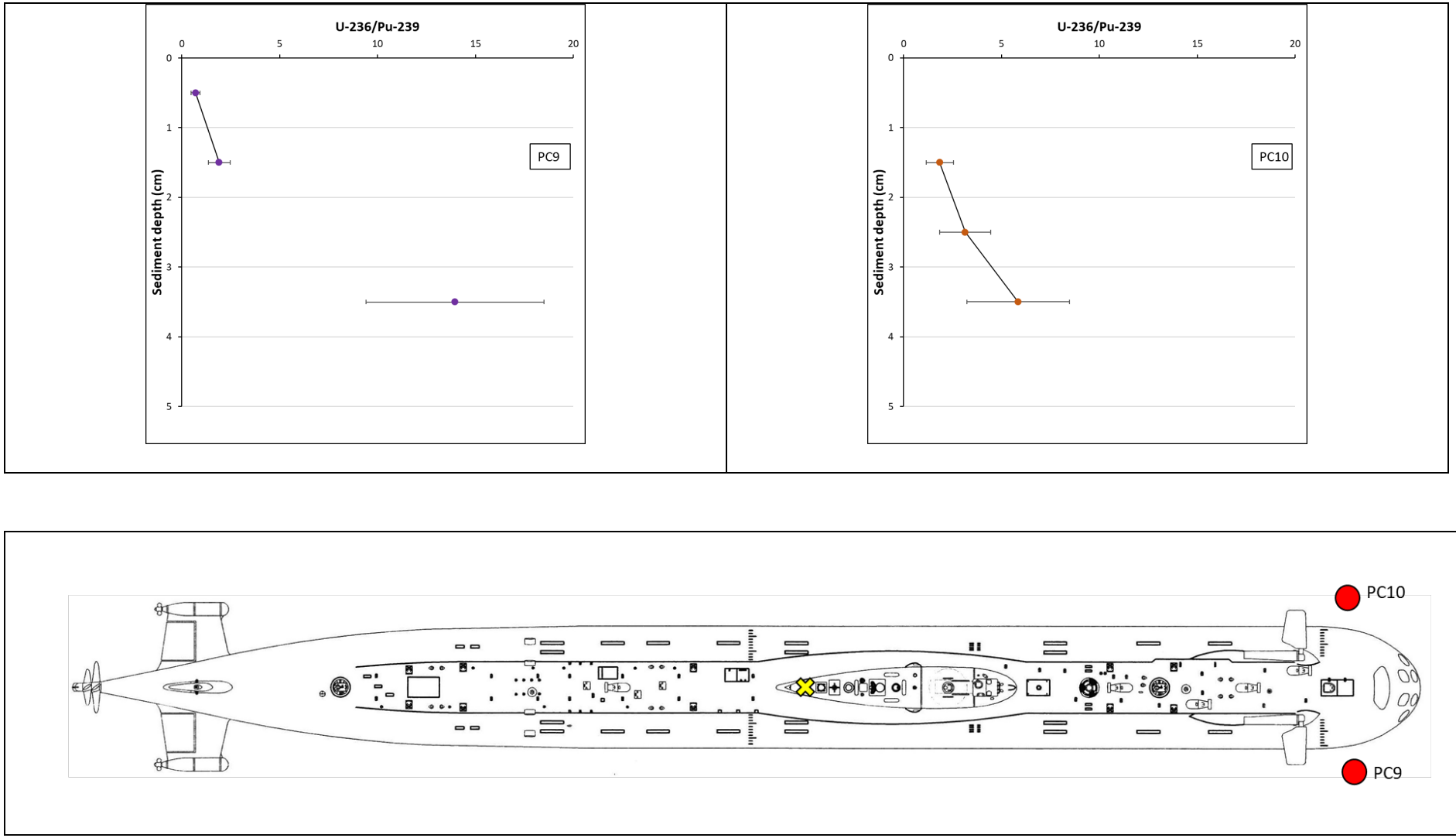

Figure 4.45. Sediment profiles of U-236/Pu-239 atom ratios in two push cores taken around the torpedo compartment of Komsomolets. The prevailing current direction flows along the submarine from the stern to the bow. Location of the ventilation pipe and metal grill is indicated by the yellow cross. Error bars show propagated measurement uncertainties (1 sigma).

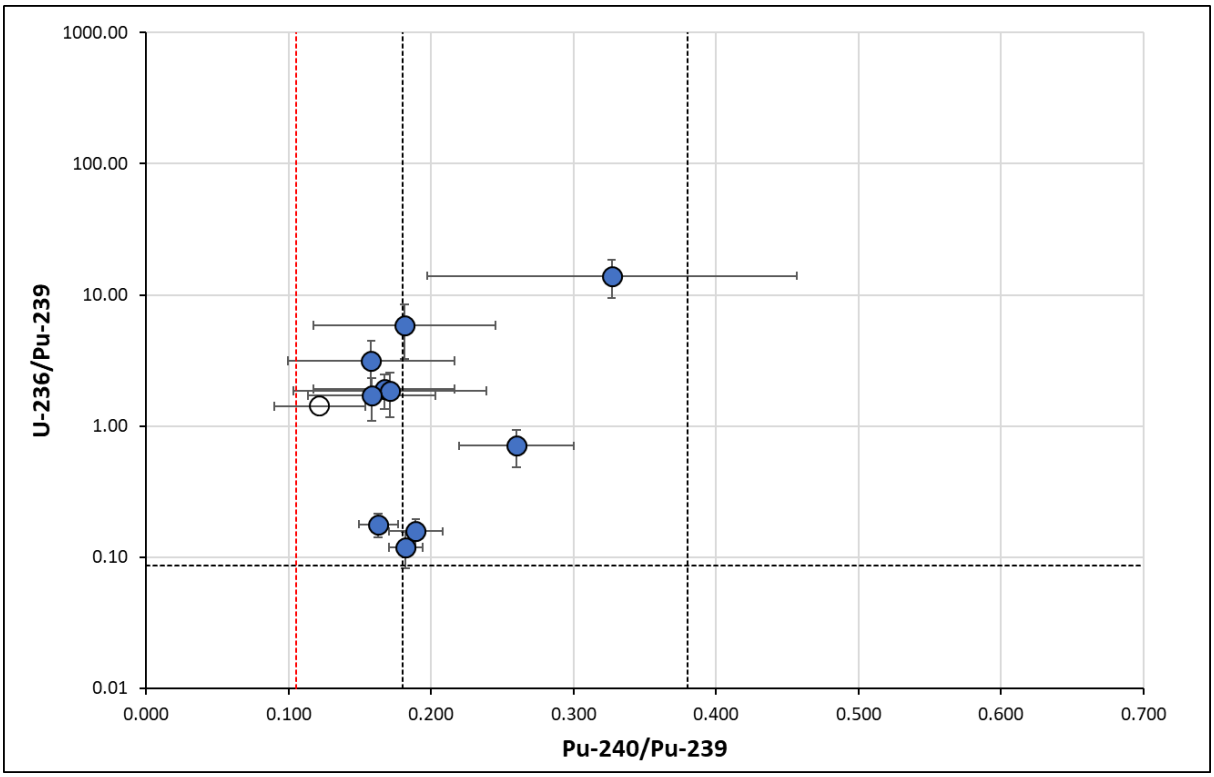

Figure 4.46. Plot showing relationship between atom ratios of U-236/Pu-239 and Pu-240/Pu-239 for sediment samples where it was possible to determine both ratios. Error bars show propagated uncertainties (1 sigma). The black horizontal dashed line shows the derived U-236/Pu-239 atom ratio for an Irish Sea sediment reference material (IAEA-385) from 1993 (Lee et al., 2001, 2008). The red vertical dashed line shows the Pu-240/Pu-239 atom ratio derived from the estimated Pu-239 and Pu-240 reactor inventories for Komsomolets (Gladkov et al., 1994; Høibråten et al., 1997). The black vertical dashed lines show the maximum (Chornobyl deposition) and minimum (global fallout) of the range of Pu-240/Pu-239 atom ratios for other sources of these plutonium isotopes to the Norwegian Sea. Plot includes one data point (open circle) where the U-239/Pu-239 atom ratio is based on a detection limit value for U-236 as this sample showed the lowest sediment Pu-240/Pu-239 atom ratio (0.122 ± 0.032).

4.4.6 Trace elements

Trace elements in push core sediments were generally within a factor of two from the lowest value to the highest value when considering all sampled cores and all sediment depths analysed, although Mn, Cd, Cu, Pb and U showed a greater degree of variation. None of the measured trace elements showed any trends with increased concentration in the surface sediments as was observed for Cs-137. The concentration of titanium in sediments around Komsomolets fell within expected values for marine sediments (Schnetger et al., 2000; Li & Schoonmaker, 2003; Wei et al., 2003). Although natural levels of titanium in marine sediments are relatively high, the lack of any obvious additional titanium signal in sediments around the submarine would support the visual evidence of little or no obvious corrosion of the outer hull. Due to the overall lack of variation between cores and with sediment depth, values for trace elements in sediments are given as overall averages and the range of all available data (Table 4.9).

However, levels of trace elements in sediments around Komsomolets were higher than compared to sediments from the open Barents Sea (e.g., Knies et al., 2006; Budko et al., 2022). Compared to quality standards for sediment set by the Norwegian Environment Agency, levels of Ni, Zn, Cu and As in some of the sediment samples would be classified as giving rise to chronic or acute toxic effects to ecosystems (Miljødirektoratet, 2016). Given that concentrations of the same trace elements were lower in the top 2 cm of sediment cores taken within ~20 m of Komsomolets and at reference site 100 m upstream from the submarine in 2013 (Flo, 2014), this would suggest that any impact is limited to the immediate area around the submarine itself.

Table 4.9. Average concentration of trace elements across all sediment cores from 0 to 10 cm depth.

Element	Unit (d.w.)	Mean (± %SD)	Min	Max
Ti	g/kg	4.1 ± 8%	2.8	5.0
V	mg/kg	143 ± 11%	102	175
Cr	mg/kg	84 ± 10%	51	100
Mn	g/kg	0.60 ± 44%	0.3	1.9
Fe	g/kg	40 ± 10%	30	64
Co	mg/kg	16 ± 10%	10	19
Ni	mg/kg	44 ± 10%	31	59
Zn	mg/kg	89 ± 14%	59	160
Cu	mg/kg	32 ± 65%	16	281
As	mg/kg	12 ± 30%	5.5	29
Rb	mg/kg	62 ± 18%	43	100
Sr	g/kg	0.19 ± 41%	0.1	0.6
Cd	mg/kg	0.13 ± 79%	0.01	0.8
Cs	mg/kg	4.0 ± 15%	2.8	6.0
Ba	mg/kg	204 ± 20%	134	380
La	mg/kg	26 ± 15%	18	39
Ce	mg/kg	57 ± 12%	40	82
Pr	mg/kg	6.7 ± 12%	4.7	9.7
Nd	mg/kg	27 ± 11%	19	37
Sm	mg/kg	5.3 ± 9%	3.8	7.2
Eu	mg/kg	1.1 ± 7%	0.8	1.4
Gd	mg/kg	4.6 ± 8%	3.5	6.1
Tb	mg/kg	0.66 ± 8%	0.5	0.9
Dy	mg/kg	3.7 ± 8%	2.7	4.8
Ho	mg/kg	0.66 ± 9%	0.5	0.9
Er	mg/kg	1.8 ± 10%	1.3	2.3
Tm	mg/kg	0.23 ± 11%	0.2	0.3
Yb	mg/kg	1.4 ± 12%	1.0	2.0
Lu	mg/kg	0.2 ± 12%	0.1	0.3
Tl	mg/kg	0.31 ± 25%	0.2	0.5
Pb	mg/kg	14 ± 24%	11	50
Bi	mg/kg	0.19 ± 10%	0.1	0.3
Th	mg/kg	8.1 ± 14%	5.4	12
U	mg/kg	1.4 ± 49%	0.9	6.4

Due to the overall lack of variation between cores and with sediment depth, values for trace elements in sediments are given as overall means (± %SD) and the minimum and maximum of all available data (n=160). Uncertainties on individual measurements were typically between 0.1% and 4%.

4.5 Radionuclides and trace elements in biota

4.5.1 Cesium-137 (Cs-137)

Results for the activity concentrations of Cs-137 in biota are given in Table 4.10. The activity concentrations of Cs-137 were below the detection limit in four of the seven samples of biota that were taken from the hull of the submarine on either side of the sail below the location of the ventilation pipe. The relatively high detection limits for these samples were due to the low sample masses once the samples had been dried. For the other three biota samples, Cs-137 activity concentrations ranged from 2.7 ± 0.2 to 20 ± 1 Bq/kg fresh weight (f.w.). Data for Cs-137 activity concentrations in soft corals is not available for the Norwegian marine environment, but lower values have been observed in other anemone (0.05 ± 0.04 Bq/kg f.w.) and sponge (0.12 ± 0.04 Bq/kg f.w.) species from the Barents Sea in 2015 (Norwegian monitoring programme, unpublished data). It is worth noting that the three species with elevated activity concentrations of Cs-137 are all suspension/filter feeders and are sessile species and the observed levels of Cs-137 are likely directly related to the releases of Cs-137 from the reactor due to the proximity of these biota to the ventilation pipe. However, these activity concentrations are still low and not at a level where any significant effects would be expected. For further comparison, activity concentrations of Cs-137 in various fish species from the Norwegian Sea in 2020 ranged from 0.07 to 0.25 Bq/kg f.w. (Norwegian monitoring programme, unpublished data). The one biota sample (a motile species) that was collected from the seafloor next to Komsomolets showed an activity concentration of Cs-137 that was below the detection limit. No other gamma emitting radionuclides were detected in these samples.

Table 4.10. Activity concentrations of Cs-137 (Bq/kg f.w.) in biota[a].

Collection location	Taxonomic description	Common name	Cs-137 (Bq/kg f.w.)
From the sides of the sail below the ventilation pipe	*Gersemia* sp.	Soft coral	20 ± 1
	Cladorhiza gelida	Carnivorous sponge	2.7 ± 0.2
	Actiniaria	Sea anemone	5.7 ± 0.7
	Amphipoda	Crustacean	<82
	Polynoidae	Scale worm	<48
	Solenogastres	Shell-less mollusc	<270
	Hydrozoa	Hydroid	<160
	Arthropoda: Copepoda	Copepod	<190
From the seafloor next to Komsomolets	*Pontaster tenuispinus*	Starfish	<1

a - All samples are based on pooled samples, except for the starfish (n=1).

4.5.2 Plutonium isotopes (Pu-239 and Pu-240) and Pu-240/Pu-239 atom ratios

Results for the combined activity concentrations of Pu-239 and Pu-240 in biota are given in Table 4.11. The combined activity concentrations of Pu-239 and Pu-240 in biota that were analysed ranged from 16 ± 1 to 51 ± 4 mBq/kg f.w. for samples collected directly from the hull of the submarine below the ventilation pipe. For the single sample collected from the seafloor the combined Pu-239 and Pu-240 activity concentration was 75 ± 4 mBq/kg f.w.. No such data for these biota types are available from other locations for direct

comparison. However, contemporary (2000 to 2018) ranges of activity concentrations of Pu-239,240 for fish and molluscs from the North Sea of 0.02 to 0.14 mBq/kg f.w. and 8 to 83 mBq/kg f.w., respectively, have been reported to the OSPAR Commission (https://odims.ospar.org/en/). For further comparison, such data is also available for a mixed Irish Sea and North Sea fish (IAEA-414) reference material from 1996 and an Irish Sea shellfish (IAEA-134) reference material from 1991. Using a dry weight to fresh weight ratio of 0.2, Pu-239,240 activity concentrations in these fish and shellfish reference materials have been reported at 24 ± 0.8 mBq/kg f.w. and 3260 ± 160 mBq/kg f.w., respectively (Lee et al., 2001; Pham et al., 2006).

The Pu-240/Pu-239 atom ratios for samples collected directly from the hull of the submarine below the ventilation pipe ranged from 0.189 ± 0.034 to 0.25 ± 0.14, while for the single sample collected from the seafloor this atom ratio was 0.160 ± 0.018 (Table 4.10). Although the latter atom ratio is somewhat lower than the value of 0.180 ± 0.014 for global fallout in northern regions (Kelley et al., 1999), the atom ratios for the other samples do not indicate uptake of any released plutonium from the reactor in Komsomolets.

Table 4.11. Combined Pu-239 and Pu-240 activity concentrations (mBq/kg f.w.) and Pu-240/Pu-239 atom ratios in biota[a].

Collection location	Taxonomic description	Common name	Pu-239,240 (mBq/kg f.w.)	Pu-240/Pu-239
From the sides of the sail below the ventilation pipe	*Gersemia* sp.	Soft coral	16 ± 1	0.193 ± 0.033
	Cladorhiza gelida	Carnivorous sponge	51 ± 4	0.189 ± 0.034
	Actiniaria	Sea anemone	27 ± 7	0.25 ± 0.14
From the seafloor next to Komsomolets	*Pontaster tenuispinus*	Starfish	75 ± 4	0.160 ± 0.018

a - All samples are based on pooled samples, except for the starfish (n=1).

4.5.3 Uranium-236 (U-236) and U-236/Pu-239 atom ratios

Results for the activity concentrations of U-236 and U-236/Pu-239 atom ratios in biota are given in Table 4.12. The activity concentrations of U-236 in biota that were analysed ranged from 7 ± 2 to <45 µBq/kg f.w. for samples collected directly from the hull of the submarine below the ventilation pipe. For the single sample collected from the seafloor the U-236 activity concentration was <34 µBq/kg f.w.. Uranium-236 is not routinely monitored in marine biota, but data is available for the mixed Irish Sea and North Sea fish reference material from 1996 and the Irish Sea shellfish reference material from 1991. Again, using a dry weight to fresh weight ratio of 0.2, U-236 activity concentrations in these fish and shellfish reference materials have been reported at 4.8 ± 1.4 and 124 ± 2 µBq/kg f.w., respectively (Lee et al., 2008).

Atom ratios of U-236/Pu-239 were only possible to determine for two biota samples. For biota, it is not possible to relate observational ratios of these radionuclides directly to known source terms due to different rates of biological accumulation of U-236 and Pu-239 by different biota types. However, for some perspective, U-236/Pu-239 atom ratios can be derived for the aforementioned fish and shellfish reference materials at 0.36 and 0.06, respectively.

Table 4.12. Activity concentrations of U-236 (µBq/kg f.w.) and atom ratios of U-236/Pu-239 in biota[a].

Collection location	Taxonomic description	Common name	U-236 (µBq/kg f.w.)	U-236/Pu-239
From the sides of the sail below the ventilation pipe	*Gersemia* sp.	Soft coral	7 ± 2	0.72 ± 0.24
	Cladorhiza gelida	Carnivorous sponge	<45	-
	Actiniaria	Sea anemone	34 ± 9	2.3 ± 0.7
From the seafloor next to Komsomolets	*Pontaster tenuispinus*	Starfish	<34	-

a - All samples are based on pooled samples, except for the starfish (n=1).

4.5.4 Trace elements

Results for the concentration of trace elements in biota are given in Table 4.13. The concentration of trace elements in three different species collected from the sides of the sail below the ventilation pipe were typically higher than those in the single biota sample that was collected from the seafloor. The differences in concentration of trace elements between biota on the side of the sail and the seafloor may reflect differences in exposure due to proximity to the releases and sessile versus motile life histories. However, inter species differences in feeding mechanisms and bioaccumulation of different trace elements should also be considered. It is likely that the observed trace element concentrations in the three species collected from the sides of the sail are directly related to the elevated levels of the same trace elements observed in releases from the ventilation pipe (e.g., Al, Mn, Cu, Zn, Cd, Ba and Pb). There is little or no trace element data available for the species sampled, but the data reported here are higher than values with a range of other biota from the Norwegian Sea and Barents Sea (Nahrgang et al., 2013; Frantzen et al., 2015; Wiech et al., 2020). In particular, the concentration of Cd in the *Gersemia* sp. soft coral is higher than the maximum value for Cd in the hepatopancreas of brown crabs (*Cancer pangurus*) from Northern Norway from a recent study (Wiech et al., 2020) and the reported ranges of Cd in a wide selection of marine taxa from around the world (Neff et al., 2002). It is difficult to assess the impact of these levels of trace metals on the biota growing on Komsomolets or in the area around the submarine, but it was notable from the video surveillance of the sail that no biota was seen growing on the upper part of the hull in the immediate area around the ventilation pipe and that there appeared to be a limit to the growth of biota with respect to the distance to the ventilation pipe (Figure 4.47).

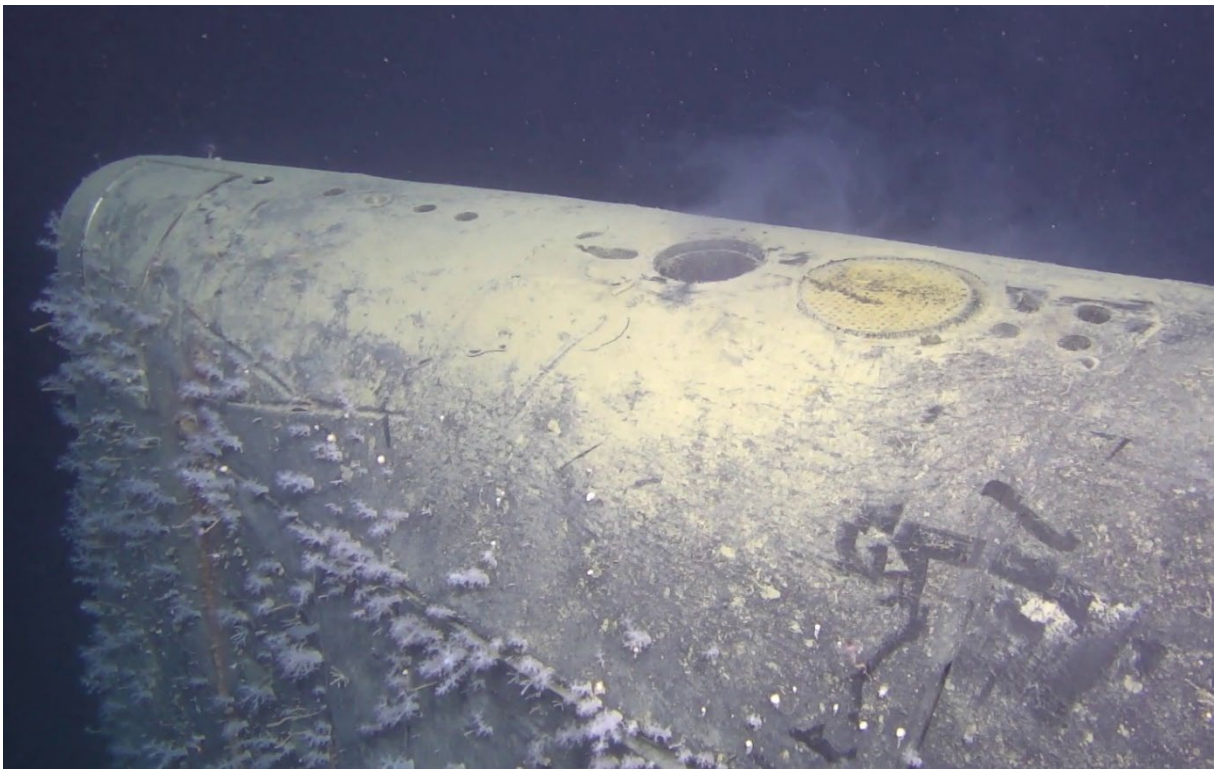

Figure 4.47. Extent of biota growth on the starboard side of the hull of Komsomolets around the ventilation pipe (Photo: IMR).

Table 4.13. Trace elements in biota

Element	Unit (f.w.)	From the sides of the sail below the ventilation pipe			From the seafloor next to Komsomolets
		Gersemia sp.	*Cladorhiza gelida*	*Actiniaria*	*Pontaster tenuispinus*
		Soft coral	Carnivorous sponge	Sea anemone	Starfish
Al	mg/kg	113 ± 7%	154 ± 11%	191 ± 23%	75 ± 2%
V	mg/kg	0.49 ± 6%	0.34 ± 15%	0.36 ± 7%	0.19 ± 4%
Cr	mg/kg	1.8 ± 23%	1.8 ± 98%	0.25 ± 17%	0.3 ± 0.4%
Mn	mg/kg	3.8 ± 8%	3.1 ± 7%	3.8 ± 6%	1.9 ± 1%
Fe	g/kg	0.28 ± 8%	0.22 ± 11%	0.22 ± 43%	0.055 ± 1%
Co	mg/kg	0.068 ± 7%	0.62 ± 102%	0.39 ± 85%	0.070 ± 2%
Ni	mg/kg	0.44 ± 4%	0.75 ± 90%	0.26 ± 5%	0.39 ± 0.3%
Cu	mg/kg	6.0 ± 17%	12 ± 24%	11 ± 98%	6.0 ± 1%
Zn	mg/kg	44 ± 11%	24 ± 38%	49 ± 20%	15 ± 1%
Ga	µg/kg	30 ± 5%	41 ± 11%	41 ± 22%	20 ± 1%
As	mg/kg	5.2 ± 3%	1.1 ± 8%	7.2 ± 5%	8.1 ± 0.2%
Zr	µg/kg	129 ± 3%	103 ± 11%	84 ± 13%	225 ± 1%
Nb	µg/kg	21 ± 7%	25 ± 74%	13 ± 19%	12 ± 0.2%
Cd	mg/kg	170 ± 3%	0.41 ± 3%	0.054 ± 19%	12 ± 0.2%
Sn	µg/kg	18 ± 6%	57 ± 16%	15 ± 10%	8.1 ± 12%
Ba	mg/kg	9.2 ± 10%	187 ± 34%	65 ± 44%	3.2 ± 1%
Ce	µg/kg	134 ± 3%	107 ± 11%	93 ± 13%	64 ± 0.3%
Eu	µg/kg	3.3 ± 2%	8.3 ± 26%	3.8 ± 18%	2.0 ± 0.4%
Hf	µg/kg	3.7 ± 7%	3.4 ± 10%	2.4 ± 15%	4.6 ± 4%
W	µg/kg	5.1 ± 6%	12 ± 21%	2.2 ± 17%	1.5 ± 0.5%
Tl	µg/kg	3.9 ± 8%	18 ± 2%	21 ± 102%	1.4 ± 1%
Pb	mg/kg	0.88 ± 23%	1.5 ± 7%	1.9 ± 2%	0.090 ± 0.4%
Bi	µg/kg	1.8 ± 15%	5.7 ± 12%	7.5 ± 42%	0.56 ± 5%
Th	µg/kg	17 ± 7%	14 ± 11%	12 ± 14%	8.4 ± 0.3%
U	µg/kg	32 ± 2%	39 ± 10%	56 ± 7%	168 ± 1%

Results above are the mean (± %SD) of three measurements, each from separate aliquots of the sample. Uncertainties on individual measurements were typically between 1% and 7%.

5 Overall conclusions

In 2019, the nuclear submarine Komsomolets was observed lying upright at a depth of around 1680 m approximately 250 km SSW from Bear Island. The inspection of the Komsomolets showed that the forward section of the submarine has suffered considerable damage to both the outer hull and inner pressure hull particularly around the torpedo compartment. The coverings and plates over the port, starboard and upper deck areas around the torpedo compartment that were installed by Russia in the 1990s were observed to be in place. This was also the case for the plugs installed over the torpedo tube openings, although in some cases the plugs did not form a complete seal over the entire tube opening. The stern section showed no obvious physical damage to the external hull, except for a number of missing deck tiles on the starboard side adjacent to the main stern ballast tank and compartment seven. Apart from the physical damage that was observed, the submarine showed little or no visible external corrosion. The exterior surfaces of the submarine were covered with a sparse layer of marine biota growth.

Due to the significant damage to the torpedo compartment, it is clear that open pathways between the marine environment and this compartment exist, in spite of the remediation work carried out by Russia in the 1990s. However, there was no indication of any release of weapon grade plutonium in either the sediment or the water column from the two nuclear warheads reported to have been in the torpedo compartment when Komsomolets sank. Based on the video evidence and previous eyewitness accounts, it can be assumed that there is an open pathway between the opening where the forward entrance hatch was located and at least compartments two and three. Although it is not possible to confirm, it is likely that further pathways exist between compartment three and compartments in the rear of the submarine, either through damaged transverse bulkheads or system tube lines that ran the length of the submarine.

The 2019 Norwegian research cruise confirmed that the previous Russian reports of releases of radionuclides from the ventilation pipe at the rear of sail but based on the observations from the first dive with the ROV, the releases are not continuous. However, it is not possible to elaborate on the frequency and duration of releases based on the limited time that the ventilation pipe was under observation. When elevated levels of radionuclides were detected in or near the ventilation pipe, a simultaneous visual release could be observed. The cause of this visual release is not known. On occasion, visual releases and elevated levels of radionuclides were detected from a metal grill next to the ventilation pipe, which has not been reported previously by Russia. Based on available schematics of Komsomolets, it is possible that the pipe under the metal grill is the air inlet for the diesel generator in compartment three, immediately forward of the reactor compartment. However, it is not known whether there is any connection or opening between the ventilation pipe and the pipe covered by the metal grill either by design or because of the accident and/or subsequent corrosion that would allow releases to pass from one pipe to the other. As is likely the case for the ventilation pipe, the air inlet pipe for the diesel generator would have been open when Komsomolets sank as the diesel generator in compartment three was in operation at the time of sinking. No obvious visual releases were observed emerging from any other opening around the submarine. During the times when the visual releases were observed, these tended to drift slowly towards the bow (i.e., northwards).

The range of Cs-137 activity concentrations in seawater samples collected from or near the ventilation pipe and metal grill when visual releases were observed were within the range of previously reported values by Russian investigations. The maximum observed activity concentration of Cs-137 in these samples was 800 000 times higher than typical background values for Cs-137 in seawater from the Norwegian Sea. For Sr-90, the maximum observed seawater activity concentration in the same samples was 400 000 times higher than typical background values for Sr-90 in seawater from the Norwegian Sea.

However, based on the results for Cs-137 and Sr-90 in samples taken at different distances from the ventilation pipe, the releases of these radionuclides from the reactor in Komsomolets appear to be rapidly diluted. Activity ratios of Cs-137 to Sr-90 taken within or close to point of release were typically around 2.2 and higher than the predicted reactor inventory activity ratio of 1:1. This is likely due to higher leaching rates of Cs-137 than Sr-90 from spent nuclear fuel. Future monitoring of the activity ratio of Cs-137 to Sr-90 in releases may provide insights into the deterioration of the nuclear fuel within the reactor. For seawater samples filtered through <0.45 um filters, higher activity concentrations of Cs-137 were observed in the dissolved phase than in the particulate phase.

The maximum observed combined activity concentration of Pu-239 and Pu-240 in seawater samples collected from or near the ventilation pipe and metal grill when visual releases were observed was 64 times higher than the average activity concentration of Pu-239,240 in bottom water sampled around Komsomolets since 1993. In general, higher combined activity concentrations of Pu-239 and Pu-240 were observed in the particulate phase than in the dissolved phase, with an indication that plutonium in the particulate phase undergoes relatively rapid vertical settling. Atom ratios of Pu-240/Pu-239 in dissolved and particulate phases of seawater samples taken from or near the ventilation pipe and metal grill were generally closer to estimated ratios for these plutonium isotopes in the reactor than to expected values for global fallout or other sources of Pu-239,240 to the Norwegian Sea. The maximum observed activity concentration of U-236 in seawater samples collected from or near the ventilation pipe and metal grill when visual releases were observed was 243 times higher than compared to available data for the North Sea. The elevated levels of Cs-137, Sr-90, Pu-239, Pu-240 and U-236 as well as atom ratios of Pu-240/Pu-239 that have been detected in releases from the reactor in Komsomolets would suggest that the nuclear fuel assemblies have been damaged and that nuclear fuel is in direct contact with seawater and deteriorating.

The releases that have occurred since Komsomolets sank in 1989 appear to have had little impact on the surrounding sediments based on the available results for Cs-137, Pu-239, Pu-240, U-236 and atom ratios of Pu-240/Pu-239. There is some evidence that marine biota growing on the hull of Komsomolets have accumulated Cs-137 that has been released from the reactor, but the observed activity concentrations are still low and not at a level where any significant effects would be expected.

Elevated concentrations of several trace elements in releases from or near the ventilation pipe and metal grill, in sediment around Komsomolets and in marine biota growing on the hull likely indicates other ongoing corrosion processes within the submarine. Any impacts from the elevated levels of some trace elements (e.g., Ni, Cu and Zn) in the releases and in sediments around the submarine are likely to be limited to the immediate area around the submarine.

Releases from the reactor in Komsomolets have been occurring since the submarine sank in 1989 and can be expected to continue in the future. Further investigations should be carried out to determine the mechanisms behind the observed releases, the corrosion processes that are occurring within the reactor and the implications of these for further releases and the fate of the remaining nuclear material in the reactor. Komsomolets provides a unique opportunity to understand the risks and consequences of releases from other sunken or dumped reactors in the Arctic as well as risks from any further accidents involving nuclear powered vessels and any other type of nuclear technologies used at sea. It is therefore important that continued monitoring of the situation and status of the submarine is carried out.

6 References

Astakhov, I.B., Druzhinin, A.A., Krylov, N.G., Korochkin, A.M., Maksimov, M.YU. 2000. Radiological Environmental Research Conducted at the Site of the Sinking of the Komsomolets Nuclear-Powered Submarine. Nuclear Physical Methods in Radioecological Investigations of Nuclear Test Sites. NATO Science Series 31: 109-114.

Blindheim, J., Føyn, L., Martinsen, E.A., Svendsen, E., Sætre Hjøllo, S., Ådlandsvik, B. 1994. The sunken nuclear submarine in the Norwegian Sea – A potential environmental problem? Fisken og Havet 7:1-46, Institute of Marine Research, Bergen, Norway.

Budko, D.F., Demina, L.L., Travkina, A.V., Starodymova, D.P., Alekseeva, T.N., 2022. The features of distribution of chemical elements, including heavy metals and Cs-137, in surface sediments of the Barents, Kara, Laptev and East Siberian Seas. Minerals, 12(3), p.328.

Bøhmer, N., Bertelsen, T. 1992. Undersøkelse av radioaktiv forurensning etter havariet med atomubåten Komsomolets. Arbeidsdokument, Statens institutt for strålehygiene, 1992:8 (In Norwegian).

Campion, P.J., 1975. Procedures for Accurately Diluting and Dispensing Radioactive Solutions. Bureau International des Poids et Mesures Monographie BIPM-1, Sèvres.Camplin, W.C., Read, R.J. 1992. Monitoring the site of a sunken nuclear submarine. Marine Pollution Bulletin 24(1): 52-55.

Cao, L., Bu, W., Zheng, J., Pan, S., Wang, Z., Uchida, S., 2016. Plutonium determination in seawater by inductively coupled plasma mass spectrometry: A review. Talanta, 151, pp.30-41.

Casacuberta, N., Christl, M., Lachner, J., Van Der Loeff, M.R., Masque, P., Synal, H.A., 2014. A first transect of 236U in the North Atlantic Ocean. Geochimica et Cosmochimica Acta, 133, pp.34-46.

Casacuberta, N., Christl, M., Vockenhuber, C., Wefing, A.M., Wacker, L., Masqué, P., Synal, H.A. and Rutgers van der Loeff, M., 2018. Tracing the three Atlantic branches entering the Arctic Ocean with 129I and 236U. Journal of Geophysical Research: Oceans, 123: 6909-6921.

Chamizo, E., Christl, M. and Fifield, L.K., 2015. Measurement of 236U on the 1 MV AMS system at the Centro Nacional de Aceleradores (CNA). Nuclear Instruments and Methods in Physics Research Section B: Beam Interactions with Materials and Atoms, 358, pp.45-51.

Choppin, G., Rydberg, J., Liljenzin, J.O., 1995. Radiochemistry and Nuclear Chemistry, 2nd ed. Butterworth-Heinemann, Oxford, UK.

Christl, M., Lachner, J., Vockenhuber, C., Lechtenfeld, O., Stimac, I., Van der Loeff, M.R., Synal, H.A., 2012. A depth profile of uranium-236 in the Atlantic Ocean. Geochimica et Cosmochimica Acta, 77, pp.98-107.

Christl, M., Casacuberta, N., Vockenhuber, C., Elsässer, C., Bailly du Bois, P., Herrmann, J. and Synal, H.A., 2015a. Reconstruction of the 236 U input function for the N ortheast A tlantic O cean: Implications for 129 I/236 U and 236 U/238 U-based tracer ages. Journal of Geophysical Research: Oceans, 120: 7282-7299.

Christl, M., Casacuberta, N., Lachner, J., Maxeiner, S., Vockenhuber, C., Synal, H.A., Goroncy, I., Herrmann, J., Daraoui, A., Walther, C., Michel, R., 2015b. Status of 236U analyses at ETH Zurich and the distribution of 236U and 129I in the North Sea in 2009. Nuclear Instruments and Methods in Physics Research Section B: Beam Interactions with Materials and Atoms, 361, pp.510-516.

Dittmann, B-A. et al. 2019. *ColPuS*, a new multi-isotope plutonium standard for Accelerator Mass Spectrometry. Nucl. Instr. and Meth. B, 438 (2019) 189-192.

Eigl, R., Srncik, M., Steier, P., Wallner, G., 2013. 236U/238U and Pu-240/Pu-239 isotopic ratios in small (2 L) sea and river water samples. Journal of environmental radioactivity, 116, pp.54-58.

Fifield, L.K., 2008. Accelerator mass spectrometry of the actinides. Quatern. Geochron. 3, 276-290.

Fifield, L.K., Tims, S.G., Fujioka, T., Hoo, W.T., Everett, S.E., 2010. Accelerator mass spectrometry with the 14UD accelerator at the Australian National University. Nucl. Instrum. Methods Phys. Res. Sect. B 268, 858-862.

Fifield, L.K., Tims, S.G., Stone, J.O., Argento, D.C., De Cesare, M., 2013. Ultra-sensitive measurements of ^{36}Cl and ^{236}U at the Australian national university. Nucl. Instrum. Methods Phys. Res., Sect. B 294, 126–131.

Frantzen, S., Maage, A., Duinker, A., Julshamn, K. and Iversen, S.A., 2015. A baseline study of metals in herring (Clupea harengus) from the Norwegian Sea, with focus on mercury, cadmium, arsenic and lead. Chemosphere, 127, pp.164-170.

Gladkov, G.A., Khlopkin, N.S., Lystsov, V.N., Nejdanov, G.A., Pologikh, B.G., Sivintsev, Y.V. 1994. Assessment and prognosis of the state of nuclear installation of submarine Komsomolets, Working Group under leadership of Academician N. S. Khlopkin, RRC “Kurchatov Institute”, Moscow, Russia.

Geckeis, H., Zavarin, M., Salbu, B., Lind, O.C., Skipperud, L., 2019. Environmental Chemistry of Plutonium, in: Clark, D.L., Geeson, D.A., Hanrahan, R.J. (Eds.), Plutonium Handbook. American Nuclear Society, pp. 1979-2118.

Gómez-Guzmán, J.M., López-Gutiérrez, J.M., Pinto-Gómez, A.R., Holm, E. 2012. ^{129}I measurements on the 1 MV AMS facility at the Centro Nacional de Aceleradores (CNA, Spain). Applied Radiation and Isotopes 70: 263-268.

Grøttheim S., 1999. Artificial Radionuclides in the Northern European Marine Environment in 1995. Distribution of plutonium, americium and radiocaesium in seawater and sediments. Cand. Scient. Thesis. Oslo: Department of Biology, Section of Marine Zoology and Marine Chemistry, University of Oslo, 1999.

Gwynn, J.P., Heldal, H.E., Flo, J.K., Sværen, I., Gäfvert, T., Haanes, H., Føyn, L. and Rudjord, A.L. 2018. Norwegian monitoring (1990–2015) of the marine environment around the sunken nuclear submarine Komsomolets. Journal of Environmental Radioactivity, 182: 2-62.

Harvey, B.R., Ibbett, R.D., Lovett, M.B., Williams, K.J. 1989. Analytical procedures for the determination of strontium radionuclides in environmental materials. Aquatic Environmental Protection: Analytical Methods Number 5. Ministry for Agriculture Fisheries and Food, Directorate for Fisheries Research.

Heldal, H.E., Varskog, P., Føyn, L., 2002. Distribution of selected anthropogenic radionuclides (137Cs, 238Pu, 239,240Pu and 241Am) in marine sediments with emphasis on the Spitsbergen–Bear Island area. Science of the Total Environment, 293(1): 233-245.

Høibraaten S., Thoresen P.E., Haugan A. 1997. The sunken nuclear submarine Komsomolets and its effects on the environment. The Science of the Total Environment 202: 67–78.

Hollister, C.D. 1992. MC-31002 'Trip report, St Petersburg, Russia. September 20-25. 1992'. Charles Davies Hollister papers, 1967-1998. MC-31, Data Library and Archives, Woods Hole Oceanographic Institution.

Hollister, C.D. 1993a. MC31 Keldysh Report 01 'Trip report of 1993 Keldysh expedition to Komsomolets'. Charles Davies Hollister papers, 1967-1998. MC-31, Data Library and Archives, Woods Hole Oceanographic Institution.

Hollister, C.D. 1993b. MC31 Article Translation 01 'Results of the new expedition (Samojlov, V.), Naval Journal, 1993'. Charles Davies Hollister papers, 1967-1998. MC-31, Data Library and Archives, Woods Hole Oceanographic Institution.

Hollister, C.D. 1994a. MC-31 Symposium 04 'International Symposium on the discussion of results of 1993 expedition to SSN "Komsomolets" and on the working out of a common concept for further research. January 31st - February 2nd, 1994, St Petersburg, Russia.'. Charles Davies Hollister papers, 1967-1998. MC-31, Data Library and Archives, Woods Hole Oceanographic Institution.

Hollister, C.D. 1994b. MC-31009 'Proceedings of the January 1994 Rubin Conference'. Charles Davies Hollister papers, 1967-1998. MC-31, Data Library and Archives, Woods Hole Oceanographic Institution.

IAEA 2004. Sediment distribution coefficients and concentration factors for biota in the marine environment. Technical Reports Series No. 422. IAEA, Vienna.

Kazennov, A. 2010. Technologies of radiation monitoring of dumped objects and aquatories. The practices of RRC "Kurchatov Institute". Presentation at the IAEA CEG Workshop on Removal of Spent Nuclear Fuel (SNF) and Radioactive Waste (RW) from Andreeva Bay, and Strategies for Handling Sunken Objects Containing SNF in the Arctic Ocean. 24 - 26 February 2010, Hague, Netherlands. https://www.iaea.org/OurWork/ST/NE/NEFW/CEG/documents/ws022010/eng/5.4KazennovEngl.pdf

Kelley, J.M., Bond, L.A., Beasley, T.M. 1999. Global distribution of Pu isotopes and 237Np. Science of the Total Environment 237–238: 483-500.

Knies J., Jensen H.K.B., Finne T.E., Lepland A., Sæther O.M., 2006. Sediment composition and heavy metal distribution in Barents Sea surface samples results from Institute of Marine Research 2003 and 2004. Report No. 2006.067. Geological Survey of Norway, Trondheim, Norway. https://www.ngu.no/upload/Publikasjoner/Rapporter/2006/2006_067.pdf

Kolstad, A.K. 1995. Tokt til Komsomolets i 1993 og 1994. StrålevernRapport 1995:7, Norwegian Radiation Protection Authority, Østerås (In Norwegian).

Kuwae, M., Finney, B.P., Shi, Z., Sakaguchi, A., Tsugeki, N., Omori, T., Agusa, T., Suzuki, Y., Yokoyama, Y., Hinata, H., Hatada, Y., Inoue, J., Matsuoka, K., Shimada, M., Takahara, H., Takahashi, S., Ueno, D., Amano, A., Tsutsumi, J., Yamamoto, M., Takemura, K., Yamada, K., Ikehara, K., Haraguchi, T., Tims, S., Froehlich, M., Fifield, L.K., Aze, T., Sasa, K., Takahashi, T., Matsumura, M., Tani, Y., Leavitt, P.R., Doi, H., Irino, T., Moriya, K., Hayashida, A., Hirose, K., Suzuki, H. and Saito, Y., 2023. Beppu Bay, Japan, as a candidate Global boundary Stratotype Section and Point for the Anthropocene series. The Anthropocene Review 10: 49-86.

Kuznetsov, A.P., Shmelev, I.P., Demidov, A.M., Efimov, B.V., Shubko, V.M. 1996. Radionuclides in the benthofauna in the region of the location of the Komsomolets atomic submarine (the Norwegian Sea). Izvestiia Akademii Nauk. Seriia Biologicheskaia 4: 467-471 (In Russian).

Kuznetsov, A.P., Shmelev, I.P., Demidov, A.M., Efimov, B.V., Shubko, V.M. 1999. Radionuclides 90Sr and 137Cs in the benthos near the nuclear submarine "Komsomolets". Izvestiia Akademii Nauk. Seriia Biologicheskaia 1: 67-74 (In Russian).

Lee, S.H., Gastaud, J., La Rosa, J.J., Kwong, L.L.W., Povinec, P.P., Wyse, E., Fifield, L.K., Hausladen, P.A., Di Tada, L.M., Santos, G.M., 2001. Analysis of plutonium isotopes in marine samples by radiometric, ICP-MS and AMS techniques. Journal of Radioanalytical and Nuclear Chemistry, 248, pp.757-764.

Lee, S.H., Povinec, P.P., Wyse, E., Hotchkis, M.A.C., 2008. Ultra-low-level determination of 236U in IAEA marine reference materials by ICPMS and AMS. Applied Radiation and Isotopes, 66: 823-828.

Li, Y.H. and Schoonmaker, J.E., 2003. Chemical composition and mineralogy of marine sediments. Treatise on Geochemistry 7: 1–35.

Lindahl, P., Lee, S.H., Worsfold, P., Keith-Roach, M., 2010. Plutonium isotopes as tracers for ocean processes: a review. Marine Environmental Research, 69(2), pp.73-84.

Livingston, H.D. and Anderson, R.F., 1983. Large particle transport of plutonium and other fallout radionuclides to the deep ocean. Nature 303: 228-231.

Lopez-Lora, M., Chamizo, E., Villa-Alfageme, M., Hurtado-Bermúdez, S., Casacuberta, N., García-León, M. 2018. Isolation of ^{236}U and ^{239,240}Pu from seawater samples and its determination by Accelerator Mass Spectrometry. Talanta 178: 202-210.

Lukashin, V.N., Vinogradov, M.E., Gordeev, V.Y., Rusakov, V.Y. 1996. Sedimentary material streams in the Norwegian Sea: data from the year-round sediment-trapping station. Transactions of the Russian Academy of Sciences-Earth Science Sections 349(5): 844-847.

Lukashin, V.N., Gordeev, V.Y., Isaeva, A.B., Rusakov, V.Y. 1998. Investigation of Vertical Fluxes of Sedimentary Material in the Norwegian Sea from August 1994 to July 1995. Geochemistry international 36(9): 830-837.

Lukashin, V.N. 2008. Geochemistry of suspended matter and sinking material in the eastern Norwegian Sea. Geochemistry International 46(7): 711-723.

Miljødirektoratet, 2016. Grenseverdier for klassifisering av vann, sediment og biota – revidert 30.10.2020. M-608. https://www.miljodirektoratet.no/globalassets/publikasjoner/m608/m608.pdf

Moghaddam, N.M., Fadaei, A.H., Zahedi, E., 2011. Evaluating the effect of using different sets of enrichment for FAs on fuel management optimization using CA. Ann. Nucl. Energy 38: 835-845.

Momoshima, N., Kakiuchi, H., Maeda, Y., Hirai, E., Ono, T., 1997. Identification of the contamination source of plutonium in environmental samples with isotopic ratios determined by inductively coupled plasma mass spectrometry and alpha-spectrometry. Journal of Radioanalytical and Nuclear Chemistry, 221, pp.213-217.

Moreno, J.A.G., 2022. Radiactive particle biotic and abiotic processes. Doctoral dissertation, Universidad de Sevilla.

Mork, K.A., Ø. Skagseth, H. Søiland, 2022, Water mass properties and distribution in the Nordic Seas during the 2010s, and in relation to the changes during the last 50 years. The Symposium on Decadal Variability of the North Atlantic and its Marine Ecosystems: 2010-2019, ICES Decadal 2022. June 20-22, 2022. Bergen, Norway.

Nahrgang, J., Brooks, S.J., Evenset, A., Camus, L., Jonsson, M., Smith, T.J., Lukina, J., Frantzen, M., Giarratano, E. and Renaud, P.E., 2013. Seasonal variation in biomarkers in blue mussel (Mytilus edulis), Icelandic scallop (Chlamys islandica) and Atlantic cod (Gadus morhua)—Implications for environmental monitoring in the Barents Sea. Aquatic toxicology, 127, pp.21-35.

Nejdanov, G. 1993. Cs-137 contamination of seawater around the "Komsomolets" nuclear submarine, in: Radioactivity and Environmental Security in the Oceans: New Research and Policy Priorities in the Arctic and North Atlantic, June 7-9, 1993, Woods Hole Oceanographic Institution, Massachusetts, USA, pp. 119-133.

Neff, J.M. 2002. Cadmium in the ocean. In: Bioaccumulation in Marine Organisms. Effect of Contaminants from Oil Well Produced Water. (ed Neff, J.M.) pp. 89-102, ISBN 9780080527840, Elsevier.

Nies, H., Harms, I.H., Karcher, M.J., Dethleff, D., Bahe, C. 1999a. Anthropogenic radioactivity in the Arctic Ocean—review of the results from the joint German project. Science of the Total Environment 237: 181-191.

Nies, H. , Karcher, M. , Bahe, C. , Backhaus, J. , Harms, I., Dethleff, D. 1999b. Transportmechanismen radioaktiver Substanzen im Arktischen Ozean-Numerische und experimentelle Studien am Beispiel der Barents- und Karasee , Berichte des Bundesamtes für Seeschiffahrt und Hydrographie Nr.21, Hamburg und Rostock, 134 p. In German.

Nyffeler, F., Cigna, A.A., Dahlgaard, H. and Livingston, H.D., 1996. Radionuclides in the Atlantic Ocean: a survey. In: International Symposium on Radionuclides in the Oceans (P. Guegueniat, P. Germain and H. Metivier Eds.), pp. 1-28 Les Editions de Physique, pp. 1-28.

Ottersen, G. 2010. A digital temperature atlas for the Norwegian Sea. ICES Journal of Marine Science, 67(8): 1525-1537.

Oughton, D.H., Fifield, L.K., Day, J.P., Cresswell, R.C., Skipperud, L., Salbu, B. 1999. Determination of $^{Pu\text{-}240/Pu\text{-}239}$ isotope ratios in Kara Sea and Novaya Zemlya sediments using accelerator mass spectrometry. In: Symposium on Marine Pollution, IAEA-SM-354, IAEA, Vienna.

Oughton, D.H., Fifield, L.K., Day, J.P., Cresswell, R.C., Skipperud, L., Di Tada, M.L., Salbu, B., Strand, P., Drozcho, E., Mokrov, Y. 2000. Plutonium from Mayak: measurement of isotope ratios and activities using accelerator mass spectrometry. Environmental science & technology, 34(10): 1938-1945.

Pham, M.K., Sanchez-Cabeza, J.A., Povinec, P.P., Arnold, D., Benmansour, M., Bojanowski, R., Carvalho, F.P., Kim, C.K., Esposito, M., Gastaud, J., Gascó, C.L., 2006. Certified reference material for radionuclides in fish flesh sample IAEA-414 (mixed fish from the Irish Sea and North Sea). Applied Radiation and Isotopes, 64(10-11), pp.1253-1259.

Qiao, J., Heldal, H.E., Steier, P., 2022. Understanding source terms of anthropogenic uranium in the Arctic Ocean–First 236U and 233U dataset in Barents Sea sediments. Science of the Total Environment, 847, p.157503.

Romanov, D.A. 2006. Fire at Sea: The Tragedy of the Soviet Submarine Komsomolets. Potomac Books Inc., Washinghton DC, USA.

Röllin, S., Sahli, H., Gnägi, L., Alvarado, J.A.C., 2020. Determination of plutonium and uranium radionuclides in glacier ice samples by MC-ICP-MS. Chimia, 74(12), pp.989-989.

Schnetger, B., Brumsack, H.J., Schale, H., Hinrichs, J. and Dittert, L., 2000. Geochemical characteristics of deep-sea sediments from the Arabian Sea: a high-resolution study. Deep Sea Research Part II: Topical Studies in Oceanography, 47(14), pp.2735-2768.

Skjerdal, H., Heldal, H.E., Gwynn, J., Strålberg, E., Møller, B., Liebig, P.L., Sværen, I., Rand, A., Gäfvert, T., Haanes, H., 2017. Radioactivity in the Marine Environment 2012, 2013 and 2014. Results from the Norwegian Marine Monitoring Programme RAME. Strålevern-rapport 2017:13. Østerås, Norwegian Radiation Protection Authority.

Skjerdal, H., Heldal, H.E., Rand, A., Gwynn, J., Kiel-Jensen, L., Volynkin, A., Haanes, H., Møller, B., Liebig, P.L., Gäfvert, T. 2020. Radioactivity in the Marine Environment 2015, 2016 and 2017. Results from the Norwegian Marine Monitoring Programme RAME. DSA-rapport 2020:04. Østerås, Direktoratet for strålevern og Atomsikkerhet.

Srncik, M., Tims, S.G., De Cesare, M., Fifield, L.K., 2014. First measurement of ^{236}U and $^{236}U/^{239}Pu$ isotopic ratios in a Southern Hemishere soil far from nuclear test or re- actor sites. J. Environ. Radioact. 132, 108–114.

Steier, P., Bichler, M., Fifield, L.K., Golser, R., Kutschera, W., Priller, A., Quinto, F., Richter, S., Srncik, M., Terrasi, P., Wacker, L., Wallner, A., Wallner, G., Wilcken, K.M., Wild, E.M., 2008. Natural and anthropogenic ^{236}U in environmental samples. Nucl. Instrum. Methods Phys. Res., Sect. B 266, 2246–2250.

Stepanov, A.V., Tsvetkov, O.S., Tishkov, V.P., Belyaev, B.N., Domkin, V.D., Ivanova, L.M., Osokina, A.A., Plekhov, V.S., Bobylev, K.L., Johannessen, O. 1999. Isotopic composition of plutonium in the bottom deposits of the Norwegian Sea and Greenland Sea and identification of the sources of contamination. Atomic Energy 87(4): 745-752.

Sivintsev, Y., 1995. Studies of nuclides composition and characteristics of fuel in dumped submarine reactors and atomic icebreaker “Lenin”. Part 2 – Nuclear submarines. Report IAEA-IASAP-5.

Vysotsky, V.L., Sivintsev, Yu.V., Sotnikov, V.A., Khokhlov, V.N. 2014. Release of man-made radionuclides into seawater from dumped and sunken nuclear- and radiation-hazardous objects Thermal Engineering 61(13): 931-945.

Wendel, C.C., 2013. Source identification of Pu and 236U deposited on Norwegian territories. PhD Thesis, Department of Plant and Environmental Sciences, Norwegian University of Life Sciences, Ås, Norway.

Wei, G., Liu, Y., Li, X., Shao, L. and Liang, X., 2003. Climatic impact on Al, K, Sc and Ti in marine sediments: evidence from ODP Site 1144, South China Sea. Geochemical Journal, 37(5), pp.593-602.

Wiech, M., Frantzen, S., Duinker, A., Rasinger, J.D. and Maage, A., 2020. Cadmium in brown crab Cancer pagurus. Effects of location, season, cooking and multiple physiological factors and consequences for food safety. Science of the Total Environment, 703, p.134922.

Yablokov, A.V., Karasev, V.K., Rumyanstsev, V.M., Kokeev, M.E., Petrov, O.J., Lystsov, V. N., Emel'yanenkov A.F., Rubtsov, P.M. 1993. Facts and Problems related to Radioactive Waste Disposal in Seas Adjacent to the Territory of the Russian Federation, Small World Publishers Inc., Moscow, Russia.

Zhurakov, A.M., Dozhdikov, S.I., Zolotkov, A.A. 1992. Corrosion stability of spent nuclear fuel in sea water. In: Proceedings of the international scientific seminar of the USSR. Atomic energy on sea, safety and ecology. S

ISSN 2535-7379

dsa@dsa.no
+47 67 16 25 00
dsa.no

1 DSA Report 01-2024
Setting up a National Technical and Scientific Support Organization for Nuclear Safety and Security

2 DSA-rapport 02-2024
Potential Dispersal of Contaminants from Hypothetical Accidents Involving the Floating Nuclear Power Plant: Akademik Lomonosov

3 DSA-rapport 03-2024
Investigation into the Radioecological Status of the Sunken Nuclear Submarine Komsomolets in the Norwegian Sea

4 DSA-rapport 04-2024
Overvaking av radioaktivitet i luft 2023

DSA
Norwegian Radiation and Nuclear Safety Authority